EVASION OF EFFLUX AND ENHANCING BIOAVAILABILITY OF AMPRENAVIR BY PRODRUG DERIVATIZATION

A DISSERTATION IN

Pharmaceutical Sciences
and
Chemistry

Presented to the Faculty of University of
Missouri-Kansas City in partial fulfillment of
the requirements for the degree

DOCTOR OF PHILOSOPHY

by

Nanda K. Mandava

B.S., Pharmacy, The Tamil Nadu Dr. M.G.R. Medical University, 2001

Kansas City, Missouri
2013

EVASION OF EFFLUX AND ENHANCING BIOAVAILABILITY OF AMPRENAVIR BY PRODRUG DERIVATIZATION

Nanda K Mandava, Candidate for Doctor of Philosophy Degree

University of Missouri-Kansas City, 2010

ABSTRACT

Millions of people worldwide have been infected with human immunodeficiency (HIV). Highly active antiretroviral therapy (HAART) has substantially improved the clinical management of HIV-1 infection. Inclusion of HIV protease inhibitors (PIs) in HAART has substantially improved clinical outcomes of HIV infected patients. However complete eradication of virus poses an unmet goal. Major challenge with current anti-HIV drug regimen is the inability of PIs to attain sufficient concentrations in sanctuary sites such as brain resulting in persistent viral replication and may lead to viral resistance. Sub-therapeutic concentration of PIs in brain leads to drug resistance and HIV associated dementia. One of the major factors which limit central nervous system (CNS) permeation of PIs is the presence of efflux proteins on brain capillary endothelial cells. There are several reports demonstrating that PIs are substrates of efflux proteins which limit their oral bioavailability and brain permeation. Various approaches have been employed to evade the efflux and improve the bioavailability, however improving brain absorption still remains as an elusive goal. The overall objective of this dissertation project was to improve oral and brain bioavailability of Amprenavir (APV) by prodrug strategies targeting nutrient transporters to bypass P-glycoprotein (P-gp) mediated efflux. APV has low bioavailability and negligible brain

absorption which is attributed by low aqueous solubility, efflux mediated by multidrug resistance proteins, extensive metabolism and protein binding. In order to improve oral bioavailability and absorption across blood brain interfaces, di-peptide and amino acid prodrugs of APV (Val-Val-APV, Gly-Val-APV, Val-APV) were synthesized and evaluated for interaction with efflux and influx transporters, enzymatic hydrolysis, and bioavailability. These prodrugs targeting peptide transporters were demonstrated to evade P-gp mediated efflux and exhibit better permeability characteristics compared to APV. All these prodrugs have higher aqueous solubility. Enzymatic stability and metabolism studies demonstrated that these prodrugs undergo enzymatic hydrolysis and regenerate parent drug which exerts pharmacological action. Oral and brain absorption of prodrugs was much higher as compared to APV in Sprague-Dawley rats. Thus transporter targeted prodrug modification of P-gp substrates could lead to shielding of these drug molecules from efflux pumps and improve bioavailability of PIs and other P-gp substrates.

APPROVAL PAGE

The faculty listed below, appointed by the Dean of School of Graduate Studies have examined the dissertation titled "Evasion of Efflux and Enhancing Bioavailability of Amprenavir by Prodrug Derivatization" presented by Nanda K. Mandava, candidate for the Doctor of Philosophy degree, and certify that in their opinion it is worthy of acceptance.

Supervisory Committee

Ashim K. Mitra, Ph.D., Committee Chair
Division of Pharmaceutical Sciences

Chi H. Lee, Ph.D.
Division of Pharmaceutical Sciences

Kun Cheng, Ph.D.
Division of Pharmaceutical Sciences

Santosh Kumar, Ph.D.
Division of Pharmacology

Y.C. Jerry Jean, Ph.D.
Department of Chemistry

CONTENTS

ILLUSTRATIONS

Figure

Page

TABLES

Table Page

ACKNOWLEDGEMENTS

I would like to extend my gratitude and appreciation for all people who helped me during my Ph.D. program. First and the foremost I would like to thank my advisor Ashim K. Mitra, Ph.D., for his excellent support, constant input in my research project and guidance in personal and professional aspects. I would like to extend my appreciation for Dr. Mitra in his trust for me and also for providing freedom for exploring different avenues of research. I also wish to sincerely thank my supervisory committee members, Chi H. Lee, Ph.D., Kun Cheng, Ph.D., Santosh Kumar, Ph.D., and Y. C .Jerry Jean, Ph.D., for their constant encouragement and valuable suggestions.

I wish to thank Dhananjay Pal, Ph.D. for training me and helping me in all cell culture techniques. I am especially thankful to him for all his encouragement, support and patiently listening to me in my good and bad times. . I would like to thank Mrs. Ranjana Mitra for her cheerful encouragement and constant support in lab. I sincerely thank Swapan Samantha, Ph.D., for synthesizing the prodrugs. I would like to specially thank Ritesh Jain, Ph.D., for all his scholarly help which aided to improve my analytical thinking, and teaching all the experimental techniques. I would like to thank Sriram Gunda, Ph.D., and Sheetal Agarwal Ph.D., for their help and support throughout my days as graduate student. I am thankful to Mitesh Patel for his constant help in experiments. I would also like to thank present and past students of Dr. Mitra who directly or indirectly helped me throughout my stay at UMKC.

I also sincerely thank Joyce Johnson and Sharon Self for their help everyday through these years. I also like to extend my gratitude to all the faculty, staff and students of Division of Pharmaceutical sciences for their help and for creating a friendly environment in school.

I would like to express my deepest gratitude for my parents Sreerama Murthy Mandava and Lakshmi Mandava for their constant support and the sacrifices they have made for me. I would like to thank one important person in my life, Sneha Pendyala, my wife who supported me in all walks of my life and provided constant encouragement and support.

I would like to acknowledge NIH for funding the project.

DEDICATED TO MY PARENTS, MY WIFE SNEHA, AND MY DAUGHTER SANNIHITHA

CHAPTER 1

INTRODUCTION

Overview

Millions of people worldwide have been infected with human immunodeficiency virus (HIV) and the syndrome remains among the top five fatal diseases. Two different retroviruses, HIV-1 and HIV-2, cause HIV infection in humans. Both are enveloped positive-stranded RNA viruses belonging to lentivirus sub-family. HIV-1 is responsible for the majority of infections globally. AIDS dementia complex (ADC) or HIV-associated dementia (HAD) develops in about 20 per cent of HIV infected patients who progress to AIDS. Although the development of highly active antiretroviral therapy (HAART) has greatly slowed the progression from HIV infection to AIDS and improved the clinical treatment of AIDS related diseases, the eradication of HIV/AIDS remains a major medical challenge. HAART constitutes a combination of protease inhibitors (PIs), non-nucleoside reverse transcriptase inhibitors (NNRTIs) and nucleoside reverse transcriptase inhibitors (NRTIs). Despite of their very good antiviral efficacy, PIs suffer from low and variable oral bioavailability, negligible brain permeation and poor pharmacokinetic (PK) profiles. Low and variable oral bioavailability is attributed by poor aqueous solubility, high affinity for membrane efflux proteins, high protein binding and extensive metabolism by CYP enzymes. Also, the existence of sanctuary sites such as brain parenchyma for HIV-1 may potentially endanger the efficacy of long-term therapy. Sub-therapeutic concentrations of PIs in the sanctuary sites like brain, lung and bone marrow cause persistent viral infection and may lead to viral resistance. Blood brain barrier (BBB) presents a significant challenge to the delivery of therapeutic agents to the brain. Tight junctions prevent free diffusion of small polar

molecules across this barrier. However, entry of large lipid soluble molecules is also limited across BBB by the presence of several ATP binding cassette (ABC) efflux transporters i.e., P-glycoprotein (P-gp) and multi-drug resistance associated proteins (MRPs) which efficiently prevent entry of drug molecules into the central nervous system (CNS).

Various strategies have been employed by researchers to evade the efflux and improve bioavailability. These approaches include co-administration of efflux protein inhibitor or modulator to control the expression and functional activity of efflux proteins, utilizing various formulations such as nanoparticulate systems, and chemical modification of drugs such that efflux can be evaded. Co-administration of modulators and inhibitors may affect the physiological activity of efflux proteins which efflux xenobiotics and toxins from cells. This may lead to adverse events and toxicities. Chemical modifications such as prodrug approach has the advantage that activity of efflux proteins is not affected. This pro-drug approach does not require any additional augmenting agent which may lead to toxicity. One of these non-substrate strategies is targeted prodrug approach. In this approach not only evading the efflux proteins, but also influx transporters such as nutrient transporters can be utilized. This approach involves utilization of influx proteins which facilitate transport of polar nutrients such as amino acids and peptides.

Prodrugs can be designed by conjugating amino acid/di-peptide promoiety such that they can be recognized and translocated by amino acid and peptide nutrient transporters expressed on epithelial (intestinal) and endothelial (brain capillary endothelial cells) cells. Another advantage of these prodrugs is the promoieties released after regeneration of parent drug are not toxic. When a compound binds to a nutrient transporter, it triggers a configurational change in the transport protein allowing its translocation across the

membrane and it is subsequently released into the cytoplasm. During this process the substrate is not freely available to efflux transporters located on the inner leaflet of the cell membrane. Circumventing P-gp/MRP2 mediated efflux not only increases absorption across intestinal mucosa but also decreases repetitive exposure to metabolizing enzymes in intestinal lumen. In addition to the possibility of enhanced intestinal permeation, prodrug derivatization of compounds may offer additional pharmaceutical, pharmacokinetic and toxicokinetic advantages such as better chemical stability, solubility and toxicity profiles. Therefore, transporter targeted prodrug derivatization strategy offers several possibilities that may prove to be advantageous for systemic delivery of PIs.

In this dissertation project novel amino acid and di-peptide prodrugs of amprenavir (APV) have been designed and synthesized such that the modified compounds become substrates of nutrient transporters. These prodrugs were evaluated for their interaction with efflux proteins, influx transporters, enzymatic stability, metabolism and systemic bioavailability

Statement of the Problem

Protease inhibitors are considered to be the most important therapeutic agents to date for the treatment of AIDS. Currently available PIs approved by FDA include Saquinavir, Ritonavir, Nelfinavir, Lopinavir, Amprenavir, Fosamprenavir, Indinavir, Atazanavir, Tipranavir and Darunavir. Despite of good antiviral efficacy, PIs suffer from unfavorable physicochemical and pharmacokinetic properties. APV has low aqueous solubility, low oral absorption and fast biotransformation into inactive metabolites. When used both alone and in combination with other antiretroviral agents, amprenavir has been demonstrated to be a highly effective inhibitor of HIV replication that reduces HIV-1RNA levels and is associated

with improved CD4+ cell counts (St Clair et al., 1996; Sadler et al., 1999; Veronese et al., 2000). Currently available formulations of amprenavir are as 50 mg and 150 mg soft-gelatin capsules or as a 15 mg/mL oral solution, with a recommended oral dose of amprenavir (capsules) for adults and adolescents of 1200 mg bid, without specific food or fluid requirements. Despite its absorption profile being relatively good for a protease inhibitor, dosing regimens of up to eight capsules twice daily are required to achieve effective plasma concentrations. This can be a problem for some patients, especially since they are likely to be facing a significant pill burden if they are following a highly active antiretroviral therapy (HAART) regimen (Falcoz et al., 2002). Oral bioavailability of APV is limited to 14-26%. Such low bioavailability is primarily attributed to extensive cellular efflux mediated by efflux protein P-glycoprotein (P-gp) and first-pass metabolism mediated by enzyme cytochrome P450 3A4 (CYP3A4). Predominantly localized P-gp limits the absorption of orally administrated drugs. Abundantly expressed in the liver and gut wall, CYP3A4 is responsible for the extensive first-pass metabolism of. APV is a good substrate for both P-gp and CYP3A4 (Kempf et al., 1997; Adkins and Faulds, 1998; Edwards et al., 2002). The efflux of drug molecules by P-gp back to intestinal lumen or blood capillaries further increases the drug exposure to cellular as well as luminal enzymes and thus causing extensive drug metabolism. The monotherapy of APV is restricted because of its low bioavailability. The combination of APV with ritonavir/ketoconazole may boost the plasma concentration of APV. However, high doses of drugs are required in order to reach sufficient therapeutic level of drug concentration, which may cause drug resistance and cytotoxicity. In order to circumvent the cellular efflux mediated by P-gp and extensive first-pass metabolism mediated by CYP3A4 and thus improving the oral absorption and bioavailability of APV,

novel amino acid and di-peptide conjugated prodrugs of APV were designed and synthesized. These amino acid, di-peptide prodrugs may become the substrates of the influx transporters expressed on intestinal epithelium and brain endothelial cells and bypass the P-gp mediated efflux.

Objectives

The objectives of this dissertation project are:

a. To synthesize relevant peptide and amino acid prodrugs of APV and characterize these compounds in terms of their molecular weights, aqueous solubilities and buffer hydrolysis
b. To study the interaction of the synthesized prodrugs of APV with the respective influx transporters, affinity of the prodrugs towards efflux proteins and metabolizing enzymes *in vitro* using appropriate cell culture models
c. To study protein binding, enzymatic hydrolysis and bioreversion of prodrugs *in vitro*
d. To investigate oral bioavailability of APV and prodrugs *in vivo* in Sprauge-Dawley rats
e. To study permeability characteristics of APV an prodrugs using *in vitro* blood brain barrier model (rat brain endothelial cells co-cultured with astrocytes)
f. To conduct *in vivo* brain microdialysis studies with amino acid prodrugs to study their brain absorption properties

CHAPTER 2

LITERATURE REVIEW

This chapter provides overview of HIV (human immunodeficiency virus) infection, current clinical management, and role of protease inhibitors in HIV therapy, setbacks of current therapy. This chapter also discusses about role of efflux proteins and influx transporters in oral and brain absorption. Various strategies to circumvent P-gp, MRP mediated efflux, and prodrug approach. This chapter would facilitate understanding of the research goals and findings presented in subsequent chapters.

Introduction to HIV and AIDS

Acquired Immune Deficiency Syndrome (AIDS) is caused by HIV. HIV is different from most other viruses since it compromises the host immune system. Over one million Americans are living with HIV/AIDS today. Worldwide, the figure is over 30 million AIDS is the final stage of HIV infection. It can take years for a person infected with HIV, even without treatment, to reach this stage. Having AIDS means that the virus has weakened the immune system to the point, at which the body is vulnerable for other opportunistic infections.

HIV Virus

Two different retroviruses, HIV-1 and HIV-2, cause HIV infections in humans. HIV enveloped single stranded RNA viruses belonging to lentivirus sub-family. HIV-1 is major cause of infections worldwide. The cross sectional view of HIV virion is shown in Figure 1.

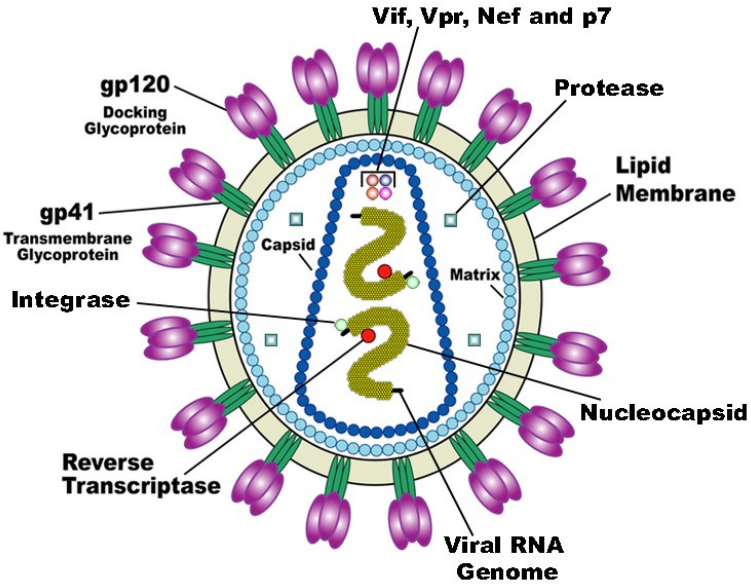

Figure 1. Stucture of HIV virion. Adapted from US NIH

HIV is an enveloped complex retrovirus. The genetic information is encoded by ~9-kb RNA and each virion has two copies of RNA. HIV-1 genome consists of nine separate genes encoding for a total of 3 structural polyproteins (Env, Gag and Pol), 4 accessory proteins (Vif, Vpr, Nef and Vpu) and 2 regulatory proteins (Rev and Tat) (Frankel and Young, 1998). The outermost covering of the virus particle, referred as envelope, is a lipid bilayer derived from the host cell plasma membrane. HIV-1 is composed of two copies of single-stranded RNA enclosed by a capsid comprising the viral protein p24. The capsid environment also contains other viral proteins such as integrase and reverse transcriptase. This capsid is in turn encapsidated by a layer of another matrix protein (MA) called p17. The HIV-1 RNA is part of a protein nucleic acid complex, which is composed of the nucleoprotein p7 and the reverse transcriptase p66 (RT). The viral particle contains all the

enzymatic equipment that is necessary for replication: a reverse transcriptase (RT), an integrase p32, and a protease p11. An envelope, which covers the viral core or nucleocapsid, is derived from host cell membrane. This core is mainly lipoidal in nature and contains some viral proteins. The major HIV protein associated with this envelope is gp120/41. The gp41 glycoprotein traverses the envelope, gp120 is present on the outer surface and is non-covalently attached to gp41. This functions as the viral antireceptor or attachment proteins. Both gp120 and gp41 glycoproteins have important role in the binding of HIV to cells in the infection process. Besides these surface proteins, HIV is also studded with human proteins (including class I and class II MHC molecules) acquired by the virus as it buds from the human cell membrane.

Life Cycle of HIV

HIV can only replicate inside human cells, therefore HIV life cycle can be divided into seven steps: entry to the cell, reverse transcription and integration, transcription and translation, and assembly and maturation (Figure 2). Life cycle of HIV-1 virus begins with binding of the virus with the CD4+ receptors present on the host cells (Dalgleish et al., 1984; Klatzmann et al., 1984). CD4+ receptors are present on the surface of many lymphocytes, which are critical part of body's immune system. In addition to binding to CD4+ receptor, HIV virus also binds to either a CCR5 or CXCR4 co-receptor protein to get entry into the host cell. The virus then fuses with the host cell and releases its genetic material and RNA into host cells. An enzyme called reverse transcriptase then converts the single stranded HIV RNA to double stranded HIV DNA. Reverse transcriptase inhibitors are an important class of drug that inhibits the conversion of viral RNA to DNA.

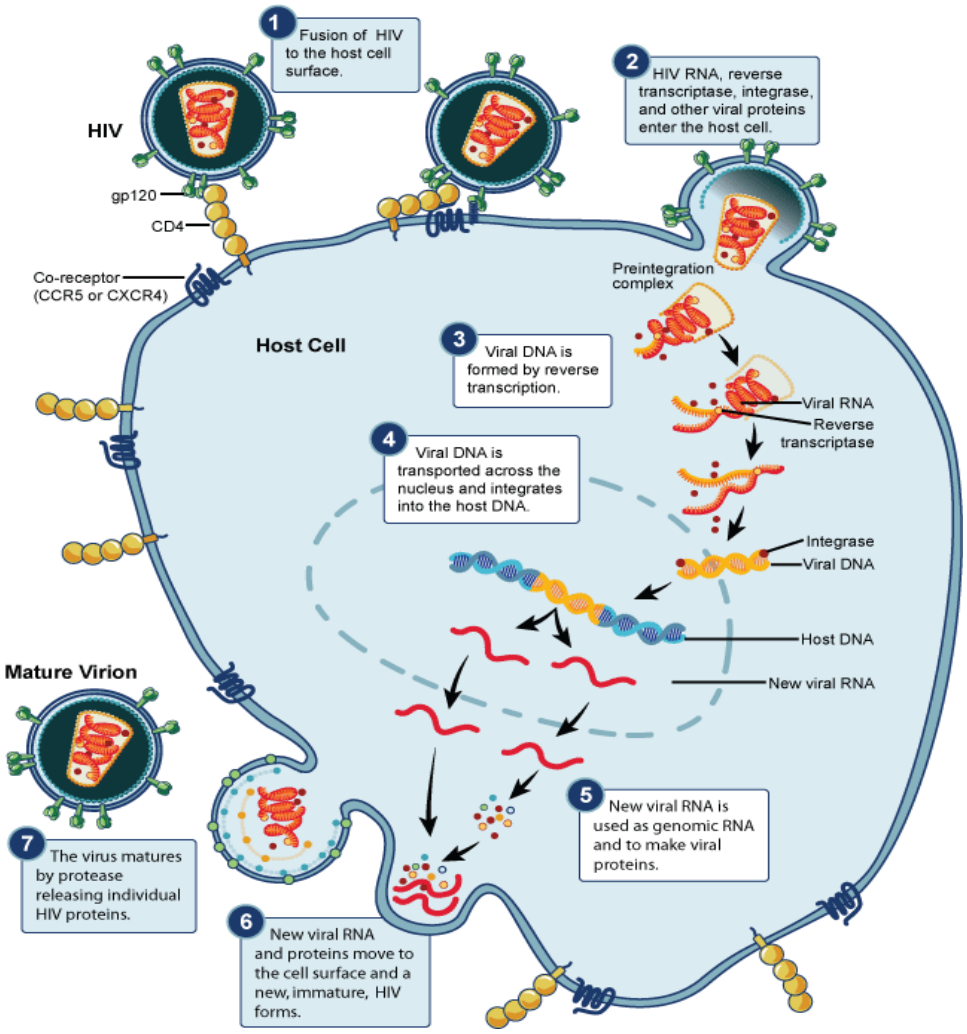

Figure 2. Stages of HIV life cycle. Adapted from NIAID

Reverse transcriptase inhibitors were the first HIV medications, and are still a critical part of treating patients with HIV. Reverse transcriptase inhibitors can be divided into two classes, nucleoside and non-nucleoside analogues, based on the structure and the mechanism by which they inhibit viral reverse transcriptase. Once the genetic material of HIV virus is converted to DNA it enters the host cell nucleus and an enzyme called integrase facilitates the integration of viral DNA into the host cell DNA. This integrated HIV DNA is now known as provirus. This provirus may remain in latent state for many years producing few or no new copies of HIV. This ability to persist in certain latently infected cells is the major barrier for the eradication or cure of HIV. Activation of the host cell results in the transcription of viral DNA into messenger RNA (mRNA) with the help of an enzyme called RNA polymerase. This new viral mRNA forms the genetic material of the next generation of the virus. The viral RNA and viral proteins assemble at the cell membrane into a new virus. Amongst the viral proteins is HIV protease, which is require to process HIV proteins into their functional form. HIV-1 PIs, one of the most potent drugs for HIV-1 treatment acts by blocking this critical maturation step of the virus. Following assembly at the cell surface, the virus then buds forth from the cell, and is released to infect another cell. Unless treated, the virus spreads throughout the body and results in the destruction of the body's immune system. The destruction of immune system leads to many opportunistic infections and further to many life-threatening complications. One important goal is to design new drug moieties which can interfere with HIV life cycle in its early stages or to develop drug moieties, which can prevent the entry of virus particles into the host cell.

HIV Associated Dementia

AIDS dementia complex (ADC) or HIV-associated dementia (HAD) develops in about 20 per cent of HIV infected patients who progress to AIDS. The actual underlying mechanisms for the pathogenesis of ADC in adults and progressive encephalopathy in infants and children still remain unclear. In approximately 30 per cent of immunosuppressed HIV infected patients, the entry of virus into the central nervous system (CNS) initiates a syndrome which is characterized by progressive motor degeneration and behavioral abnormalities (Price et al., 1988). Although the virus infects the brain at an early stage of HIV infection, neurological complications including dementia, sensory neuropathy and myelopathy tend to occur at an advanced stage of AIDS. Cells primarily harboring the virus in brain are the microglial cells and macrophages. Macrophage activation within the CNS and peripheral nervous system (PNS) appears to be a critical factor in the development of HAD and sensory neuropathies (Kamerman et al.). Brain cells, other than macrophages also get infected with HIV-1. Non-productive infection of astrocytes with the expression of *nef* and *rev* has been reported with HIV-related encephalopathy in infants (Tornatore et al., 1994; Ranki et al., 1995). Observed neuronal dysfunction and loss of neurons in advanced HAD (20-40% in the frontal lobe) may be due to indirect factors such as neurotoxins and cytokines. Astrocytosis induced during brain infection may also be a critical event in HAD, as dopamine system may be damaged, which may have profound effects in clinical manifestation of HAD.

Current HIV Treatment Options

The knowledge about the life cycle of HIV-1 and the necessity to combat the virus has led to the development of many anti-HIV agents. Currently, 25 drugs belonging to six

different categories had been approved by the US FDA for the treatment of HIV (Flexner, 2007; Greene et al., 2008). As depicted in Figure 2, the life cycle of HIV-1 includes several steps starting from viral entry and finishing with maturation of released viral particles. Accordingly, drugs were designed to inhibit viral entry (by inhibiting the chemokine CCR5 coreceptor), to inhibit viral fusion (by inhibiting TM/gp41), to inhibit reverse transcription of viral RNA into DNA (by inhibiting RT), to inhibit integration of viral DNA into host genome (by inhibiting IN) and/or to inhibit maturation of released viral particles (by inhibiting PR) Table.1 summarizes the current anti-HIV drugs belonging to different classes approved by the USFDA.

Protease Inhibitors (PIs)

Protease (PR) plays a prominent role in the maturation of released virions. It is a 99-residue protein belonging to the class of aspartic acid proteases, functioning as a catalytic dimer (Pearl and Taylor, 1987; Oroszlan and Luftig, 1990; Wlodawer and Erickson, 1993; Louis et al., 2007). PR helps in processing Gag-Pol and Pol polyproteins into mature functional and structural proteins. In the absence of PR, the nascent virions are non-infectious and hence the spreading of HIV-1 is halted. Thus, PR seems to be an indispensable target in the treatment of HIV-1. The presence of efflux transporters and extensive plasma protein binding (90–99%) of PIs lowers the effective concentration of drugs in the viral sanctuary sites (Nath and Sacktor, 2006; Kwara et al., 2008; Pokorna et al., 2009). In order to maximize drug concentration, a low dose of RTV (pharmacokinetic enhancer / booster) is administered. This combination significantly decreased HIV progression due to enhancement of pharmacokinetic properties of coadministered drug.

Table 1. Summary of drugs approved by the USFDA for HIV treatment.

Drug Category	Generic name	Brand Name®
CCR5 Antagonists (entry inhibitors)	Maraviroc	Selzentry
Fusion Inhibitors	Enfuvirtide	Fuzeon
Non-nucleoside Reverse Transcriptase Inhibitors (NNRTIs)	Nevirapine	Viramune
	Delavirdine	Rescriptor
	Efavirenz	Sustiva
	Etravirine	Intelence
	Rilpivirine	Edurant
Nucleoside Reverse Transcriptase Inhibitors (NRTIs)	Zidovudine	Retrovir
	Didanosine	Videx
	Stavudine	Zerit
	Lamivudine	Epivir
	Abacavir	Ziagen
	Tenofovir	Viread
	Lamivudine	Epivir
Integrase Inhibitors	Raltegravir	Isentress
Protease Inhibitors	Saquinavir (SQV)	Invirase
	Ritonavir (RTV)	Norvir
	Indinavir (IDV)	Crixivan
	Nelfinavir (NFV)	Viracept
	Amprenavir (APV)	Agenerase
	Fosamprenavir (FPV)	Lexiva
	Lopinavir (LPV)	Kaletra (in combination with RTV)
	Atazanavir (ATV)	Reyataz
	Tipranavir (TPV)	Aptivus
	Darunavir (DPV)	Prezista

This significant finding was first reported by Kempf et al, where they have shown that RTV potently inhibited the cytochrome P450 (CYP)-mediated metabolism of SQV, IDV, NFV and APV (Kempf et al., 1997). This reported by Kempf et al, where they have shown that RTV potently inhibited the cytochrome P450 (CYP)-mediated metabolism of SQV, IDV, NFV and APV (Kempf et al., 1997). This finding was considered as a milestone in the development of HIV therapeutics and currently all the marketed PIs, expect for NFV, are co-administered with RTV. Currently marketed PIs are listed in Table 1.

The introduction of highly active anti-retroviral therapy (HAART), *i.e.*, combinations of PIs with nucleoside reverse transcriptase inhibitors (NRTIs) or non-nucleoside reverse transcriptase inhibitor (NNRTIs) has resulted in suppression of HIV viral replication and progression. However, this regimen encountered with many problems including: compliance, resistance, interactions and adverse effects. Compliance in HAART is frequently observed due to higher pill burden. The development of antiviral drug resistance due to high mutation rate and lack of proof reading capacity of viral RT also leads to treatment failure (Doyon et al., 1996; Mammano et al., 1998). Also, complications arise due to metabolism of PIs and NNRTIs *via* the same pathway (CYP-P450) (de Maat et al., 2003). The long term adverse effects of antiretrovirals such as visceral fat accumulation (within the abdomen, on the upper back and around the neck), metabolic disorders (hyperlipidemia, hypertriglyceridemia and insulin resistance), hepatotoxicity and increased cardiovascular risks still remains a major problem (Nolan et al., 2005; Shibuyama et al., 2006; Wohl et al., 2006). Taken together, although the current therapeutics are successful in reducing viral load, there are several disadvantages associated with them. Novel PIs with better pharmacokinetic properties, simple dosage regimen, little/no resistance and side effects are desirable at this point.

HAART has proven successful in suppressing systemic viral burden, but brain has proven to be a sanctuary site where the virus can reside relatively unchecked by therapeutic intervention (Thomas, 2004). The major obstacle in the delivery of PIs to the brain is the blood brain barrier. In addition to the tight cellular junctions at BBB the presence of efflux transporters (P-gp, MRP) are the primary factors limiting the entry of PIs into the brain. All protease inhibitors are substrates of ATP dependent efflux pumps (P-gp, MRP) which actively extrude PIs from the brain. Hence, brain serves as a sanctuary site for HIV-1 and potentially endanger the efficacy of long term therapy (Crowe and Sonza, 2000; Yeni et al., 2004). Also, complete eradication of HIV-1 may not be possible due to latently infected cells in the CNS which can lead to drug resistance and finally treatment failure. Thus, the presence of efflux proteins and metabolizing enzymes may result low oral bioavailability and sub-optimal drug concentrations, particularly in sanctuary sites, resulting in consumption of a large dose of PIs to maintain adequate drug concentration in the brain tissue leading to significant toxicity. Thus, in HIV pharmacotherapy, adequate drug concentrations in the brain are needed for anti-viral efficacy. For optimal brain delivery of the HIV protease inhibitors, circumvention of the membrane specific efflux transporters is essential.

Brain Drug Delivery

Several therapeutic agents are unsuccessful in treating CNS disorders due to ineffective delivery to brain. Drug delivery to brain poses a great challenge even though brain is highly perfused with blood flow. This is due to the physiological barriers which separate brain tissue from blood circulation and control transport of several compounds including nutrients. Barriers attributing to low brain bioavailability of drugs are BBB and BCSFB. Important functions of these barriers are to impede free diffusion between brain

fluids and blood, and to provide transport processes for essential nutrients, ions and metabolic waste products (Redzic, 2011).

Treatment of neurodegenerative diseases, brain cancers and infections require therapeutic drug concentrations in the brain. Drug delivery to central nervous system (CNS) poses several challenges for researchers in drug development because of limited access for therapeutic agents. Low brain absorption of therapeutic agents is mainly attributed to two physiological barriers, blood-brain barrier (BBB) and blood-cerebrospinal fluid barrier (BCSFB). BBB is formed by polarized endothelial cells of brain microvasculature and several other cell populations such as astrocytes and pericytes which support endothelial cells collectively in restricting entry and exit of nutrients and xenobiotics. The BCSFB is located at choroid plexus and formed by epithelial cells which are connected by tight junctions. Stroma and fenestrated blood vessels are present underneath the epithelial cells. These blood vessels lack tight junctions but tight junctions between epithelial cells restrict the entry of drugs into cerebrospinal fluid (CSF) (Scherrmann, 2002). Even though brain is highly vascularized, these barriers separate brain from general blood supply. BBB and BCSFB play an important role in controlling entry of nutrient and therapeutic agents into brain, thus maintain brain homeostasis. Other than cellular tight junctions, various efflux proteins such as P-glycoprotein (P-gp), multidrug resistance proteins (MRPs) and breast cancer resistant protein (BCRP) are highly expressed on BBB and contribute significantly to limit brain absorption of drugs.

Blood-Brain Barrier (BBB)

Brain is protected from foreign organisms and toxic substances by BBB. It is made up of three layers, inner endothelial cell layer which forms wall of brain capillaries, basement

membrane and feet processes of astrocytes and pericytes. Figure 3 is the schematic representation of BBB and other components of vascular unit and their arrangement. Brain capillaries have a complex morphology which provides special characteristics to endothelial cell layer with respect to diffusion of solutes. Brain endothelial cells (BECs) are interconnected by tight junctions (TJs) and occlude paracellular spaces. Moreover BECs exhibit minimal pinocytotic activity. In addition these BECs are secluded by astrocytic end feet and pericytes on brain side which further restrict permeability of various drugs. Overall BBB exhibits very high transendothelial electrical resistance (TEER) values, around 1500 Ωcm^2, which is very high compared to other tissues which ranges from 3-33 Ωcm^2 (Crone and Christensen, 1981). Thus BBB provides very high resistance to permeability of solutes, drugs and xenobiotics. As mentioned earlier other than BECs, other cell populations which attribute to barrier properties of BBB include astrocytes and pericytes. Both astrocytes and pericytes help in differentiation and maintenance of BBB function. Astrocytes account for 60% of total non-neuronal cell population which provide biochemical support for endothelial cells, transport essential nutrients to nervous tissue and maintain extracellular ion balance. They also play a crucial role in repair and scarring processes following injuries and inflammation (Sarafian et al.). Pericytes secrete growth factors which are important for maturation and remodeling of vascular system. They are involved in transport across BBB and regulation of vascular permeability (Allt and Lawrenson, 2001).

Blood-Cerebrospinal Fluid Barrier (BCSFB)

The BCSFB is another barrier which restricts entry of systemically administered drugs into CNS. BCSFB functions in conjunction with BBB and meninges to safeguard brain. CSF is secreted from choroid plexus epithelium (CPE) and circulates through

ventricles around brain and spinal cord (Engelhardt and Sorokin, 2009). Choroid plexus (CP) are villous structures floating in cerebrospinal fluid and attached to ventricular ependyma. The ependyma is continuous with the epithelial layer of CP composed of single layer of cells. These CPE cells constitute BCSFB (Abbott et al.).

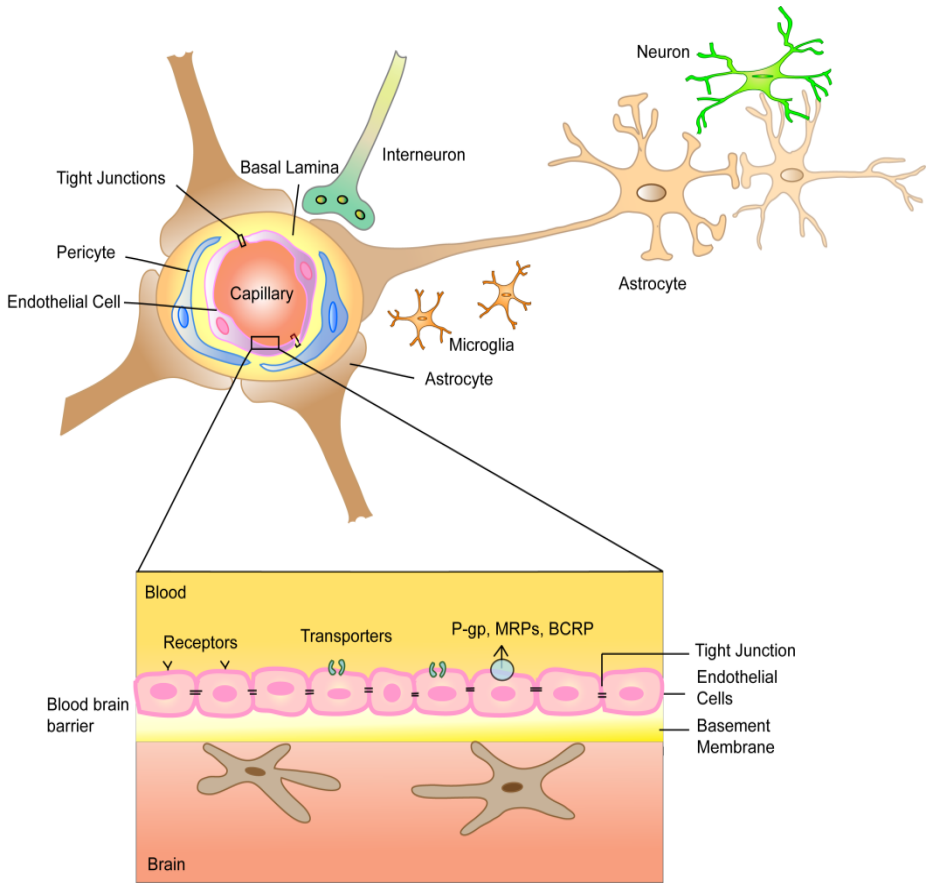

Figure 3. Schematic representation of the blood–brain barrier (BBB)

Tight junctions are present in CP epithelium restricting solute transport. Tight junctions on BCSFB are distinct and exhibit less restriction to diffusion of solutes in comparison with BBB (Johanson et al., 2005). In addition to TJs, CP epithelium is fortified with organic acid transporter system which is responsible for driving organic acids in CSF to blood. Hence variety of therapeutic organic acids, such as zidovudine, methotrexate and penicillin, cannot gain access to brain parenchyma. Arachnoid epithelium serves as another barrier for transport of drugs in to the brain. Arachnoid is one of the three meninges, underlying dura, covers entire CNS as a protective sheath and separates extracellular fluids of CNS from rest of the body (Abbott et al.; Abbott, 2002). However, low surface area and avascular nature of arachnoid makes it less significant interface for solute exchange from blood to CNS (Abbott, 2005). All these barriers form a combination of physical, transport and metabolic barriers resulting in restricted environment for solute entry into brain. Various approaches have been attempted for improving brain permeation of drugs. Some of the common approaches have been discussed in the following sections.

ABC Efflux Transporters

The ABC super family is one of the 16 subfamilies that are driven by ATP. There are seven subfamilies classified as ABC transporters (ABCA – ABCG). This family includes clinically significant MDR pumps, P-gp and MRP, all of which confer resistance to anticancer drugs. Remaining transporters are mainly expressed in a number of pathogenic fungi and parasitic protozoa, where they confer resistance to antimicrobial drugs (Legare et al., 2001). Although, most ABC proteins were discovered as drug transporters, these proteins frequently translocate a wide range of substrates, including dyes, ionophoric peptides, lipids and steroids. Members of the ABC family share extensive homology and domain

organization. The general structure of ABC transporters is composed of two homologous halves, each containing six putative transmembrane domains (TMDs) and an ATP-binding domain located towards the cytoplasm. There are a number of exceptions to this structural arrangement. For example, MRP1 – 3 and MRP6 – 7 have a third membrane spanning domain (MSD) with five TMDs (Bakos et al., 1996; Hipfner et al., 1997). BCRP, in comparison, is a half transporter (6) and is believed to dimerize in order for it to participate in transport activity that result in substrate tropism corresponding to different dimerization partners. Both nucleotide binding sites are necessary for the efflux of substrates (Urbatsch et al., 1995).

P-glycoprotein (MDR1)

P-glycoprotein (P-gp) is a 170–kDa phosphorylated and glycosylated plasma membrane protein belonging to the ABC super family of transport proteins encoded by MDR. P-gp was discovered by Juliano and Ling in 1970s and is the most widely studied efflux transporter till date (Juliano and Ling, 1976). This ABC transporter has been proposed to act as a "hydrophobic vacuum cleaner" because of its ability to remove lipids as well as drug molecules from intracellular environment. It is the primary active drug efflux pump which binds and translocates molecules against a concentration gradient at an expense of ATP hydrolysis (Katragadda et al., 2005).

The most striking property of P-gp is its broad substrate specificity. Substrates of P-gp include anticancer agent, H2-receptor antagonists, HIV protease inhibitors, antibiotics, anti-hypertensives, steroids, linear and cyclic peptides, calcium channel blockers, corticoids and immunosuppressive agents (Schinkel and Jonker, 2003). P-gp plays a major role in drug disposition by limiting the absorption and accumulation of xenobiotics and conferring

resistance to a diverse range of compounds. P-gp expression has been documented in a wide range of normal tissues like kidney, adrenal gland, liver, small intestine, colon, lung, prostate, skin, spleen, placenta, heart, skeletal muscle, stomach, blood brain barrier (BBB), and ovary (Ambudkar et al., 2003). P-gp is predominantly expressed on apical membrane of lower GI tract, brain, testis and kidney. Its constitutive expression in wide range of tissues suggests its role as a barrier to xenobiotic entry into the cells (Thiebaut et al., 1987; Cordon-Cardo et al., 1989).

P-gp on Intestinal Epithelium

In humans, P-gp is highly expressed on the apical surface of superficial columnar epithelial cells of ileum and colon, and expression gradually decreases proximally into the jejunum, duodenum, and stomach (Ho et al., 2003). It is extensively localized on the villus tip of enterocytes which is the main site for absorption of orally administered drugs. Involvement of P-gp in drug absorption was first demonstrated *in vitro* with Caco-2 cells (Hunter et al., 1993). Later, role of P-gp in pharmacological aspects was demonstrated in *mdr1a(-/-)* knockout mice (Sparreboom et al., 1997). The results obtained in this study demonstrated that paclitaxel following oral administration in *mdr1a*(-/-) knockout mice exhibited a six fold increase area under curve (AUC). Similar results were obtained with HIV protease inhibitors indinavir, nelfinavir and saquinavir (Kim et al., 1998). Intestinal absorption of vinblastine and acebutolol increased 2.2- and 2.6-fold, respectively, when co-administered with cyclosporine, which is a known P-gp inhibitor (Terao et al., 1996). These results clearly indicate the role of P-gp in oral absorption of various therapeutic agents.

P-gp at the Blood–Brain Barrier

High level of P-gp is expressed on luminal side of brain endothelial cells (i.e., facing blood side) (Cordon-Cardo et al., 1989). Therapeutic agents which are substrates of P-gp trying to enter the endothelial cells from the blood side are effluxed out immediately, blocking their entry into brain parenchymal cells. HIV protease inhibitors represent one of the most potent therapeutic classes developed so far for the treatment of HIV. However, being the substrates of P-gp, these compounds are poorly transported across BBB. As a result, success rate in treating HIV-related dementia is on the lower side (Golden and Pollack, 2003). Treatment failure in many CNS diseases, including Alzheimer's disease, multiple sclerosis and Parkinson's is primarily due to low brain uptake of therapeutic agents (Vogelgesang et al., 2004). Several studies have shown that the P-gp expression on the BBB restricts the entry of HIV-1 protease inhibitors into the brain (Edwards et al., 2002; Park and Sinko, 2005). Recent studies in multidrug resistant-1a (MDR-1a) knockout mice demonstrated increased levels of protease inhibitors in mouse brain (Washington et al., 2000; Salama et al., 2005). Thus, P-gp expression plays a major role in the disposition of the drugs across the BBB. Better drug delivery strategies bypassing P-gp mediated efflux and improving brain concentration of PIs, are essential to improve drug efficacy and lower treatment failure. Several strategies have been developed to inhibit or bypass P-gp mediated efflux. Various P-gp inhibitors are often co-administered with P-gp substrates (therapeutic agents) resulting in higher bioavailability (Tolcher et al., 1996). However, systemic administration of P-gp inhibitors is limited by their toxicity resulting from high doses required to inhibit P-gp in-vivo. Although various approaches have been explored to

overcome P-gp mediated drug efflux, P-gp still remains a major barrier to oral and CNS drug absorption.

Multidrug Resistance Associated Proteins (MRPs)

RP family contains at least nine members: MRP-1 and its eight homologs, known as MRP2-9.These membrane proteins mediate the ATP-dependent unidirectional efflux of glutathione, glucuronate, or sulfate conjugates of lipophilic drugs. In addition to many anionic conjugates, a number of unconjugated amphiphilic anions can serve as substrates for MRPs. Recent reports have identified MRP in the brain capillary endothelium and human brain microvessels. Of the nine MRP isoforms currently identified, a recent report identified MRP homologues MRP1, MRP4, MRP5, and MRP6 in both primary cultured bovine brain endothelial cells and capillary-enriched bovine brain homogenates. MRP7 has been identified in brain homogenate, but its exact localization has not been determined. MRP-2 has been identified in the apical (luminal) membrane of rat brain capillary endothelium (Miller et al., 2000). Expression of various isoforms of MRP and other efflux proteins is shown in Figure 4.

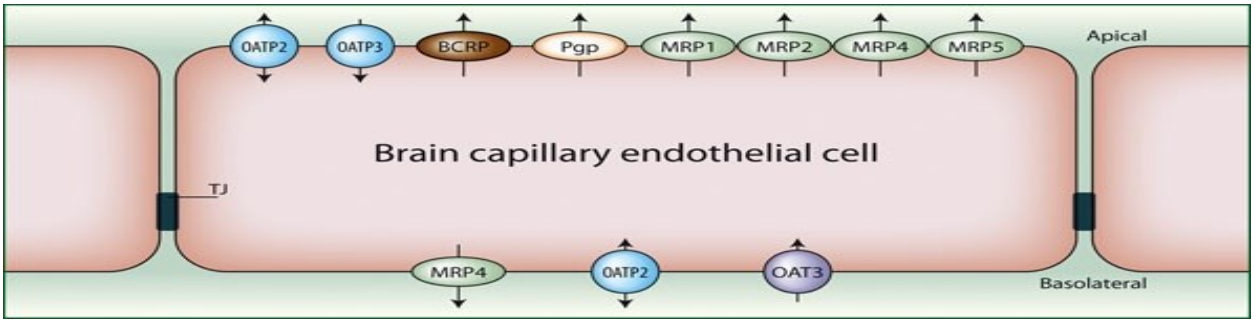

Figure 4. Vairous efflux proteins expressed on brain capillary endothelial cells. Reproduced with permission (W Lösche et al., 2005)

Recent studies revealed that MRPs play a significant role *in-vivo* in the absorption of saquinavir across BBB (Park and Sinko, 2005). However various literature reports suggest that APV is not a very good substrate of MRP1 and has little interaction with MRPs (van der Sandt et al., 2001).

Plasma Protein Binding

The pharmacokinetic and pharmacodynamic properties of drugs are largely a function of the reversible binding of drugs to plasma or serum proteins. Plasma proteins include albumin, α_1-acid glycoprotein (AAG), lipoproteins and α, β and γ globulins (Huang and Ung; Kremer et al., 1988). Generally, the unbound drug is available for diffusion or transport across cell membranes, and for interaction with pharmacological targets (e.g. receptor, ion channel, transporter, and enzyme) (Rowland, 1984). Plasma protein binding of a drug also influences its distribution, elimination, and drug action. Highly plasma protein bound drugs are confined to the vascular space, resulting in low volume of distribution. In contrast, drugs that remain largely unbound in plasma are generally available for distribution to other organs including brain. Higher plasma protein binding of drugs is associated with low efficacy. Most HIV-protease inhibitors (PIs) bind to AAG. When tested in-vitro against wild type HIV, AAG is responsible for the decrease in activity of the current PIs exhibiting high plasma protein binding. Most PIs are highly bound to plasma proteins, nelfinavir (99% bound), lopinavir (99%), saquinavir (98%), ritonavir (98%), amprenavir (90%) and indinavir (60%) (Anderson et al., 2000; Boffito et al., 2003; Barrail et al., 2006). Determination of both total and unbound plasma drug concentrations is, therefore, necessary to assess drug availability and anti-HIV efficacy. Furthermore, an increase in unbound drug fraction may increase drug availability at the target site.

Metabolizing Enzymes

Cytochrome P450 (CYP) is the most prevalent drug metabolizing enzymes and is present predominantly in the intestine and liver. CYP3A4 is the most abundant form in the CYP-family (Kolars et al., 1992). CYP3A group represents the major drug-metabolizing enzyme and accounts for approximately 30% of hepatic CYP and more than 70% of intestinal CYP activity. Moreover, CYP3A is estimated to metabolize between 50% and 70% of currently administered drugs (Watkins, 1997). CYP3A4 enzyme is present in the liver and enterocytes (Guengerich et al., 1986). A significant amount of CYP3A is expressed in the enterocytes to metabolize xenobiotics during their transit across intestinal epithelium. According to recent reports, CYP3A5 is also polymorphically expressed in small intestine and contributes significantly to drug metabolism (Shen et al., 1997). Although hepatic metabolism can make a major contribution to systemic drug elimination, a combination of hepatic and intestinal drug metabolism appears to have a major influence on pre-systemic or first-pass drug loss. CYP3A4 has wide substrate specificity. It can metabolize various structurally diverse therapeutic agents. CYP3A4 and P-gp have a considerable overlap in substrate specificity and tissue distribution. Which may further reduces the drug concentration in blood affecting drug bioavailability and therapeutic efficacy. For drugs which are common substrates of P-gp and CYP3A4, such as HIV PIs, P-gp efflux increases drug exposure to CYP3A4 in the intestinal lumen which leads to more extensive metabolism by CYP3A4 (Watkins, 1997; Benet and Cummins, 2001). The metabolism of xenobiotics via phase I functionalization and phase II conjugation converts drugs to water soluble metabolites which can be excreted from the body and reduce the potential toxicity. Although the ultimate elimination of the parent drug and its metabolites from the body is necessary, the

extensive early-stage metabolic processing of orally administrated drugs is undesirable since the drug concentration in system circulation and targeted tissues cannot reach the therapeutic level.

Amprenavir undergoes extensive first pass metabolism by CYP3A4. Ketoconazole (selective CYP3A4 inhibitor) inhibited the formation of major amprenavir metabolites. 3.7 μM of ritonavir completely inhibited the biotransformation of amprenavir by human liver microsomes (Treluyer et al., 2003). Metabolism of ritonavir, on the other hand, is caused by CYP3A4 and CYP2D6. It significantly inhibits the metabolism of CYP3A4 substrates like nifedipine and CYP2D6 substrates like dextromethorphan, when administered in combination (Hsu et al., 1998). In addition to oxidative metabolism, conjugation reactions may play an important role in detoxification of xenobiotics from the small intestine. Specific molecules are effluxed into intestinal lumen after being conjugated with a glucuronide or sulfate moiety within enterocytes. Transport systems responsible for the cellular efflux of the conjugated metabolites and organic anions have been characterized recently (Leslie et al., 2001).

Strategies to Overcome P-gp and MRP Mediated Efflux

Developing drug strategies to circumvent P-gp and MRP mediated efflux is an unmet need in drug delivery. Designing drug molecules with no interaction with these efflux pumps is limited due to the fact that modification of drug molecule can result in loss of potency and biological stability. Another challenge for designing effective drug molecules is that till date 3D crystal structure of P-gp and MRP is not elucidated and poorly understood. However, some of the strategies have been adopted that have resulted in partial of full circumvention of

P-gp and MRP mediated efflux. Some of those strategies are discussed in the following paragraphs.

Various approaches have been studied by researchers to circumvent P-gp mediated efflux and first –pass metabolism there by to improve oral bioavailability of poorly absorbed drugs. One of the approaches is co-administration of P-gp and/or CYP3A4 modulators or inhibitors to inhibit the function of P-gp and/or CYP3A4 (Eagling et al., 1999; Patel and Mitra, 2001). Some of the inhibitors/modulators are laniquidar (R101933), ocl44-093 (ONT-093), zosuquidar (LY335979), elacridar (GF-120918) and tariquidar (XR9576). Although this approach result in higher bioavailability, success of this approach is hindered by side effects due to alteration of normal physiological roles of these proteins and increasing the cytotoxicity due to the high doses required to inhibit the functions of these proteins. Synthesis of lipophilic ester prodrugs to enhance transport across epithelial cells constitutes one such strategy (Chang et al., 1987). Although this approach has been successful to some extent, lowered aqueous solubility of these modified compounds often proves to be a challenge in the development of orally bioavailable dosage forms. Other strategies to enhance drug absorption from the intestine include the formulation of nanospheres and microspheres (Hodges et al., 1995; Thomas et al., 1996). Application of polymers which transiently perturb the tight junctions between epithelial cells is another approach (Kotze et al., 1998; Dorkoosh et al., 2004). However, to date, these approaches have met with limited success. Membrane fluidizing agents and penetration enhancers have also been investigated (Shao et al., 1994). However, cellular toxicities have, for the most part, limited their use. Prodrugs targeted towards membrane transporters expressed on epithelial cells are perhaps the most exciting of all the current drug delivery strategies (Anand et al., 2002).

Pro-drug (PD) and Pro-Pro-Drug (PPD) Approach

The unfavorable physicochemical properties such as low aqueous solubility and physiological properties such as substrate for efflux proteins, high CYP3A4 metabolism and high protein biding attribute to low bioavailability of PIs (Watkins, 1997; Wacher et al., 1998). The presence of efflux transporter (P-gp, MRP) imposes a major obstacle for the entry of PIs across the intestinal epithelium and BBB. Co-administration of several agents that are P-gp substrates/inhibitors are often employed to improve permeability characteristics of these agents. However, lack of specificity and high concentrations required to inhibit efflux process often results in unacceptable toxicities and limits their usefulness. This co-administration may also affect the physiological function of efflux proteins and may lead to related toxicities. Potentially promising approach to improve oral bioavailability and brain permeation of PIs is by circumventing efflux transporters at both intestinal epithelium and BBB. Prodrug seems a viable approach for improving brain bioavailability of PIs. We propose to develop amino acid and di-peptide conjugated prodrugs of HIV PIs and we hypothesize that the resultant prodrugs will generate enhanced brain bioavailability. The ligand coupled PIs will permeate brain capillary endothelial cells efficiently by binding and translocating via influx membrane transporters and bypass membrane efflux pumps like P-gp and MRPs. The approach is depicted in Figure 5, where a drug, which is a substrate for an efflux transporter, is converted to a substrate of a targeted influx transporter (amino acid, peptide and vitamin) by coupling to a pro moiety. The resultant prodrug is not recognized by the efflux transporters and is ferried across the membrane. We named di-peptide prodrug as pro-pro-drug (PPD), each “pro” representing an amino acid promoiety. In the pro-pro-drug strategy, following oral administration of pro-pro-drug (di-peptide conjugated drug) may

evade the efflux at intestinal epithelium and circumvent the efflux. By circumvention of efflux, pro-pro-drug exposure to metabolizing enzymes in the intestinal lumen will be minimized. Once the di-peptide prodrug reaches systemic circulation, PPD may undergo enzymatic degradation and generate PD and some amount of drug (Figure.6). Systemically generated PD can be identified by nutrient transporters expressed on BBB and circumvent the efflux. This may lead to enhanced permeation across BBB. Major advantage of this PPD approach is to be able to target two nutrient transporters expressed on two different barriers. Design of PPDs targeting such active transport processes represents paradigm shift from the traditional prodrug approach. The nutrient transporters described in the following sections will be targeted for this purpose.

Nutrient Transported to be Targeted

Various nutrient transporters apart from efflux transporters are expressed on epithelial (intestinal) and endothelial (brain vascular endothelial) cells these influx transporters are responsible for active transport of various nutrients such as amino acids, peptides and vitamins. Intestinal peptide transporter and amino acid transporters are targeted in this project. Expression pattern of these transporters and functionality are discussed in the following section.

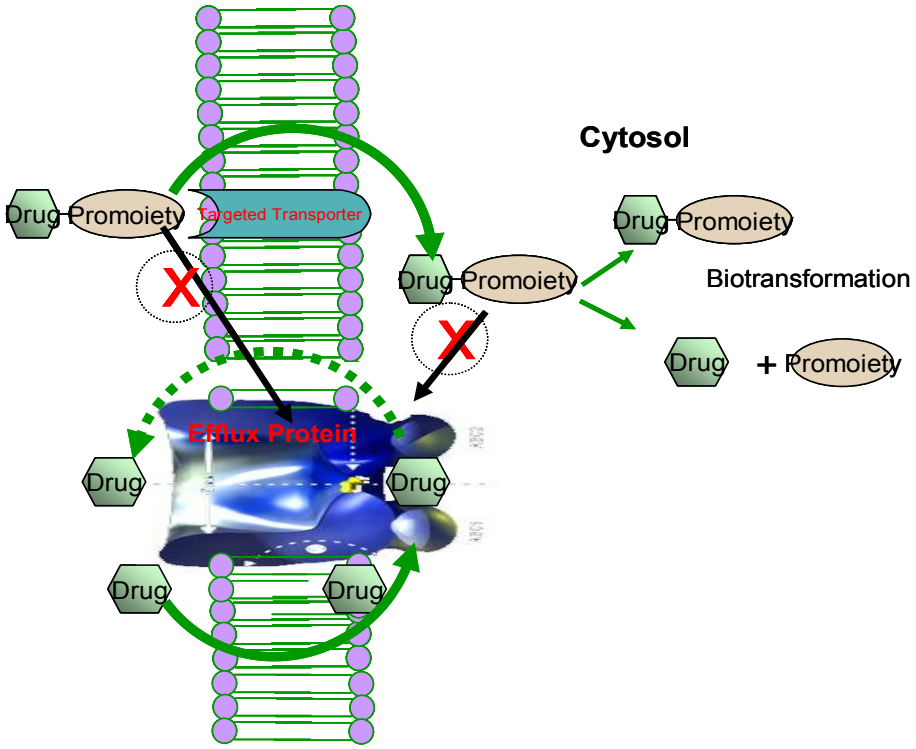

Figure 5. Circumvention of membrane efflux by prodrug derivatization targeting influx transporters

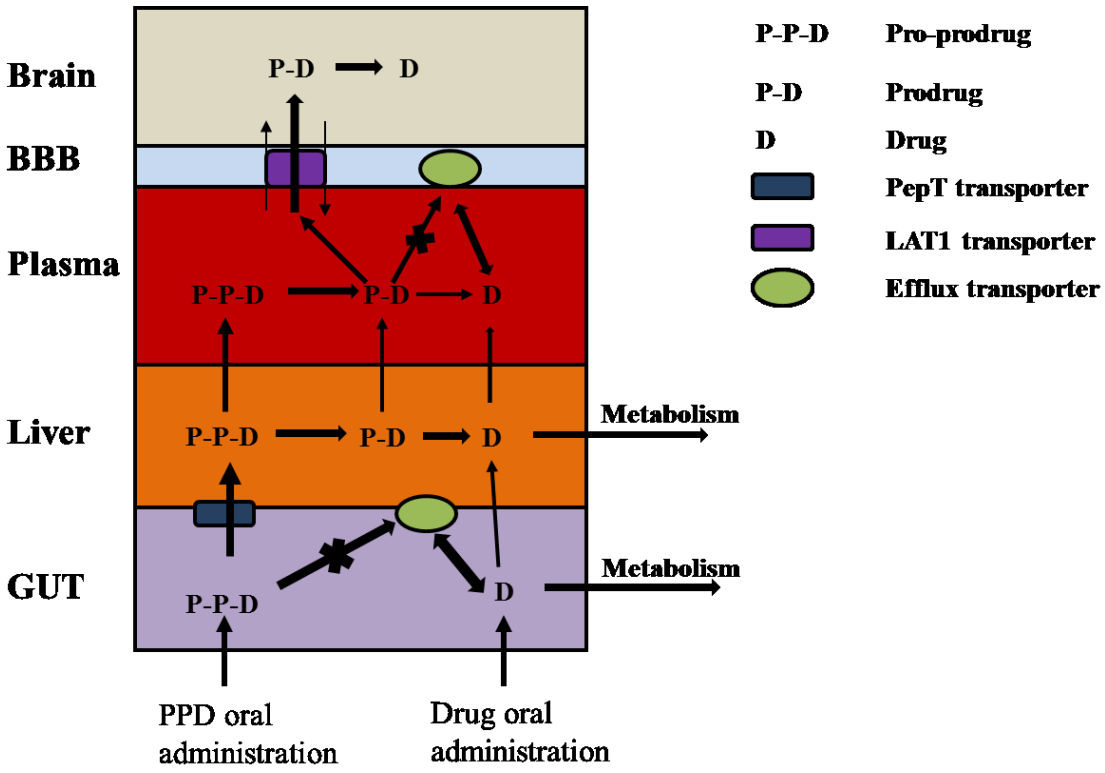

Figure 6. Hypothetical mechanisms involved in pro-pro-drug approach to improve oral and brain bioavailability

Peptide Transporter System

Peptide transporters are the most versatile proteins available for drug transport. Belonging to *peptide transporter* (PTR) family, it serves as an integral membrane protein especially in the intestinal membrane to accept various di- and tri-peptides as substrates, thereby acting as both nutrient and drug transporter (Terada and Inui, 2004; Rubio-Aliaga and Daniel, 2008). Peptide transporter or PEPT as it is commonly referred to, is a solute carrier protein and is classified into two broad classes: PEPT1 (SLC15A1) and PEPT2 (SLC15A2), differing in their tissue localization, substrate specificity, affinity as well as transporter capacity (Rubio-Aliaga and Daniel, 2002). Both PEPT1 and PEPT2 are highly expressed in various epithelia however, PEPT1 is involved in translocation of di- and tri-peptides and peptidomimetic analogues in the small intestine whereas PEPT2 is primarily localized on the renal tubular epithelium (Rubio-Aliaga and Daniel, 2008). These transporters are also found in other tissues such as brain, lungs, bile duct and pancreas (Rubio-Aliaga and Daniel, 2002). In addition to peptide transporters, PTR family also consists of two peptide histidine transporters, namely PHT1 and PHT2, involved in specifically translocating histidine and a few selected di- and tri-peptides (Rubio-Aliaga and Daniel, 2008). Not much work has been reported on PHTs; however, PEPT has gained a lot of attention recently as a drug delivery target. Intestinal PEPT not only provides uptake of di- and tri-peptides, but also functions as a possible vehicle site for the delivery of pharmacologically active peptidomimetics i.e. β-lactam antibiotics, ACE inhibitors, bestatin, thrombin inhibitors and rennin inhibitors (Yang et al., 1999; Rubio-Aliaga and Daniel, 2008). Both PEPT1 and PEPT2 are considered an ideal target for drug delivery because of its high capacity and affinity towards di- and tri-peptide moieties. Therefore, if a drug exhibits low

oral bioavailability such as acyclovir and ganciclovir, conjugation with a moiety which is easily recognizable by the transporter makes the adduct a substrate for the transporter. This prodrug, in other words, can be defined as a derivatized drug which is a substrate for the influx transporter, in this case PEPT. Thus derivatization of the drug molecule allows the newly formed substrate to be ferried across the lipid bilayer membrane. Physico-chemical property such as water solubility is also improved based on the amino acid chosen for derivatizing the drug. Once the di-peptide prodrug is translocated across the intestinal lipid bilayer utilizing the PEPT, it is broken down into amino acid prodrug by peptidases. The newly generated amino acid intermediate then reaches the target tissue such as brain utilizing the amino acid transporter for permeation. Since peptide transporters are robust and high capacity transporters, their utilization to ferry the prodrugs of PIs across the physiological barriers may prove to be a highly effective strategy (Yang et al., 2001).

Amino Acid Transport Systems

Amino acid transporters are present in all mammalian cells and translocate nutrient amino acids. Final steps in biotransformation of proteins result in the formation of di/tri peptides and amino acids, while translocation of these di/tri peptides involves a peptide transporter (PepT1), absorption of amino acids involves several transport systems. Amino acid transport systems are mainly classified according to sodium ion dependency and substrate specificity. These transport systems are broadly divided into Zwitterionic, Cationic and Anionic amino acid transporters. Due to the presence of multiple transport systems and overlapping substrate specificities, transport of amino acids across a cell membrane is a highly complex phenomenon. Depending upon the capacity and affinity, amino acid transporters can move not only naturally occurring amino acids but also structurally related

compounds such as antiparkinsonian agent L-Dopa, anticancer agent melphalan, thyroid hormones and gabapentin (Goldenberg et al., 1979; Su et al., 1995). These findings implicate that amino acid transport system could be utilized as a potential drug delivery tool to enhance the bio-availability of poorly permeable drug molecules. Small neutral amino acids are transported predominantly by Na^+ dependent transport system such as ASC (for Ala-, Ser-, and Cys-preferring), system A (for Ala-preferring) & $B^{0,+}$ (neutral and cationic amino acids preferring) and Na^+-independent transport system ASC, LAT (large neutral amino acids preferring) and $b^{0,+}$. Systems, $b^{0,+}$, y^+L and $B^{0,+}$ translocate a wide range of substrates, including cationic and neutral amino acids, differing however in their interactions with inorganic monovalent ions such as Na^+.

Due to their Localization on a variety of tissues including intestinal, nasal and BBB amino acids transporters may prove to be a useful target in transporter targeted drug delivery (Hundal and Taylor, 2009). Currently, nine amino acid transport systems (Figure 7) have been reported to be present at the brain capillary endothelium of the BBB (Smith, 2000). Among these types, large neutral amino acid transporter, system L, and cationic amino acid transporter, system y+, are present on the BBB as Na^+ independent systems. Similarly, Na^+ dependent amino acid transporter such as system x^-, neutral and/or cationic amino acid transporters, system A, B^{O+}, and ASC, and a beta-amino acid systems are also known to be present on the BBB. Among these types, system L has broad substrate specificity for relatively large neutral amino acids such as phenylalanine, tyrosine, leucine and is known to transport CNS acting drugs such as L-dopa, lacrofen and gabapentin (Tsuji and Tamai, 1999). System x^- transports anionic amino acids, such as aspartic acid and glutamic acid at BBB (Tamai and Tsuji, 2000). CAT-1 and CAT-2 were cloned as y+ transporters. Although

both of them are expressed in brain, only CAT-1 is present at BBB and mediates the transport of cationic amino acids like lysine, arginine and ornithine (Stoll et al., 1993). Presence of such a transport system can lead to the design of compounds, with enhanced permeability across the BBB.

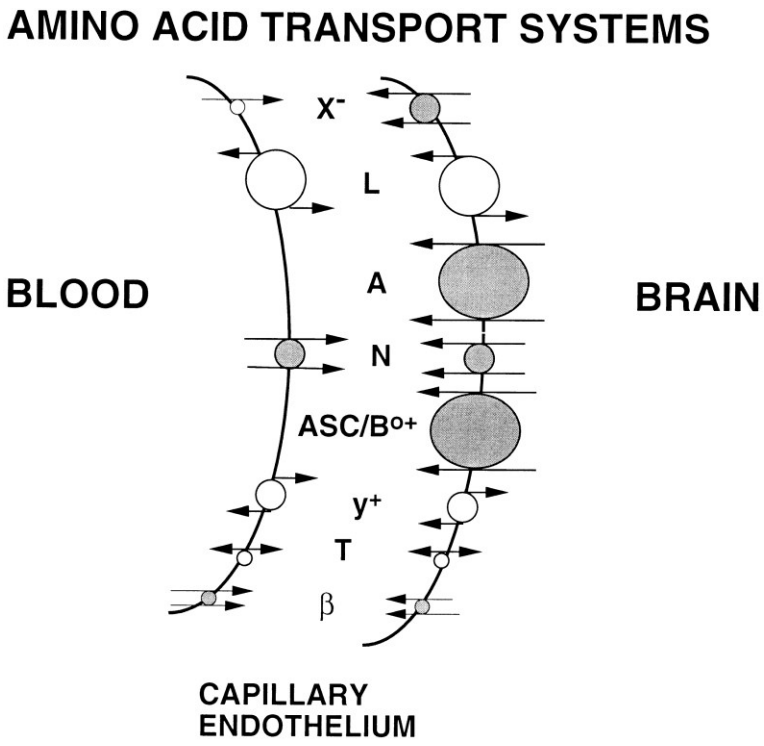

Figure 7. Various amino acid transport systems expressed on BBB (Smith, 2000)

CHAPTER 3

CIRCUMVENTION OF P-GP MEDIATED EFFLUX AND ENHANCING PERMEABILITY OF AMPRENAVIR BY PRODRUG DERIVATIZATION

Rationale

Current drug therapy for HIV-infected patients usually consists of a combination of HIV protease inhibitors and nucleoside reverse transcriptase inhibitors, which has resulted in a dramatic reduction of viral load in plasma and many tissues of infected patients (Conway et al., 1998). Although both classes of drug are potent agents in the therapy of HIV infection, combination therapy is more effective than the use of only one class of drug (Gulick et al., 1997; Cameron et al., 1998). Protease inhibitors (PIs) have been an important constituent of 'highly active anti-retroviral therapy' (HAART) which has substantially improved clinical outcomes of AIDS patients. However, complete eradication of HIV infection still remains an elusive goal. Sub-therapeutic concentrations of PIs in the sanctuary sites like brain, lung and bone-marrow cause persistent viral infection and may lead to viral resistance. One of the factors that may limit therapeutic efficacy of PIs is cellular efflux mediated by proteins like P-glycoprotein (P-gp) (Kim et al., 1998).

Amprenavir (APV) belongs to PIs and is an orally active nonpeptide inhibitor of the HIV aspartic protease enzyme. This enzyme plays an essential role in the post-translational processing of the *gag* and *gag-pol* gene products into key structural proteins and replication enzymes of HIV. Inhibition of HIV protease, therefore, results in the inhibition of processes necessary for viral maturation and proliferation (Moyle and Gazzard, 1996). Despite of good antiviral efficacy, APV suffers from low oral and brain bioavailability. APV exhibits low oral bioavailability, about 14-26%. APV like other PIs is a substrate of efflux protein, P-gp

and extensively metabolized by CYP3A4 (van der Sandt et al., 2001; Tran et al., 2005; Acharya et al., 2006). These reasons attribute to low oral bioavailability of APV. Hence APV is administered in combination with other PIs or NRTIs. One of the major factors limiting low oral absorption is cellular efflux mediated by P-glycoprotein (P-gp). P-gp is 170 kDa membrane bound protein highly expressed on intestinal epithelium. P-gp is localized at villus tip of enterocytes, main site for drug absorption, and effluxes drugs back into intestinal epithelium limiting oral absorption and ultimately low therapeutic efficacy (Jain et al., 2005; Agarwal et al., 2008). Various approaches have been attempted to improve oral absorption of drugs which are P-gp substrates. For example co-administration of P-gp inhibitors along with P-gp substrates, modulating expression of efflux proteins and chemical modification of drugs such that efflux can be evaded (Agarwal et al., 2008). Modulating P-gp expression or co-administration of high doses of P-gp inhibitors may lead to systemic toxicities by inhibiting physiological function of efflux proteins. Chemical modification of molecules such as prodrug approaches have an advantage of evading efflux without affecting physiological function of efflux proteins. Moreover evasion of efflux will also minimize drug exposure to metabolizing enzymes in intestinal lumen (Jain et al., 2005). Apart from efflux proteins, various nutrient transporters are also expressed on cell membranes of intestinal epithelium and BBB. These nutrient influx transporters are responsible for transport of nutrients across cells. Peptide and amino acid transport systems on intestinal epithelial cells are well established. Among the nutrient transporters, peptide transporters serve as promising targets due to their broad substrate specificity and high capacity. Peptide transporter targeted prodrug approach has been well established (Jain et al., 2007; Jain et al., 2008; Talluri et al., 2008). Prodrugs designed such that they can evade efflux by P-gp and utilize peptide

transporter for translocating across intestinal epithelium, may exhibit better absorption and improved bioavailability. Hence the objective of present study is to investigate the feasibility of evading efflux and enhance permeability of APV by prodrug derivatization. Di-peptide prodrugs of APV have been synthesized. Based on the previous publications L-Val-L-Val and L-Gly-L-Val exhibited better affinity for peptide transporter, hence were chosen as promoities and di-peptide prodrugs of APV were synthesized. Aqueous solubility of the prodrugs was determined. Cytotoxicity studies were performed in MDCKII-WT cells. In order to study interaction of these prodrugs with both efflux and influx transporters, MDCKII-MDR1 cells were employed. MDCKII-MDR1 cell line is genetically engineered to overexpress P-gp and well established model to study drug-transporter interactions. Cellular accumulation and bi-directional transport studies were performed.

Materials and Methods

Materials

Unlabeled (ulb) amprenavir (APV) and P-gp inhibitor, GF120918 (GF), were generous gifts from GlaxoSmithKline Ltd., respectively. [3H]glycylsarcosine (3H-GS) (4 Ci/mmol) was purchased from Moravek Biochemicals (Brea, CA, USA). MK-571 (MK) was purchased from Biomol (Plymouth Meeting, PA, USA). HPLC grade DMSO and methanol were obtained from Fisher Scientific Co. (Pittsburgh, PA, USA). These solvents were used neat for preparing stock solutions of all drugs and inhibitors. Trypsin–EDTA solution, Dulbecco's modified Eagle's medium (DMEM) was obtained from Invitrogen (Carlsbad, CA, USA) and fetal bovine serum (FBS) was obtained from Atlanta Biologicals (Lawrenceville,GA,USA). Transwell® inserts and uptake plates were procured from Corning

Costar Corp. (Cambridge, MA, USA). All other chemicals were of analytical reagent grade and were obtained from Fisher Scientific or Sigma Chemicals.

Methods

Cell Culture

Studies were performed with stable Madin-Darby canine kidney cells type II transfectants overexpressing hP-gp/MDR1 (MDCKII-MDR1 cells; passages 5 to 15); hMRP2 (MDCKII-MRP2 cells; passages 5 to 25) ; and wild type MDCKII cells generously provided by Drs. A. Schinkel and P. Borst, The Netherlands Cancer Institute, Amsterdam. These cell lines were cultured in T-75 flasks with DMEM (with high glucose and glutamine concentrations) supplemented with 10% FBS, 1% nonessential amino acids, penicillin 100μg/mL and streptomycin 100U/mL. The medium was changed every alternate day; cells were harvested and passaged *via* trypsinization at 80 to 90% confluence (about 4 days of growth). Cells were also grown on collagen coated Transwell® inserts (12-mm) with transparent polyester membranes. Transwell® inserts were coated with type 1 rat tail collagen (100μg/cm^2), equilibrated with medium, and seeded at a 25,000 cells/cm^2 density. Following seeding, medium was changed every alternate day, and transport or uptake studies were performed after incubation of 5-7 days.

Solubility Studies

Solubilities of the prodrugs were determined in distilled deionized water (DDW). Saturated drug solutions were prepared in silicone coated microcentrifuge tubes and kept at room temperature for 24h in a shaker bath. At the end of 24h, the undissolved drug was removed by ultracentrifugation at 25000g for 5min. The supernatant was appropriately diluted and drug concentration was measured with LC/MS/MS.

Buffer Stability Studies

Hydrolytic Stability of prodrugs was determined at various pH values. Buffers, HCl (pH 1.4), phthalate (pH 3.4 and 5.4), phosphate (pH 7.4), and boric acid (pH 9.4), were prepared and ionic strength was adjusted to 0.1M. The buffer strength was also adjusted to 50 mM for all the buffers. Stock solutions of prodrugs (0.5-1 mg/mL) were prepared in methanol and used immediately for stability studies. Aliquots (9.8 mL) of the buffer were placed in screw capped vials and allowed to equilibrate at 37°C. Prodrug stock solution containing 50 µg of prodrug (0.1 to 0.05 mL) was subsequently added to the buffer and vials were placed in a water bath maintained at 37°C and rotated at 60 rpm. Samples (0.2 mL) were collected at appropriate time interval for up to 7 days. Samples were immediately stored at -80°C until further analysis. All experiments were conducted at least in triplicate.

Cytotoxicity Studies

Cytotoxicity of the prodrugs was determined in MDCKII-WT cells using an aqueous non-radioactive cytotoxicity kit based on the MTS assay. The assay determines cell *via*bility based on the mitochondrial conversion of a water-soluble tetrazolium salt [3-(4,5-dimethylthiazol-2-yl)-2,5-diphenyltetrazolum bromide; MTT] to the water-insoluble blue formazan product. The cytotoxicity kit is supplied as a salt solution of MTT (known as MTS) with an electron coupling reagent PMS (phenazine methosulfate). PMS has enhanced chemical stability, which allows it to be combined with MTS to form a stable solution eliminating the need to solubilize formazan crystals using an external source. Briefly, cells were grown in 96 well tissue culture plates at 10,000 cells per well for 24h prior to drug treatment. Culture medium was then replaced with 100µl of medium containing serial dilutions of the prodrugs (5-250µM). Cells were then incubated for 4h at 37°C under 5%

CO_2. After the treatment period was over, 20µl of MTS stock solution was added to each well. After addition of the MTS dye, the cells were incubated for 2h at 37°C. Cell *via*bility was then assessed by measuring absorbance at 485nm on an automated plate reader (Biorad, Hercules, CA). The quantity of formazan product as measured by the amount of 485nm absorbance is directly proportional to the number of living cells in culture.

Uptake Studies

Uptake studies were conducted with confluent cell monolayers, 5-7 days post seeding for MDCKII cells. Medium was aspirated and cells were washed three times with DPBS. All drug solutions were prepared immediately prior to an experiment. The study was initiated by adding 1mL of drug solution (in the presence or absence of competing substrates) to the wells. Incubation was carried out over a period of 15min at 37°C. At the end of an incubation period, drug solution was removed and the cell monolayer was washed three times with ice-cold ice-cold PBS. Cells were lysed overnight with 1mL 0.1% (w/v) Triton X-100 in 0.3N sodium hydroxide at room temperature. Aliquots (500µL) were withdrawn from each well and transferred to *via*ls containing 5mL scintillation cocktail. Samples were then analyzed with a Beckman scintillation counter (Model LS-6500, Beckman Instruments, Inc.). Uptake was normalized to the protein content of each well. Amount of protein in the cell lysate was quantified by the method of Bradford utilizing BioRad protein estimation kit (BioRad, Hercules, CA).

Transport Studies

APV transport was evaluated with monolayers of MDCKII-MDR1 cell line. All transport studies were performed with Dulbecco's modified phosphate-buffered saline (DPBS) containing glucose (1g/L) and HEPES (20mM) at pH 7.4. Drug solutions were

prepared immediately prior to initiating a transport study. APV and prodrugs (VA,VVA and GVA) were dissolved in methanol (not exceeding 2% v/v as the final concentration) and inhibitors were separately dissolved in DMSO (not exceeding 2% v/v as the final concentration) to prepare a stock solution and then diluted with DPBS to the specified final concentrations. Control solutions contained the same amount of methanol/DMSO as the drug solutions. Volumes of test solutions added were 0.5 and 1.5mL, for apical (A) and basolateral (B) chambers respectively. Prior to initiating an experiment, cultured monolayers were rinsed and equilibrated for 30min with DPBS. Drug solution was added either in the donor or receiving chamber for A to B and B to A transport study. Samples (100µL) were withdrawn from the receiving chamber at predetermined time points (15, 30, 60, 90, 120, 150, 180) and were replaced with equal volume of DPBS to maintain sink conditions. Dilutions were taken into account for the calculations. Samples were stored at −80˚C until further analysis. All the experiments were performed at 37˚C in triplicate.

Sample Preparation

Uptake and transport study samples were analyzed with LC/MS/MS. Sample preparation was carried out using liquid-liquid extraction technique. Verapamil was employed as an internal standard (IS) for analysis. The organic solvent, methyl- tert-butyl ether was utilized to extract the drug from the aqueous phase. Briefly, 50µl of IS was added to the transport sample (100µl). Each sample was mixed with 500µl of organic solvent. All samples were vortexed again for 1-2min to allow enough time for the drug to partition into the organic phase. For efficient separation of the aqueous and organic layers, samples were centrifuged at 25000g for 5min and then were stored at -20ºC for sufficient time to allow freezing of the aqueous layer. The organic layer was decanted and samples were dried in

vacuum. The residue was reconstituted in 100µl of 70:30 acetonitrile: DDW and 0.1% formic acid to allow efficient solubilization of the dried drug. This reconstituted extract was injected onto the LC/MS/MS for analysis. Standard solutions in buffer were also extracted and quantified exactly following the same procedure. Relative extraction efficiency (ratio of area for analyte *VS* area for IS) for APV, VA, VVA and GVA was approximately 50-70%.

HPLC Analysis

Buffer stability samples were analyzed by a reversed phase HPLC technique. The HPLC system was comprised of HP 1050 pump, Waters dual wavelength absorbance UV detector, and an Alcott auto sampler (model 718AL HPLC). A C(12) Lima column (250 x 4.6mm; Phenomenex, Torrance, CA) was employed for the separation of analytes. Mobile phase composed of 50mM phosphate buffer: methanol: acetonitrile (39:22:39%; v/v/v) and the pH was adjusted to 5.9 with ortho-ophosphoric acid. Flow rate was maintained at 0.8mL/min and detection wavelength was set at 215nm. Elution times for APV, V-APV, VV-APV and for GV-APV were 6,8,16, 14 and 12 minutes respectively.

LC/MS/MS Analysis

QTrap® LC/MS/MS mass spectrometer (Applied Biosystems, Foster City, CA, USA) equipped with Agilent 1100 Series quaternary pump (Agilent G1311A), vacuum degasser (Agilent G1379A) and autosampler (Agilent G1367A, Agilent Technology Inc., Palo Alto, CA, USA) was employed to analyze samples from transport and metabolism studies. HPLC separation was performed on reverse phase XTerra® MS C18 column with dimensions of 4.6 x 50 mm and particle size of 5 µm. Mobile phase (70% acetonitrile and 30% water containing 0.1% formic acid) was continuously pumped through the column at a constant flow rate of 0.2 mL/min. The sample (20µl) was injected. Electrospray ionization in the

positive mode was employed in the sample introduction. The detection was operated in multiple-reaction monitoring (MRM) mode. Precursor ion of analytes and internal standard were determined from spectra obtained during the infusion of standard solutions using an infusion pump connected directly to the electrospray source. As a result of the very soft ionization provided by the electrospray ion source, only singly charged molecular ions were observed. Each of these precursor ions was subjected to collision-induced dissociation to determine the secondary ions. The precursor and the secondary ions generated were; APV + 506.3/155.9; VVA + 704.4/156.1; GVA + 662.4/156.0; VA + 605.4/156.0 and Verapamil (IS) + 455.3/165.1. The turbo ion spray setting and collision gas pressure were optimized (IS Voltage: 5500V, temperature: 300°C, nebulizer gas: 40psi, curtain gas: 40psi). MS/MS was performed using nitrogen as collision gas. Other ion source parameters employed were: declustering potential (DP): 50V; collision energy (CE): 70V; entrance potential (EP) 5V; and collision cell exit potential (CXP) 3V. Peak areas for all components were automatically integrated by using Analyst™ software, and peak-area ratios (area for analyte *VS* area for IS) were plotted *vs.* concentration by weighted linear regression (1 *VS* concentration). The analytical data resulting from prodrugs with MRM method show a significant linearity that extends to nmol range. The limits of quantification were found to be 10 ng/mL for APV and 50 ng/mL for VA, VVA and GVA. This method gave rapid and reproducible results.

Data Analysis

Cumulative amounts of prodrugs (VVA or GVA), the intermediate VA and the parent drug APV, generated during transport across the cell monolayers were plotted as a function of time to determine permeability coefficients. Linear regression of the amounts transported as a function of time yielded the rate of transport across the cell monolayer (dM/dt). Rate

divided by the cross-sectional area available for transport (A) generated the steady state flux as shown in Eq. 1.

$$Flux=(dM/dt)/ A \quad \text{Eq. 1}$$

In all the transport studies, slopes obtained from the linear portion of the curve were used to calculate permeability values. Permeability was calculated by normalizing the steady state flux to the donor concentration (C_d) of the drug or prodrug as shown in Eq. 2.

$$Permeability=Flux/C_d \quad \text{Eq. 2}$$

Statistical Analysis

All experiments were conducted at least in triplicate and results are expressed as mean ± S.D. Statistical comparison of mean values was performed with Student t test (Graph Pad INSTAT, version 3.1). A value of $*P < 0.05$ was considered to be statistically significant.

Results and Discussion

Synthesis and Identification of Prodrugs

The synthesis of di-peptide prodrugs of APV involves conjugation of pro-moiety to the free hydroxyl group in APV. The carboxylic group of the amino acid or peptide can form the ester linkage with saquinavir which may improve the delivery of conjugated drug through transporters expressed on various tissues. There is an ester group between drug and immediate amino acid; an amide linkage between first amino acid and terminal amino acid. Both ester and peptide linkages are readily cleaved by esterases and peptidases present in tissues. Steglich esterification was employed to synthesize the prodrugs. Overall synthetic

scheme for Valine-APV (VA), Valine-Valine-APV (VVA) and Glycine-Valine-APV (GVA) is described in Figure 8.

Synthesis of Val-Amprenavir(4)

Commercially available BocVal-OH (429mg, 1.97mmol) was dissolved in dry DMF (10mL) and cooled it down to 0^{o}C using ice bath. DCC (356mg, 1.72mmol) was added and stirred for 1h at same temperature. In a separate reaction flask Amprenavir (500mg, 0.98mmol) was dissolved in DMF and add DMAP (120mg, 0.98mmol) and continued stirring for 10 min at room temperature under inert atmosphere to activate the secondary hydroxyl group of the Amprenavir(1). It was added in to the reaction mixture through a syringe and allowed it to come to the room temperature and continued stirring for 48h. Small portion of the reaction mixture was taken out and injected it in LC/MS to ensure the complete conversion of the starting material to product. Reaction mixture was filtered and solvent was evaporated at room temperature under reduced pressure to get crude product. The product Boc-Val-Amprenavir(3) was purified by silica column chromatography using 50% Ethylacetate/ Hexane as eluent with 93% yield. To deprotect the N-Boc Group, **N**-Boc-Val-Amprenavir was treated with 80% TFA/ CH_2Cl_2 at 0^{o}C for 2.5h. The filtrates were evaporated *in vacuo* to constant weight. The crude products were purified by recrystallization from cold diethyl ether to get the final product Val-Amprenavir (4) with an excellent yield (98%). The prodrug was dried under vacuum for 10h before biological evaluation.

Synthesis of Val-Val-Amprenavir (4)

BocVal-Val-OH (187mg, 0.59mmol) was dissolved in dry DMF (5mL) and cooled it down to 0^{o}C using ice bath. DCC (106mg, 0.51mmol) was added and stirred it for 1h at same temperature. In a separate reaction flask Amprenavir (150mg, 0.29mmol) was dissolved in

DMF and DMAP (37mg, 0.29mmol) was added followed by stirring for 10min at room temperature under inert atmosphere to activate the secondary hydroxyl group of the Amprenavir(1). This was added in to the reaction mixture through a syringe and allowed to come to the room temperature and stirring was continued for 48h. Small portion of the reaction mixture was taken out and injected it in LC/MS to ensure the complete conversion of the starting material to product. Reaction mixture was filtered and solvent was evaporated at room temperature under reduced pressure to get crude product. The product Boc-Val-Val-Amprenavir (5) was purified by silica column chromatography using 50% Ethyl acetate/ Hexane as eluent with 87% yield. Val-Val-Amprenavir (6) was achieved after deprotection of the N-Boc group using TFA/ DCM (4:1) followed by recrystallization from cold diethyl ether.

Synthesis of Gly-Val-Amprenavir (9)

Commercially available BocGly-OH (163mg, 0.92mmol) was dissolved in DMF (4mL) and cooled it down to 0^{o}C using ice bath. DCC (165mg, 0.80mmol) was added and stirred it for 1h at same temperature. In a separate reaction flask Val-Amprenavir(4) (500mg, 0.46mmol) was dissolved in DMF, and triethylamine (2mL) was added and stirring was continued for 10min at room temperature under inert atmosphere to neutralize the TFA salt as well as activate the primary amine group of Val-Amprenavir. This was added to reaction mixture, removed from ice bath and continued stirring for 48h. Reaction mixture was filtered and solvent was evaporated at room temperature under reduced pressure to get crude product. The product BocGly-Val-Amprenavir (8) was purified by silica column chromatography using 70% Ethyl acetate/ Hexane as eluent with 87% yield. The final product Gly-Val-Amprenavir (9) was achieved after deprotection of the N-Boc group following the same

procedure as mentioned for the synthesis of Val-Amprenavir. Synthetic schemes are provided as Figure 8.

Synthesis of Val-Amprenavir (4):

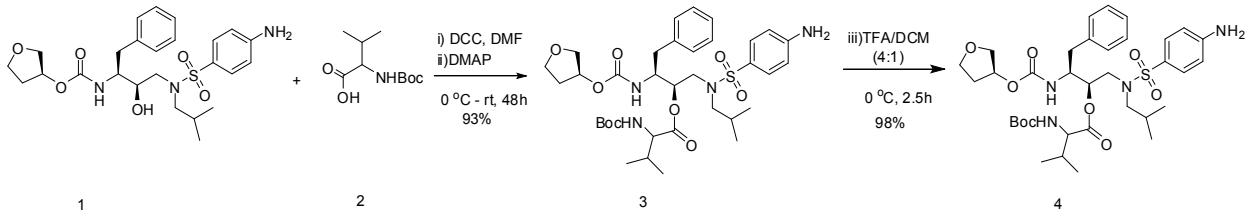

Synthesis of Val-Val-Amprenavir (6):

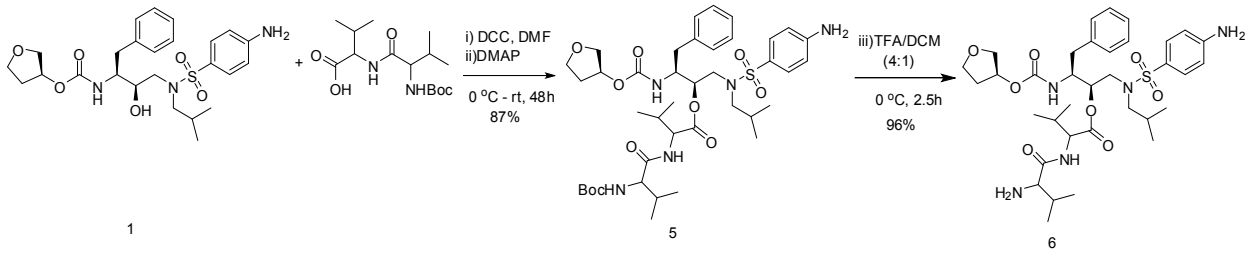

Synthesis of Gly-Val-Amprenavir (9):

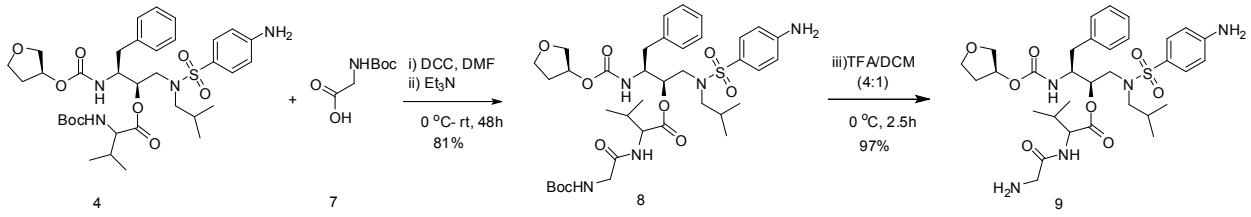

Figure 8. Synthetic scheme for Valine-APV (VA), Valine-Valine-APV (VVA) and Glycine-Valine-APV (GVA)

Identification of the Prodrugs

Mass analysis was carried out using the same LC-MS/MS spectrometer as mentioned earlier under Enhanced Mass (EMS) mode. Electron-spray Ionization (ESI) was used as an ion method and was operated in positive and negative ion modes. In the IR spectra for prodrugs, characteristic peak for –OH group at 3200-3400 cm^{-1} was not observed. ^1H NMR spectra were recorded on Varian Mercury 400 Plus spectrometer using tetra methyl silane as an IS. Chemical shifts (δ) are reported in parts per million relative to the NMR solvent signal.

VA (4): Yellowish solid; LC/MS(M/z): 605.4,; ^1H NMR ($CDCl_3$) δ: 0.75, [6H, CH_3; valine], 1.01 [6H, CH_3], 2.0 [1H, NH_2; valine], 3.75 [2H,CH_2-CH_2; tetrahydrofuran], 3.99 [2H, CH_2-CH; tetrahydrofuran], 5.0,5.11 [-CH-; methane], 6.74, 6.74, 7.68, 7.68 [4H, aromatic], 7.08, 7.12, 7.12, 7.21, 7.21 [5H, aromatic], 7.08, 7.12, 7.21, 7.68, 7.68, 6.74 [6H, aromatic], 8.0 [1H, NH-C=O; sec. amide].

VVA (6): White solid; LC/MS(M/z): 704.4,; ^1H NMR ($CDCl_3$) δ: 0.7-1.0 [12H, CH_3,val-val], 1.1 [6H, CH_3], 2.0 [1H, NH_2; valine], 3.75 [2H,CH_2-CH_2; tetrahydrofuran], 3.99 [2H, CH_2-CH; tetrahydrofuran], 5.0,5.11 [-CH-; methane], 6.74, 6.74, 7.68, 7.68 [4H, aromatic], 7.08, 7.12, 7.12, 7.21, 7.21 [5H, aromatic], 7.08, 7.12, 7.21, 7.68, 7.68, 6.74 [6H, aromatic], 8.0 [2H, NH-C=O; sec. amide].

GVA (9): Yellowish solid, LC/MS(M/z): 662.6,; ^1H NMR ($CDCl_3$) δ: 0.8-1.1 [12H, CH_3], 2.1 [1H, NH_2; glycine], 3.75 [2H,CH_2-CH_2; tetrahydrofuran], 3.99 [2H, CH_2-CH; tetrahydrofuran], 4.0 [1H, NH_2, aromatic], 5.0,5.11 [-CH-; methane], 6.74, 6.74, 7.68, 7.68

[4H, aromatic], 7.08, 7.12, 7.12, 7.21, 7.21 [5H, aromatic], 7.08, 7.12, 7.21, 7.68, 7.68, 6.74 [6H, aromatic], 8.0 [2H, NH-C=O; sec. amide].

Aqueous Solubilities

Solubility studies were carried out in DDW. Saturation solubility values of V-APV, VV-APV and GV-APV were found to be, 0.61± 0.07, 0.36 ± 0.06 and 0.47 ± 0.12 mg/mL respectively relative to 0.04 ± 0.008 mg/mL for APV. These values are much higher relative to APV which is practically insoluble in water. Such increase in solubility offers an added benefit for a drug like APV which is almost completely insoluble in water and may offer some formulation-related advantages.

Buffer Stability

Degradation rate constants for APV prodrugs are summarized in Table 2. Stability of V-APV, VV-APV and GV-APV was examined within a pH range of 1.4-9.4. Apparent first order degradation kinetics was observed for all the prodrugs. APV prodrugs exhibited similar pH rate profiles within the pH range studied with VV-APV and GV-APV being more stable than Val-APV. No appreciable degradation of prodrugs was noticed even at pH 1.4 for 7 days at 37^{o}C. Increased susceptibility to hydrolysis was observed as the pH was raised toward the alkaline range. It is clear from these studies that prodrugs are prone to alkali hydrolysis.

Table 2. Half-lives (hr) and degradation rate constant (k_{obs}) of APV prodrugs as a function of pH. Phthalate (pH 3.4 and 5.4), phosphate (7.4), and borate (pH 9.4) buffers (50 mM)

pH	**V-APV**		**VV-APV**		**GV-APV**	
	k_{obs} ($hr^{-1} \times 10^4$)	**$t_{1/2}$ (hr)**	**k_{obs} ($hr^{-1} \times 10^4$)**	**$t_{1/2}$ (hr)**	**k_{obs} ($hr^{-1} \times 10^4$)**	**$t_{1/2}$ (hr)**
1.4	ND	ND	ND	ND	ND	ND
3.4	31.4 ± 2.1	221 ± 2	24.2 ± 3.5	286 ± 13	24.9 ± 2.1	278 ± 26
5.4	101.9 ± 13	68 ± 11	57.3 ± 5.6	121 ± 9	60.3 ± 4.9	115 ±12
7.4	330 ± 46	21 ± 3	112 ± 17	62 ± 4	144 ± 14	48 ± 4
9.4	756 ± 126	9 ± 1.4	317 ± 41	22 ± 3.3	355 ± 35	19 ± 2

were employed. Hydrochloric acid was used to prepare the pH 1.4 solution. Ionic strength adjusted to 0.1 M with KC1. Studies were conducted at 37ºC. Values reported are mean ± SD (n=3)

ND: No degradation detected

Cytotoxicity Studies

Cytotoxicity of the prodrugs was determined using MTT assay. Results are depicted in Figure 1. Medium containing no drug was used as negative control. Medium containing DMSO at 2% was also tested to confirm that DMSO is not cytotoxic at that concentration. Triton X was used as positive control. At the end of 4h, 5-50µM of prodrug concentrations (VA, VVA and GVA were not significantly cytotoxic but when used at concentrations of 100 and 250µM, GVA exhibited some cytotoxicity to the cells. For transport experiments that were carried out for 3h, the concentrations of VVA and GVA used were 25µM which are not cytotoxic to the cells.

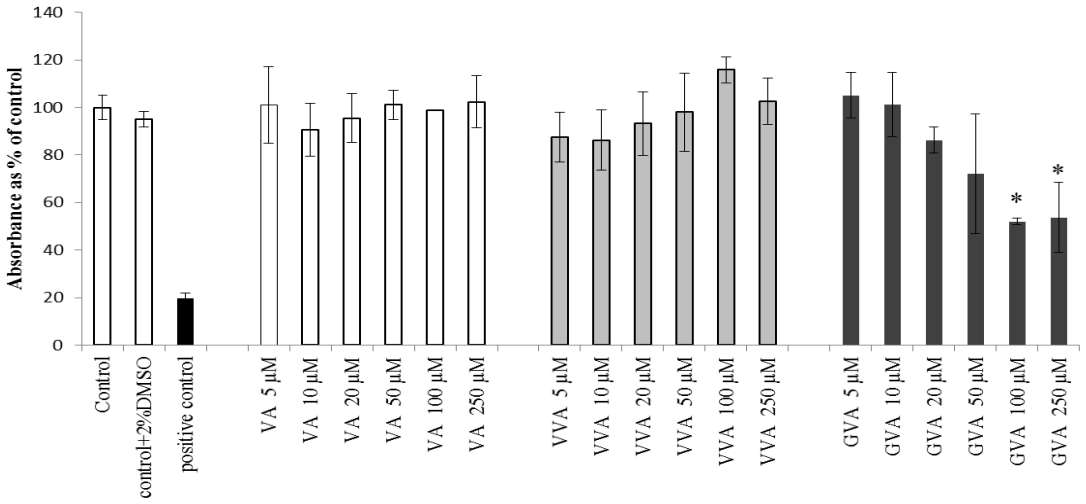

Figure 9. Cytotoxicity of Prodrugs in MDCKII-WT cells determined by MTS assay. Asterisk (*) represents statistical difference compared to control at $p<0.05$

Interaction of APV, Val–Val–APV and Gly–Val–APV with P-glycoprotein

Uptake of APV, VA, VVA and GVA by MDCKII-MDR1 cells, was studied. Equimolar concentrations (25 μM) are used. Approximately 2-3 fold increase in cellular accumulation of VA, VVA and GVA compared to APV was observed (Figure 10). This increase in the cellular uptake of prodrugs may be due to reduced affinity of prodrugs for efflux proteins. To further delineate interaction of these prodrugs with P-gp, uptake of a P-gp substrate [3H]digoxin (0.5 μCi/mL) was studied in presence of P-gp inhibitor GF120918, APV and prodrugs. GF120918 is a well-established inhibitor of P-gp. Equimolar concentrations (25 μM and 50 μM) of APV, VA, VVA and GVA were used. A fourfold increase in uptake of [3H]digoxin was observed in presence of GF120918 at 2 and 5 μM concentrations. A three folds increase in uptake of [3H]digoxin was observed in presence of APV and only two fold increase was observed in presence of VVA and GVA (Figure 11). The increase in uptake of [3H]digoxin in presence of GF is due to inhibiting activity of P-gp. However this increase in uptake was inhibited by prodrugs VA, VVA, and GVA. But inhibition in uptake is more compared to parent drug APV. These results demonstrate that prodrugs have lower affinity for P-gp compared to parent drug APV.

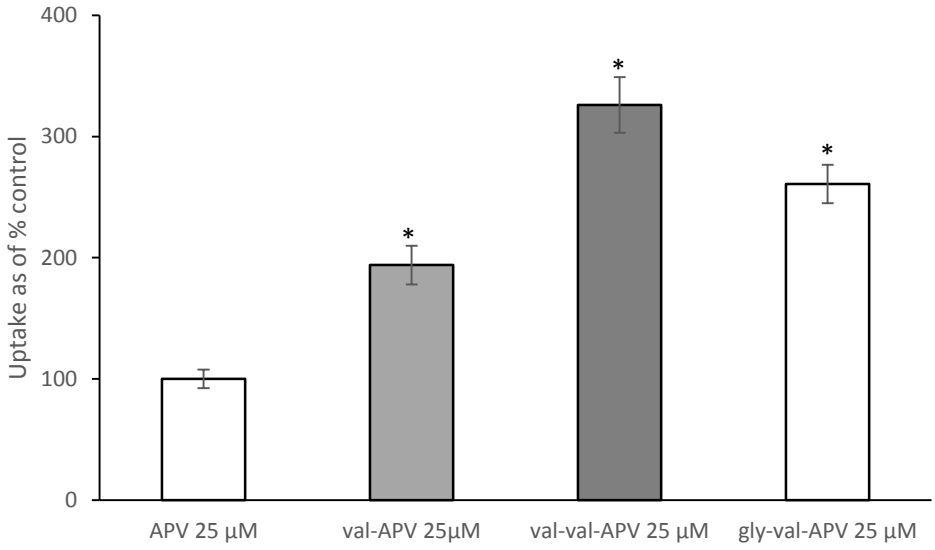

Figure 10. Uptake of 25 µM APV, V-AAPV, VV-APV, GV-APV in MDCKII-MDR1 cells (*) indicates statistical significant difference compared to Uptake in presence of APV at $p<0.05$.

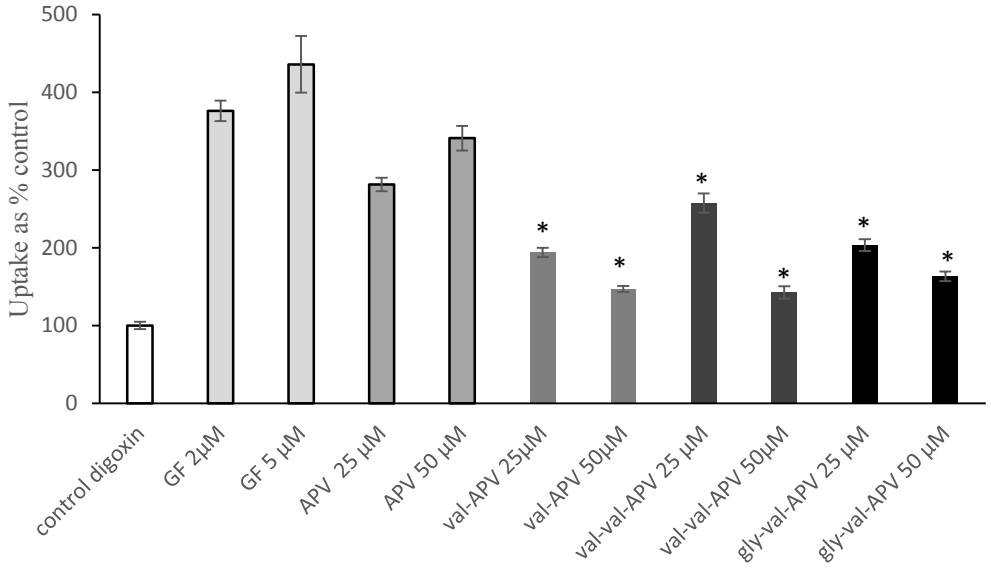

Figure 11. Uptake of [3H] digoxin in MDCKII-MDR1 cells in presence of APV, V-APV, VV-APV, GV-APV at 25 µM and 50 µM concentrations. Data points expressed as mean ± SD. (*) indicates statistical significant difference compared to Uptake in presence of APV at $p<0.05$.

Interaction with Peptide Transporters in MDCKII-MDR1 Cells

Uptake of 3H-glycylsarcosine (GS), a model substrate for peptide transporters, in the presence of unlabeled glysar and prodrugs was carried out to determine if the prodrugs are recognized by the peptide transporters. Uptake of 3H-glysar (0.5μCi/mL), was inhibited in the presence of unlabeled glysar GS, at concentration 20mM. Uptake of 3H-GS was also significantly lower (more than 50%) in the presence of relatively low amounts of prodrugs (25 and 50 μM) as demonstrated in Figure 12. These studies suggest that peptide transporters are expressed and functional, and the prodrugs are recognized by these membrane proteins.

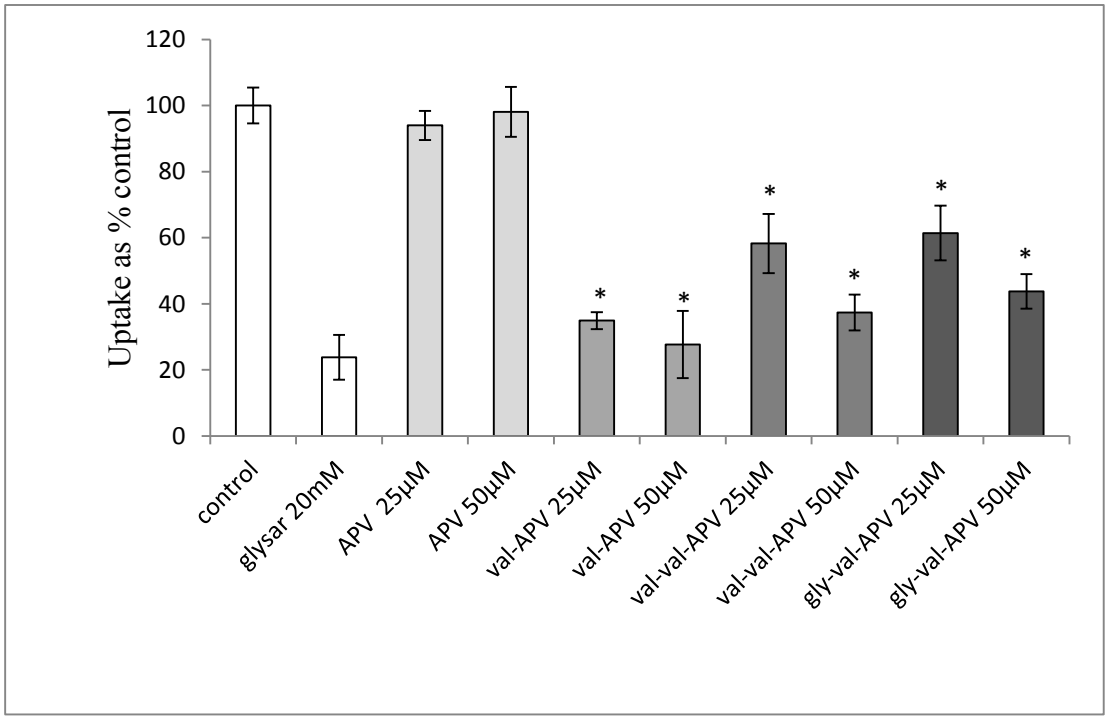

Figure 12. Uptake of [3H] glysar (0.5 μCi/mL) by MDCKII-MDR1 cells in absence (control) and in presence of 20 mM unlabeled glysar, APV, val-APV, val-val-APV and gly-val-APV

at 25 μM and 50μM concentrations). Data is expressed as mean ±SD. * $P<0.05$ which represents statistical significant difference compared to control.

Transport across MDCKII-MDR1

To further test our hypothesis that prodrug modification of APV can bypass P-gp mediated efflux and increase absorption, transepithelial transport studies were conducted in MDCKII-MDR1 cell monolayers. The difference in apical to basolateral and basolateral to apical clearly indicates the involvement of P-gp in transport of substrates. The apical cell layer expresses functional efflux protein P-gp, as well as influx (peptide) transporters; which makes it convenient for us to compare the permeability values of both the parent drug and the prodrugs in the same cell line. For P-gp substrates A-B transport will be significantly lower than B-A. Ratio of B-A and A-B permeability, termed as efflux ratio, will be close to unity for drugs which are not substrates and higher than one for substrates. Permeabilities of the prodrugs (25μM) were compared with APV (25μM) across the apical cell layer of the MDCKII-MDR1. Absorptive permeability (A-B) of APV was 1.1×10^{-6} cm/s and secretory permeability was found to be 4.5×10^{-6} cm/s (Table 3). The efflux ratio of APV is approximately 4. This asymmetric permeability is due to the expression of P-gp on apical membrane. In presence of GF120918 (5 μM) efflux ratio was 1.3 (Figure 13). This clearly demonstrates that APV is good substrate for P-gp. A-B permeability of VVA and GVA were found to be 6.27×10^{-6} cm/s and 7.1×10^{-6} cm/s respectively. Both prodrugs also exhibited asymmetric permeabilities however; efflux ratio for both prodrugs was between 1.5 and 2. This result clearly indicates that the prodrugs have significantly lower affinity for P-gp compared to drug. Bidirectional transport studies of prodrugs across MDCKII-

MDR1 were studied in absence and presence of glysar (20mM) to delineate the interaction of prodrugs with peptide transporters. Results are depicted in Figure 14. Glysar is well established substrate of peptide transporter. Permeability of VVA and GVA were found to be 7.9 $\pm$ 0.7x10^{-6} cm/sec and 9.8 $\pm$ 1.2x10^{-6} whereas 1.6$\pm$ 0.2x10^{-6} for APV. In presence of glysar (20mM) permeability of VVA and GVA reduced to 3.2 $\pm$ 0.5x10^{-6} cm/sec and 2.9 $\pm$ 0.6 x10^{-6} cm/s respectively. Peptide transporters are known to be expressed on apical membrane of MDCKII-MDR1 cells. The change in absorptive permeability of prodrugs is due to competitive binding of glysar to peptide transporter. Cellular accumulation and bidirectional transport results of prodrugs in presence of glysar clearly demonstrate that the prodrugs are substrates for peptide transporters.

Table 3. Apparent permeabilities (Papp) of APV and its prodrugs (25µM) across MDCKII-MDR1 cells Values are expressed as mean ± SD

Compound	**P_{app} (A-B) (×10^{-6} cm/s)**	**P_{app} (B-A) (×10^{-6} cm/s)**
APV	1.1 ±0.2	4.5 ± 0.3
APV + GF	1.9 ± 0.3	2.8 ± 0.1
V-APV	4.39 ± 0.3	5.9 ± 0.4
VV-APV	6.27 ± 0.2	8.2 ± 0.9
GV-APV	7.1 ±0.5	10.8 ± 1.0

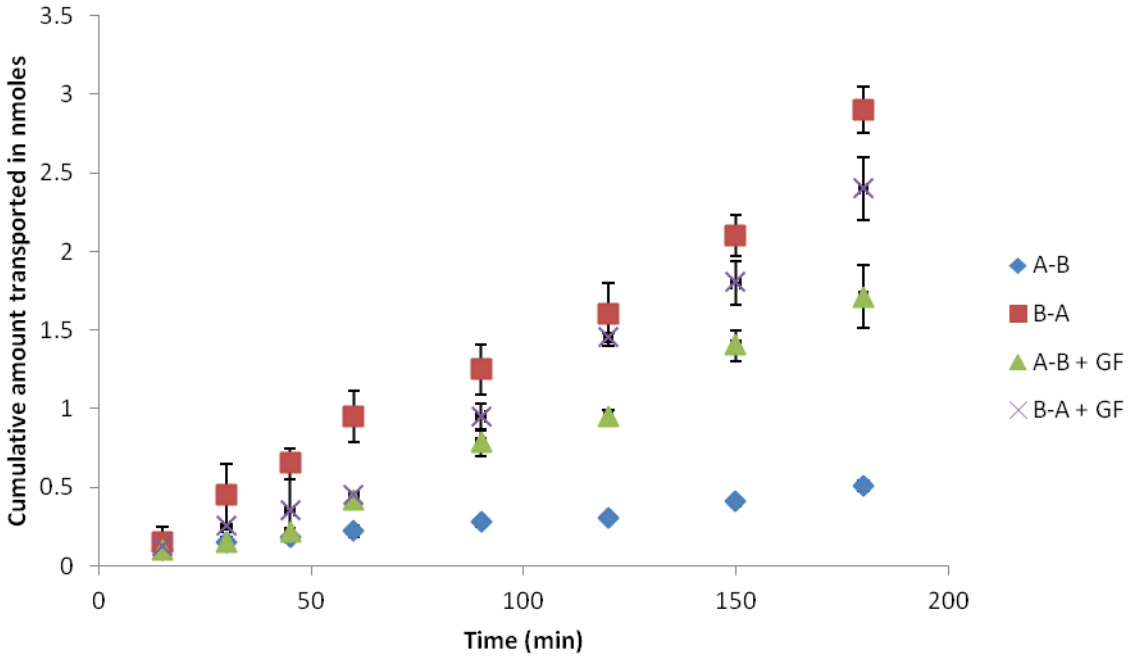

Figure 13. Bidirectional transepithelial transport of APV (25 µM) across MDCKII-MDR1 cell monolayers in presence and absence of GF 120918. Data points are expressed as mean ± S.D. (n=4).

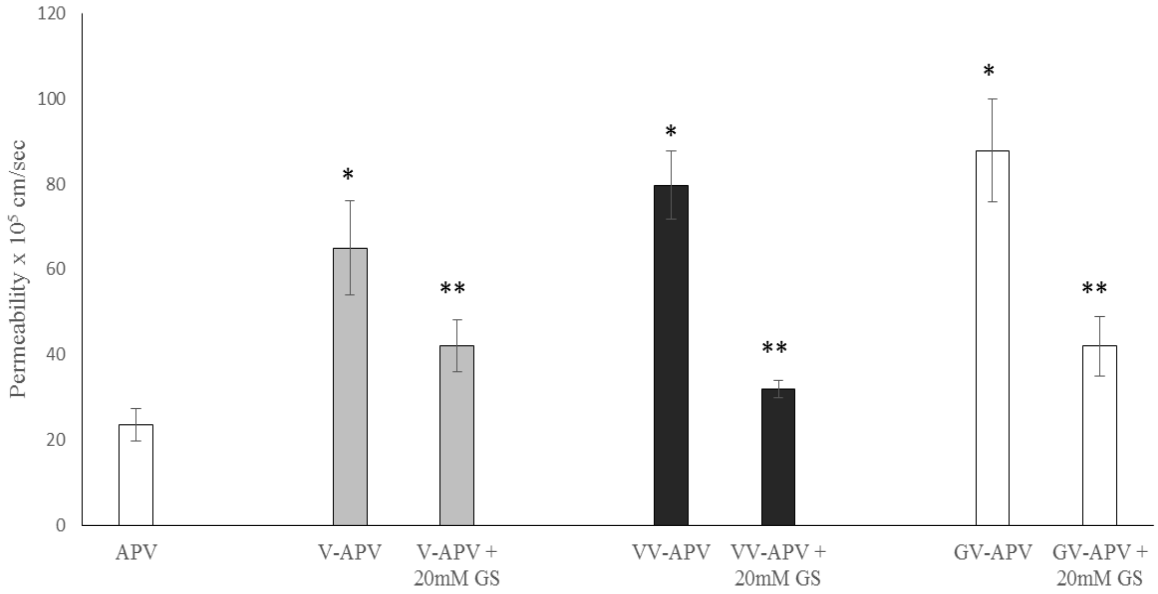

Figure 14. Permeabilities of VA, VVA and GVA relative to APV across MDCKII-MDR1 cells and in presence of 20 mM glysar. (*) represent statistical significant difference from control at $p<0.05$. (**) represent statistical significant difference from prodrug without glysar at $p<0.01$

Conclusions

Di-peptide prodrugs of APV, L-valine-L-valine-Amprenavir (VVA) and L-glycine-L-valine-Amprenavir were synthesized and evaluated for drug-transporter interactions *in vitro*. Synthesized prodrugs were identified by LC-MS/MS and NMR studies. Both prodrugs exhibited better inherent aqueous solubility compared to parent drug. VA, VVA and GVA exhibited less affinity for efflux protein P-gp compared to drug. Efflux ratios obtained from permeability studies clearly indicate that prodrugs have less affinity for P-gp compared to drug. Uptake and transport studies in presence of glysar clearly suggest that these prodrugs are substrates for peptide transporters, hence can evade the efflux and exhibit better permeability characteristics compared to drug resulting in improved bioavailability. Evasion of efflux may reduce the drug exposure to intestinal metabolizing enzymes and also minimize the chance of developing resistance on chronic APV exposure. Thus efficient delivery of APV will result in improved therapeutic efficacy and clinical outcomes. Results

obtained from this study clearly demonstrate di-peptide prodrug derivatization is a viable strategy to improving the oral absorption of APV.

CHAPTER 4

PROTEIN BINDING, METABOLIC AND ENZYMATIC STABILITY OF AMPRENAVIR PRODRUGS

Rationale

Amprenavir (APV) is a potent inhibitor of the human immunodeficiency virus and shares some pharmacokinetic properties with other protease inhibitors. The protease inhibitors, the mainstay of life-prolonging drug combinations used in the treatment of patients with acquired immunodeficiency syndrome (AIDS), are highly bound to plasma proteins, predominantly to alpha1- acid glycoprotein (AAG) (Boffito et al., 2003). *In vitro* studies have shown that the antiviral efficacy of the protease inhibitors was attenuated by the addition of human AAG to the medium. Like almost all of the commercially available HIV protease inhibitors, amprenavir exhibits a high degree of binding to plasma proteins (90%). The *in vitro* studies have shown that the plasma protein to which amprenavir primarily binds is AAG. APV is also substrate for cytochrome P450 3A4 and has inhibitory and inducing properties leading to a number of drug interactions. APV shares some pharmacokinetic properties with other protease inhibitors: it is a substrate for cytochrome P450 3A4 and has inhibitory and inducing properties leading to a number of drug interactions (Barry et al.,

1999). Approximately 90% binds to plasma proteins, predominantly to AAG (Sadler et al., 2001). The recommended dose is 1200 mg bid (or 1400 mg fosamprenavir bid), but this can be halved by pharmacoenhancement with low-dose (100 mg) ritonavir, a potent CYP3A inhibitor (Sadler and Stein, 2002). It is now recognized that virologic efficacy of protease inhibitors is dependent on both their pharmacokinetic and pharmacodynamic properties. Briefly, unbound concentrations of the antiretroviral drug have to exceed the concentration that inhibits viral replication *in vitro* (determined by IC_{50} or IC_{90}), and the inhibitory quotient, is the ratio of plasma trough concentration to *in vitro* IC_{50} or IC_{90}, as proposed to measure the *in vivo* potency of antimicrobial agents.(Piliero, 2002; Aarnoutse et al., 2003). Therefore, an increase in plasma AAG level under pathological conditions may result in treatment failure in such patients (due to higher binding and the resultant lower concentration of the free drug) unless the dosages of the drugs are adjusted appropriately.

The majority of drugs bind reversibly to plasma proteins (e.g., serum albumin, AAG, lipoproteins) or other biological materials, such as erythrocytes (Kremer et al., 1988; Schmidt et al., 2008). In addition, there are also plasma proteins which have a high affinity towards certain hormones (e.g., transcortin, thyroxine-binding globulin). Of these proteins, human serum albumin (HSA) and AAG are frequently the main binding partners for drugs in plasma (Israili and Dayton, 2001; Bertucci and Domenici, 2002). While HSA is primarily responsible for the binding of acidic drugs, basic drugs display greater affinity for AAG (Piafsky, 1980; Kopecky et al., 2003). Neutral drugs can be bound to both HSA and AAG. However, these are general statements and are not a steadfast rule, since some drugs can bind to both HSA and AAG. Moreover, unlike HSA, AAG concentrations fluctuate dramatically in various disease conditions and inflammations (Israili and Dayton, 2001). This may

severely affect therapeutic efficacy of drugs which primarily bind to AAG. Plasma concentration of AAG is 0.4-1.1 mg/dL and may change under various physiological and pathological conditions (such as during the acute-phase reaction), resulting in alteration of the binding of various drugs and other ligands. Changes in drug binding and, consequently, alteration in the levels of unbound (free) drug (C_f) can have a significant effect on both the pharmacokinetics and pharmacodynamics of a drug (Meijer and Van der Sluijs, 1987; Belpaire and Bogaert, 1989). The binding of drugs to plasma proteins is often the first controlling step in drug distribution. Binding is an important determinant not only of drug action (both therapeutic and toxic) but also of disposition (Dayton et al., 1973; Wilkinson, 1983; Belpaire and Bogaert, 1989).

Cytochrome P450 (CYP) is the most prevalent drug metabolizing enzymes and is present predominantly in the intestine and liver. CYP3A4 is the most abundant form in the CYP-family (Kolars et al., 1992). CYP3A group represents the major drug-metabolizing enzyme and accounts for approximately 30% of hepatic CYP and more than 70% of intestinal CYP activity. Moreover, CYP3A is estimated to metabolize between 50% and 70% of currently administered drugs (Watkins, 1997). CYP3A4 enzyme is present in the liver and enterocytes (Guengerich et al., 1986). A significant amount of CYP3A is expressed in the enterocytes to metabolize xenobiotics during their transit across intestinal epithelium. All currently available HIV-1 protease inhibitors are metabolized by CYP3A4 (Jayakanthan et al.). As the HIV-1 treatment employs HAART practice, the co-administration of protease drugs leads to CYP3A4-related drug-drug interactions occur for metabolic clearance and for which elevated plasma concentrations are associated with serious and/or life-threatening events. The simple reason for this is to one drug modulates the metabolism of other (drug-

drug interactions) by simple competition for the same active site, and/or by binding in an allosteric region of the same enzyme (Tanaka, 1998). Amprenavir undergoes extensive first pass metabolism by CYP3A4. Ketoconazole (selective CYP3A4 inhibitor) inhibited the formation of major amprenavir metabolites. 3.7 μM of ritonavir completely inhibited the biotransformation of amprenavir by human liver microsomes (Treluyer et al., 2003). Metabolism of ritonavir, on the other hand, is caused by CYP3A4 and CYP2D6. It significantly inhibits the metabolism of CYP3A4 substrates like nifedipine and CYP2D6 substrates like dextromethorphan, when administered in combination (Hsu et al., 1998). In addition to oxidative metabolism, conjugation reactions may play an important role in detoxification of xenobiotics from the small intestine. Specific molecules are effluxed into intestinal lumen after being conjugated with a glucuronide or sulfate moiety within enterocytes.

Prodrugs are designed to be therapeutically inactive until *in vivo* activation to the parent drug, hence reliable *in vivo* activation of the prodrug is considered critical for their pharmacological activity (Han and Amidon, 2000). Thus controlling the mechanism of *in vivo* activation of prodrugs can be critical for prodrug delivery. Enzymatic and chemical processes are known to play an important role in the hydrolysis of prodrugs and it is well known that enzymatic processes play dominant role than chemical process (Anand et al., 2003). It is also well known that hydrolytic enzymes are present ubiquitously in all biological fluids and tissues. For example, esterases are expressed throughout the body and can be utilized in the hydrolysis of an ester functional group. The prodrug to drug conversion can take place by various enzymes in different tissues, by peptidases in the intestine (Das and Radhakrishnan, 1976); by esterases in the skin (Roy and Manoukian, 1994); by

phosphomonoesterases in plasma; by β-glucuronidases at tumor tissue (Watanabe et al., 1981). Hydrolases (esterases, peptidases, lipases, glycosidases, etc.) are enzymes well suited to use for drug inactivation since they are ubiquitously distributed. Insertion of ester bonds susceptible to enzymatic cleavage may represent one approach to make the action of a drug more restricted to the site of application (Graffner-Nordberg et al., 1998).

Di-peptide drugs synthesized have an ester linkage between drug and the first amino acid and peptide linkage between two amino acids. Hence, two major pathways of enzymatic degradation are possible. One possible pathway is regeneration of amino acid prodrug from di-peptide prodrug by aminopeptidases followed by regeneration of parent drug from enzymatic hydrolysis by esterases such as carboxylesterases and cholinesterases. Another possible enzymatic hydrolytic pathway is regeneration of parent drug directly from di-peptide prodrug through enzymatic hydrolysis by esterases. In order to clearly understand the fate of prodrug and its permeation into brain, clear understanding of enzymatic hydrolysis pathways is necessary.

The objective of this study is to determine protein binding affinity of APV prodrugs to plasma protein AAG and determining the binding affinities. Moreover APV is metabolized by CYP3A4 enzyme. Metabolic stability of APV prodrugs compared to drug was evaluated. For prodrugs to regenerate parent drug, enzymatic hydrolysis of prodrugs is necessary and rate limiting step in our pro-pro-drug (PPD) approach to improve oral and brain absorption simultaneously. Hence enzymatic stability of prodrugs in presence and absence of peptidase and esterase inhibitors was performed to delineate major pathway of enzymatic hydrolysis.

Materials and Methods

Materials

APV was a generous gift from GlaxoSmithKline USA, (Philadelphia, PA). All the prodrugs used in the study were synthesized according to the methods noted in Chapter 3. Sprague–Dawley rat plasma was purchased from Valley Biomedical Inc. (Winchester, VA). IGS Sprague–Dawley rat liver microsomes were obtained from XenoTech LLC (Lenexa, Kansas). Bestatin was purchased from USB Corporation (Cleveland, Ohio). Eserine and 4-(hydroxymercuri) benzoic acid sodium salt (PCMB) were obtained from Sigma Chemical Co. (St. Louis, MO). Human alpha 1-acid glycoprotein (AAG) was obtained from Sigma Chemical Co. (St. Louis, MO). Ketoconazole was obtained from Sigma Chemical Co. (St. Louis, MO). All other chemicals and solvents were purchased from Sigma Chemical Co. (St. Louis, MO) or Fisher Scientific Co. (Pittsburgh, PA). Male Sprague-Dawley rats were obtained from Charles River Laboratories (Wilmington, MA). Tissues were harvested in accordance to protocols approved by the IACUC at University of Missouri-Kansas City.

Determination of *in vitro* Protein Binding

The protein binding of APV and prodrugs in rat plasma were determined using ultra-filtration technique reported previously (Barrail et al., 2006). Briefly, stock solutions (100 µL) of APV or prodrugs in isotonic phosphate-buffered saline (IPBS), pH 7.4, containing 8 g/L NaCl, 0.2 g/L KCl, 1.44 g/L Na_2HPO_4, and 0.24 g/L KH_2PO_4, were added into 900 µL blank rat plasma to yield final concentrations of 10 µM. Equal volume of fresh IPBS (pH7.4) replaced drug solutions to be used as control to evaluate non-specific adsorption and plasma binding. During the 30 min-equilibration at 37°C, spiked plasma samples were agitated gently every 10 min. Then 500 µL samples were transferred to Amicon ultra-0.5mL centrifugal filters (10 k NMWL, Millipore Corporation, Bedford, MA) and centrifuged at 10,000 ×g, 37°C, for 1 h. Around 250 µL of ultra-filtrate containing the unbound drug was

obtained in basolateral chamber. After centrifugation, aliquots of filtered (200 µL) and unfiltered (20 µL, diluted with IPBS to 200 µL) samples were taken and analyzed using LC-MS/MS immediately to calculate protein binding of drugs in rat plasma. Unbound fraction (f_u) was calculated by the ratio of drug in the filtered samples to the sum of filtered and unfiltered samples. Similarly to determine the affinity of APV and prodrugs, various concentrations of drugs ranging from 1-50 µM were incubated with 0.5 mg/mL of AAG dissolved in IPBS. Solutions were incubated for 30 minutes at 37°C. These solutions were transferred to Amicon ultra-0.5mL centrifugal filters (10 k NMWL, Millipore Corporation, Bedford, MA) and centrifuged at 10,000 ×g, 37°C, for 1 h. 250 µL of ultra-filtrate containing the unbound drug was obtained in basolateral chamber. After centrifugation, aliquots of filtered (200 µL) and unfiltered (20 µL, diluted with IPBS to 200 µL) samples were taken and analyzed using LC-MS/MS immediately to determine unbound drug concentration.

Stability in Rat Liver Microsomes

Rat liver microsomes were employed to study the prodrug affinity for CYP3A4 relative to APV. Individual incubations (final volume 1mL) consisted of 0.2 mg/mL microsomal protein in 100mM phosphate buffer (pH 7.4) with final concentrations of 5mM magnesium chloride, 5mM glucose 6-phosphate, 1mM b-NADP1, and 1U/mL glucose 6-phosphate dehydrogenase. The drug/prodrug (25 µM), buffer, and microsomes were mixed and kept at 37°C for 5min. The reaction was initiated by adding the NADPH generating system. Incubations were conducted at 37°C. The metabolic reaction was stopped by adding equal volumes of ice-cold acetonitrile: methanol (5:4) mixture. Samples were stored at −80˚C until further analysis. Both time dependent and concentration dependent stability studies were performed.

For time dependent degradation studies, various test compounds (25µg/mL) were incubated with activated liver microsomal solution, respectively. Degradation study was conducted for a period of 2 h. At predetermined time points 100 µL of samples were withdrawn and equal volume of acetonitrile was added to terminate the degradation process. Samples were stored at -80° C until further analysis with LC-MS/MS. For concentration dependent degradation studies, various concentrations of test compounds ranging from (1-20 µM) were incubated with activated microsomal solution for 5 min. Enzymatic degradation was terminated by adding equal amount of acetonitrile and samples in -80° C until further analysis with LC-MS/MS. To determine the effect of ketoconazole, which is well known substrate of CYP3A4, drugs/prodrugs were incubated for five minutes with microsomes in presence and absence of ketoconazole.

Stability in Tissue Homogenate

Male Sprague-Dawley rats were euthanized by a lethal injection of sodium pentobarbital through the tail vein (100 mg/kg). Intestinal segments, livers and brain were isolated and stored at -80°C. Tissues were homogenized in 10 mL of chilled isotonic phosphate buffered saline (IPBS) with a tissue homogenizer (Multipro variable speed homogenizer, DREMEL; Racine, WI) in an ice bath. Subsequently, the homogenates were centrifuged at 14,000g for 25 min at 4°C to remove cellular debris, and the supernatant was used for hydrolysis studies. Suitable dilutions were made to achieve a final protein concentration of 1.0 mg/mL. Protein content was determined according to the method of Bradford (Bradford, 1976) with BioRad protein estimation kit. Supernatant was equilibrated at 37°C for about 30 minutes prior to initiation of an experiment. Intestinal, liver and brain homogenate studies were initiated by adding 0.5 mL of l00µM prodrug stock solution to 4.5

mL of tissue homogenate. The control consisted of 4.5 mL of IPBS instead of supernatant. Aliquots (50µL) were withdrawn at appropriate time interval for up to 24 hr. Samples were immediately diluted with equal volumes of ice-cold acetonitrile:methanol (5:4) mixture to stop the enzymatic reaction and then stored at -80°C until further analysis. Apparent first order rate constants were calculated and corrected for any chemical hydrolysis observed in the control

Enzymatic Hydrolysis Studies

Enzymatic hydrolysis of APV prodrugs was determined in triplicate in rat plasma in the presence or absence of various hydrolytic enzyme inhibitors. Frozen Sprague–Dawley rat plasma was thawed quickly before experiment and diluted to 85% (v/v) with IPBS (pH 7.4) to maintain the pH of solution. Prior to the initiation of hydrolysis study, plasma and intestinal homogenate were equilibrated at 37ºC for 15 min after adding enzyme inhibitors. The concentrations for enzyme inhibitors PCMB (*p*-chloromercuribenzoic acid), eserine, bestatin, were 1, 1, and 0.5 mM respectively, were well within the acceptable range. Hydrolysis was initiated in a test tube by the addition of APV or prodrug solution to 1mL plasma or intestinal homogenate in the presence or absence of enzyme inhibitor. Final prodrug concentration in the reaction mixture was 25µM. Test tubes were incubated at 37ºC in a shaking water bath (45 rpm) and aliquots (50 µL) were withdrawn at appropriate time intervals for up to 24 h. Samples were immediately diluted with 50 µL chilled acetonitrile to quench the reaction, and centrifuged at 12,500 rpm for 15 min to precipitate protein. The supernatants were stored at -80ºC until further analysis by LC–MS/MS.

Sample Preparation and Analysis

Protein binding, enzymatic and liver microsomal stability samples were analyzed using a highly robust and sensitive LC-MS/MS technique. Samples were prepared using liquid-liquid extraction technique and verapamil (100 nM) as internal standard. Briefly, 100 µL of verapamil and acetonitrile was added to each sample. Then, 600 µL of water saturated ethyl acetate was added and samples were vortexed for 2 min. This process allowed test compounds to partition between organic and aqueous phase. Following vortexing, samples were centrifuged at the speed of 10,000 rpm for 7 min for separation of two layers. Approximately, 500 µL of organic layer was carefully separated and evaporated under reduced pressure for 45 min. The residue was reconstituted in 100 µL solution of 70 % acetonitrile and 30% water containing 0.1% formic acid and analyzed using LC-MS/MS technique. Similarly, standard solution of test compounds (0.3-5 µg) were extracted and analyzed with LC-MS/MS.

LC-MS/MS analysis

Protein binding, enzymatic and microsomal stability samples were analyzed using LC–MS/MS technique. QTrap® LC–MS/MS mass spectrometer (Applied Biosystems/Sciex) equipped with Agilent 1100 series quaternary pump (Agilent G1311A), vacuum degasser (Agilent G1379A), and autosampler (Agilent G1367A) was used. Electrospray ionization (ESI) in positive mode was used for sample analysis. Test compounds were detected in multiple-reaction monitoring (MRM) mode. Briefly, test compounds were separated using a reverse phase XTerra® MS C18 column with dimensions of 4.6 x 50 mm and particle size of 5 µm. Mobile phase (70% acetonitrile and 30% water containing 0.1% formic acid) was continuously pumped through the column at a constant flow rate of 0.25 mL/min. 20µL of samples were injected in the system and chromatographs were obtained for 5.5 min.

Precursor ions of test compounds were determined from spectra which are generated with the infusion of standard solutions to the electrospray source with the aid of an infusion pump. Each of these precursor ions is subjected to collision-induced dissociation to produce product ions. Precursor and product ion for test compounds were APV + 506.3/155.9; VVA + 704.4/156.1; GVA + 662.4/156.0; VA + 605.4/156.0 and Verapamil (IS) + 455.3/165.1. The turbo ion spray setting and parameters were optimized (IS voltage: 5500 V, temperature: 300° C, nebulizer gas: 40 psi, curtain gas: 40 psi). Nitrogen gas was used as collision gas. Other operational parameters included declustering potential (DP): 95 V; collision energy (CE): 70 V; entrance potential (EP): 8.5 V; and collision cell exit potential (CXP): 4.0 V. These parameters were generated by running analytes of interest in quantitative optimization mode. The analytical data for each test compounds generated with MRM method generated a significant linearity up to ng/mL range. With the help of this method, rapid and reproducible results were successfully obtained. Peak areas for test compounds and internal standard were determined using Analyst™ software.

Data Analysis

For protein binding studies, unbound drug concentrations vs. concentration was plotted. Scatchard plot, bound/free vs. bound of saturation binding data was plotted. The binding data was fit into ligand binding model as given below. The data was analyzed using Prism® (GraphPad Software, La Jolla, CA).

$$B = B_{max} \times \frac{C_u}{K_d + C_u} + NS \times C_u \quad \text{.....Eq. 1.}$$

Where K_d is the equilibrium dissociation constant, B_{max} is binding capacity, C_u is fraction unbound and NS is non-specific binding. In order to avoid the non-specific binding, pure

AAG was used instead of plasma and siliconized tubes or coated with Sigmacote® were used to avoid drug binding to plastic.

For oxidative metabolism studies, K_e and $t_{1/2}$ of each drug in rat liver microsomes were calculated by plotting the natural logarithm of drug concentrations versus time. The data of metabolic rates (substrate turnover per minute per milligram microsomal protein) were fit to Michaelis–Menten equation by nonlinear regression to determine the kinetic parameters *K*m and *V*max. Data modeling was conducted using KaleidaGraph (Synergy Software, Reading, Pennsylvania). *In vitro* intrinsic clearance (CL_{int}) was subsequently represented by dividing *V*max by *K*m as shown in Eq. 2.

$$V = V_{max} \times \frac{[S]}{K_m + [S]} \quad \text{..... Eq. 2.}$$

Where *V* represents the total rate of uptake, *V*max is the maximum uptake rate for the carrier-mediated process, *K*m (Michaelis–Menten constant) is the concentration at half-saturation, and [*S*] is the substrate concentration. For hydrolytic metabolism study in rat plasma and tissue homogenate, degradation rate constants (K_d) were calculated by plotting the natural logarithm of drug concentrations against time, and $t_{1/2}$ were estimated by degradation rate constants.

Results and Discussion

Protein Binding

APV and prodrugs (10µM) were incubated in rat plasma for 30 minutes at 37ºC. From the samples obtained by ultrafiltration followed by centrifugation, unbound fraction of the drug was determined. Results are summarized in Table 4.Unbound fraction of VVA and GVA was found to be 1.41 ±0.16 and 1.18 ±0.08 whereas 0.68 ±0.09 for APV. Unbound fraction of VA is comparable to drug (0.82 ±0.1). Percentage of unbound drug was found to

be 7 for APV & 13 and 11 for VVA and GVA. This data clearly suggest that the di-peptide prodrugs have less or comparable binding to plasma proteins. However this study was performed using plasma where several plasma proteins are present. Other than plasma proteins, various enzymes are also present because of which we may not exactly translate this data into exclusive protein binding.

In order to delineate the affinity of APV and prodrugs to plasma AAG, concentration dependent protein binding studies were performed. Physiological concentration of AAG varies from 0.4 to 1.1 mg/mL. Hence various concentrations of drugs were incubated with 0.5 mg/mL AAG in IPBS pH 7.4. Free unbound fraction of drug/prodrug was measured after ultrafiltration followed by centrifugation. The data obtained was fit into saturation binding model and binding parameters Equilibrium dissociation constant (K_d) and binding capacity (B_{max}) were calculated using Graphpad Prizm® software. To minimize the non-specific binding, drug binding was determined in AAG solution and all siliconized tubes or Sigmacote® coated tubes were employed. The results obtained were depicted in Table 5. The saturation binding data and Scatchard plots were depicted in Figure 15 (for APV and V-APV) and Figure 16 for (VV-APV and GV-APV). The X-intercept from the Scatchard plot gives B_{max} and Y-intercept gives B_{max}/K_d. As explained earlier, K_d is equilibrium dissociation constant, concentration at which binding site is half occupied. $1/ K_d$ gives the affinity and B_{max} is the binding capacity. APV exhibited K_d value of 5.99 ± 1.02 μM whereas VA, VVA and GVA has K_d of 7.43 ± 1.55, 9.88 ± 1.63 and 11.44 ± 1.9 μM respectively. These results clearly demonstrate that VVA and GVA exhibited reduced affinity in binding to AAG compared to drug. VA has reduced or equal affinity for binding to AAG. However, B_{max} values for drug and prodrugs were comparable. B_{max} value of APV was found to be 17.35

nmoles/mg and VA, VVA and GVA has B_{max} values 19.03, 19.44 and 24.57 nmoles/mg. Decrease in affinity and comparable binding capacity clearly suggest that the prodrugs are easily displaceable from protein compared to drug. Moreover, reduced AAG binding affinity may result in increased free drug concentration available for therapeutic efficacy. Other than plasma, AAG is known to be present in various organs in the body including vascular endothelial cells. Hence it is advantageous to have more unbound drug in brain vascular endothelial cells.

	Unbound fraction (*f*u)	**Percentage of unbound drug**
APV	0.68 ±0.09	7
V-APV	0.82 ±0.1*	9
VV-APV	1.41 ±0.16*	13
GV-APV	1.18 ±0.08*	12

Table 4. Unbound fraction (f_u) of APV and prodrugs (10 μM) in rat plasma. Data represented are mean ± SE (n = 4). *P < 0.05 statistical difference between APV and prodrug values.

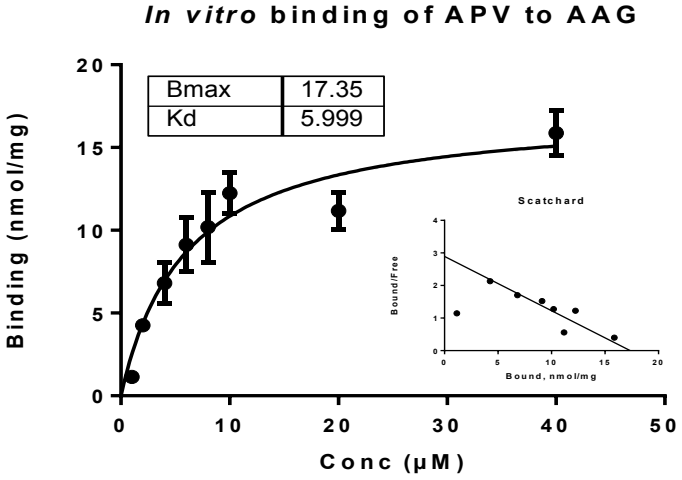
In vitro binding of APV to AAG
Bmax 17.35
Kd 5.999
Binding (nmol/mg)
Conc (µM)
Scatchard
Bound/Free
Bound, nmol/mg

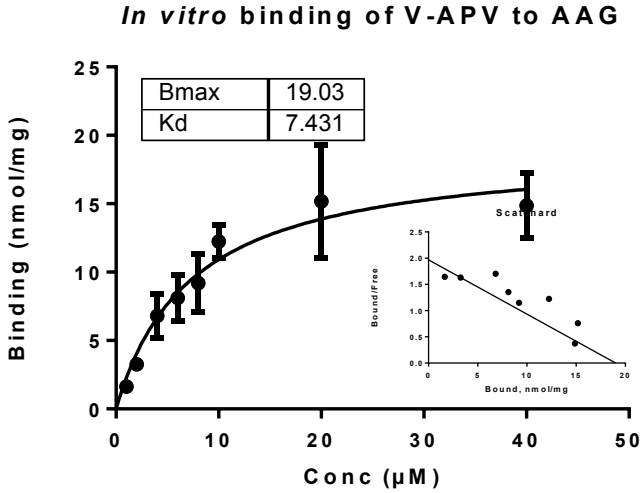
In vitro binding of V-APV to AAG
Bmax 19.03
Kd 7.431
Binding (nmol/mg)
Conc (µM)
Scatchard
Bound/Free
Bound, nmol/mg

Figure 15. *in vitro* Saturation protein binding kinetics of APV (top) and V-APV (bottom) obtained by incubating 1-50µM of APV and V-APV with 0.5 mg/mL of plasma protein alpha 1- acid glycoprotein(AAG). Values are expressed in mean ± SD.

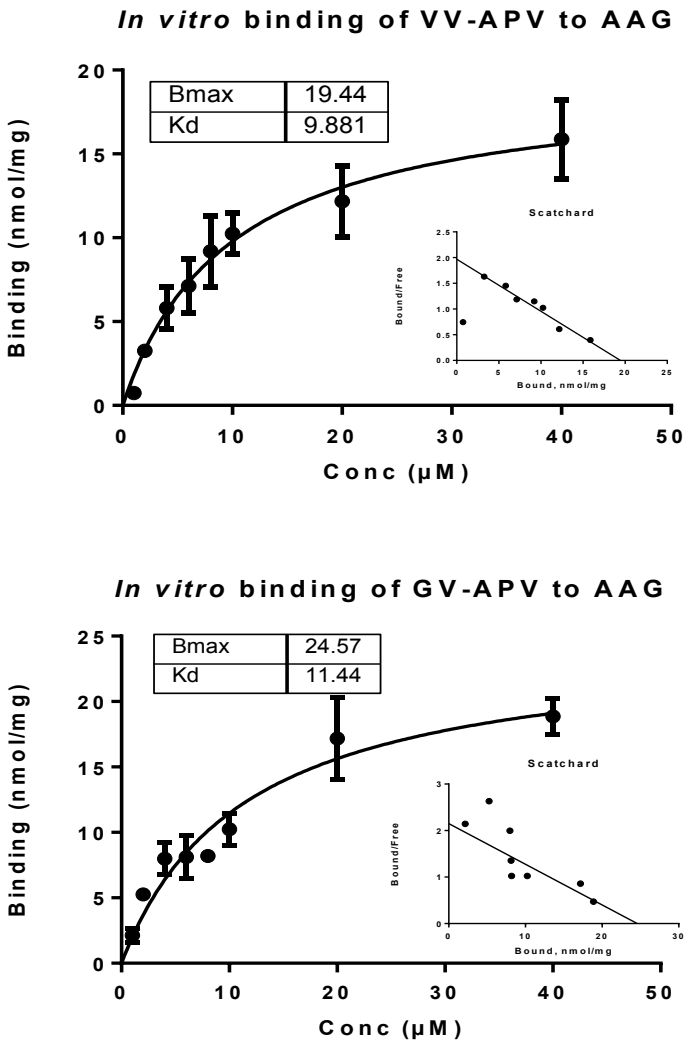

Figure 16. *in vitro* Saturation protein binding kinetics of VV-APV (top) and GV-APV (bottom) obtained by incubating 1-50μM of VV-APV and GV-APV with 0.5 mg/mL of plasma protein alpha 1- acid glycoprotein(AAG). Values are expressed in mean ± SD.

Table 5. *in vitro* protein binding kinetic parameters of APV, V-APV, VV-APV and GV-APV obtained by incubating 1-50μM of APV and V-APV with 0.5 mg/mL of plasma protein alpha 1- acid glycoprotein(AAG). (*) indicates statistical significant difference compared to APV at $p<0.05$. Values are expressed in mean ± SD.

	K_d (μM)	**B_{max} (nmoles/mg)**
APV	5.99 ± 1.02	17.35 ± 1.06
V-APV	7.43 ± 1.55	19.03 ± 1.53
VV-APV	9.88 ± 1.63*	19.44 ± 1.35
GV-APV	11.44 ± 1.9*	24.57 ± 2.8

Metabolic stability Studies

APV undergoes extensive first pass metabolism and primarily metabolized by CYP3A4. Hence we tried to determine the metabolic stability of prodrugs and affinity of prodrugs toward CYP3A4 in comparison to drug. Metabolic stability of APV and prodrugs in rat liver microsomes (0.2 mg/mL) was determined. Degradation rate constant and half-life were determined. The first order degradation rate profiles (percentage of drug/prodrug remaining vs. time) were shown in Figure 17. Degradation rate constants and half-lives were given in Table 6. Degradation rate constant of amino acid prodrug V-APV was found to be 0.009 min^{-1} whereas 0.013 min^{-1} for APV. Di-peptide prodrugs VV-APV and GV-APV exhibited 1.76 and 1.65 times slower degradation compared to drug with degradation rates 0.0068 and 0.0071 min^{-1} respectively. These results clearly suggest that the di-peptide prodrugs have slightly reduced affinity for metabolic enzymes in rat liver microsomes and exhibited 1.7 times longer half-lives.

In order to further confirm these results, concentration dependent metabolism was performed. APV and prodrugs with concentrations ranging from 1-20μM were incubated with 0.2 mg/mL rat liver microsomes for 10 minutes. By fitting the data in Michaelis-Menten kinetic model, we determined K_m and V_{max} values. The results were depicted in Table 7. prodrugs exhibited slightly low affinity with K_m values 9.1 ± 2.4 μM for VA, 9.3 ± 3.0 μM for VVA and 9.9 ± 3.7 μM for GVA whereas Km for APV is 6.2 ± 2.0 μM. These results

clearly demonstrate that the prodrugs have less affinity for metabolizing enzymes. Intrinsic clearance of drug/prodrugs was calculated from ratio of V_{max} and K_m. Among all the prodrugs VV-APV has less intrinsic clearance (0.22 mL/min/mg protein) compared to APV (0.36 mL/min/mg protein). To further compare the metabolic stability of prodrugs vs. drug, stability of drug/prodrugs was determined after incubating in 0.1 mg/mL rat liver microsomes for 10 minutes in presence and absence of ketoconazole (10μM). Ketoconazole is a well-known inhibitor of CYP3A4. In presence ketoconazole, amount of APV remaining is approximates 40% more compared to control which is APV without ketoconazole. Results from this study are represented in Figure 18. For all the prodrugs these is no significant difference was observed between control and in presence of ketoconazole. This study was performed with very low concentration of microsomes (0.1mg/mL) in order to compare the metabolic stability and affinity of prodrugs for CYP enzymes. From all these studies it is clear that prodrugs have better metabolic stability than APV and slightly lower affinity for CYP enzymes. Thus these prodrugs may bypass first pass effect to a significant amount compared to drug.

Table 6. Degradation rate constants and half-lives of APV and prodrugs in rat liver microsomes. Study was conducted in rat liver microsomes (0.2 mg/mL) at 37°C. Values are expressed as mean ± SD (n=4)

	$k_{obs} \times 10^2$ (min^{-1})	**$t_{1/2}$ (min)**	**Fold difference in $t_{1/2}$**
APV	1.21 ± 0.09	57 ± 8	
V-APV	0.95 ± 0.01	73 ± 5	1.26
VV-APV	0.68 ± 0.01	101 ± 12	1.76

GV-APV	0.71 ± 0.01	95 ± 7	1.65

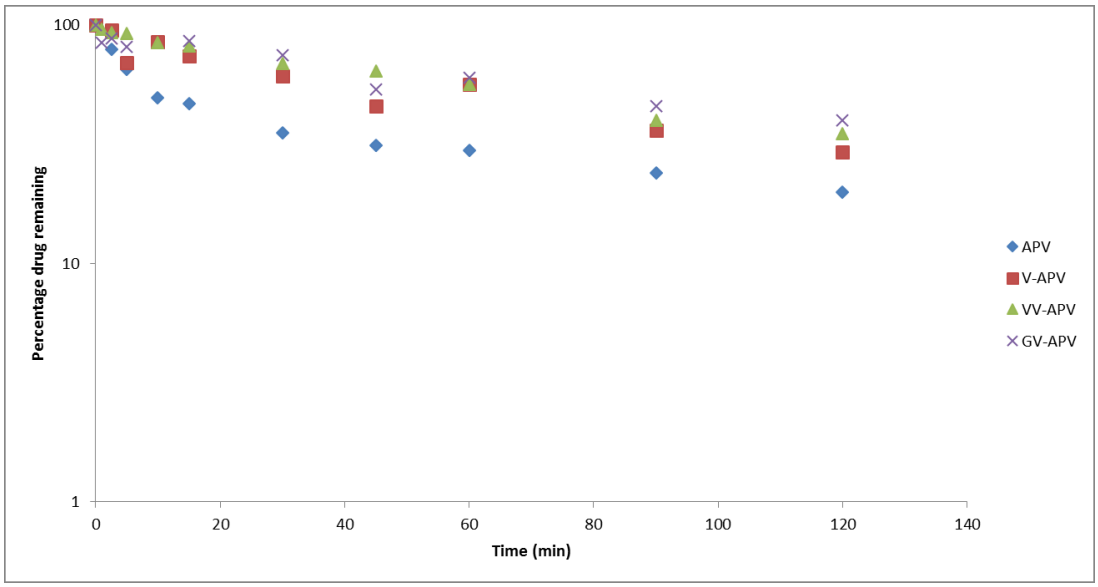

Figure 17. Enzymatic degradation profiles of APV and prodrugs (10μM) in rat liver microsomes (0.2mg/ml) at pH 7.4 for two hours.

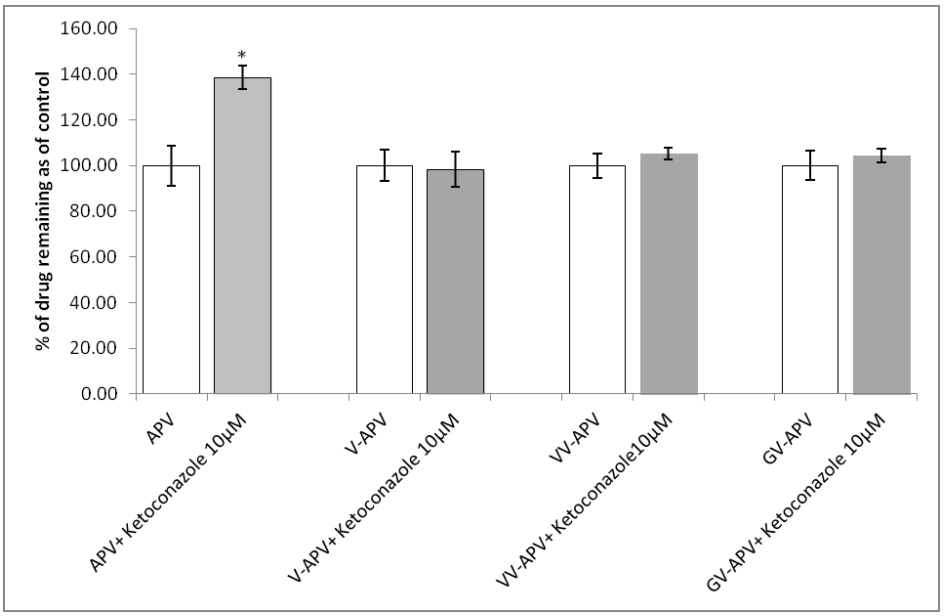

Figure 18. Amount of drug/prodrug remaining after 5 min incubation with rat liver microsomes (0.1 mg/ml), in presence and absence of Ketoconazole. *Data points are expressed as mean ±SD, n=4. (*)* represents significant difference from control

Table 7. Kinetic parameters K_m, V_{max} and *in vitro* intrinsic clearance (CL_{int}) of APV and prodrugs in 0.2 mg protein/mL rat liver microsomes (mean ± SD, n = 3).

Compounds	**V_{max} (nmoles/min/mg protein)**	**K_m (μM)**	**CL_{int} (mL/min/mg protein)**
APV	2.3 ± 0.4	6.2 ± 2.0	0.38 ± 0.03
V-APV	3.2 ± 0.5	9.1 ± 2.4	0.31 ± 0.02
VV-APV	2.0 ± 0.3	9.3 ± 3.0	0.22 ± 0.01
GV-APV	3.0 ± 1.0	9.9 ± 3.7	0.29 ± 0.02

Stability in Tissue Homogenates

The half-lives for prodrugs of APV in intestinal, liver and brain homogenate have been summarized in Table 8. The di-peptide ester prodrugs are first converted to amino acid prodrug and then further degraded to the active parent drug, APV. The major pathways of enzymatic hydrolysis appeared to be cleavage of the peptide and ester bond. There was no significant difference in the half-lives of Val- Val-APV and Gly-Val-APV in liver and intestinal homogenates. Significant difference between V-APV and di-peptide prodrugs was noted.

Table 8. Half-lives (hr) of APV prodrugs in intestinal, brain and liver homogenate (1 mg/mL). Studies were conducted at 37°C. Values reported are mean ± SD (n=3).

compound	Intestinal homogenate (t ½ mins)	Brain Homogenate (t ½ mins)	Liver homogenate (t ½ mins)
V-APV	220 ± 15	120 ± 13	25 ± 6
VV-APV	290 ± 40	173 ± 12	32 ±2
GV-APV	230 ± 10	140 ± 13	22 ± 5

Enzymatic stability studies

Enzymatic stability of prodrugs was measured in rat plasma (85%) diluted with IPBS to maintain the pH (7.4). In plasma all the prodrugs, VA, VVA, and GVA exhibited better stability. First order degradation rate constants and half-lives were determined by plotting log concentration vs. time and are shown in Table 9. The di-peptide prodrugs VVA and GVA have half-life of 64 ± 9 and 28 ± 2 minutes respectively whereas half-life of VA was found to be 50 ± 13 minutes. Among all the prodrugs VVA exhibited better stability.

The di-peptide prodrugs VVA and GVA have ester linkage between valine and APV and a peptide linkage between both amino acids. In order to determine the hydrolytic pathway, degradation profile of prodrugs in plasma in presence and absence of enzyme inhibitors was performed. The di-peptide prodrug may undergo enzymatic hydrolysis at two possible positions. The possible enzymatic degradation pathways are depicted in figure 19. One possibility is enzymatic bioreversion of PPD to PD by plasma amino peptidases followed by subsequent conversion of PD to D. Another possibility is simultaneous activity of both aminopeptidases and carboxylesterases which result in formation of PD and D simultaneously from PPD. Another possibility is direct activity of esterases on PPD generating D directly without forming the intermediate PD. For the proposed hypothesis, to improve brain absorption, mean residence time of PD is necessary and rate limiting step. In

Oder to determine which the most predominant pathway is, we determined the stability of prodrugs in plasma in presence of bestatin (0.5mM), eserine (1mM) and PCMB (1mM). Bestatin is a competitive and specific inhibitor of aminopeptidases. Eserine is cholinesterase irreversible inhibitor whereas PCMB is carboxyl esterase inhibitor and sulfhydryl group modifier. First order degradation rate constants and half-lives are given in Table 9.

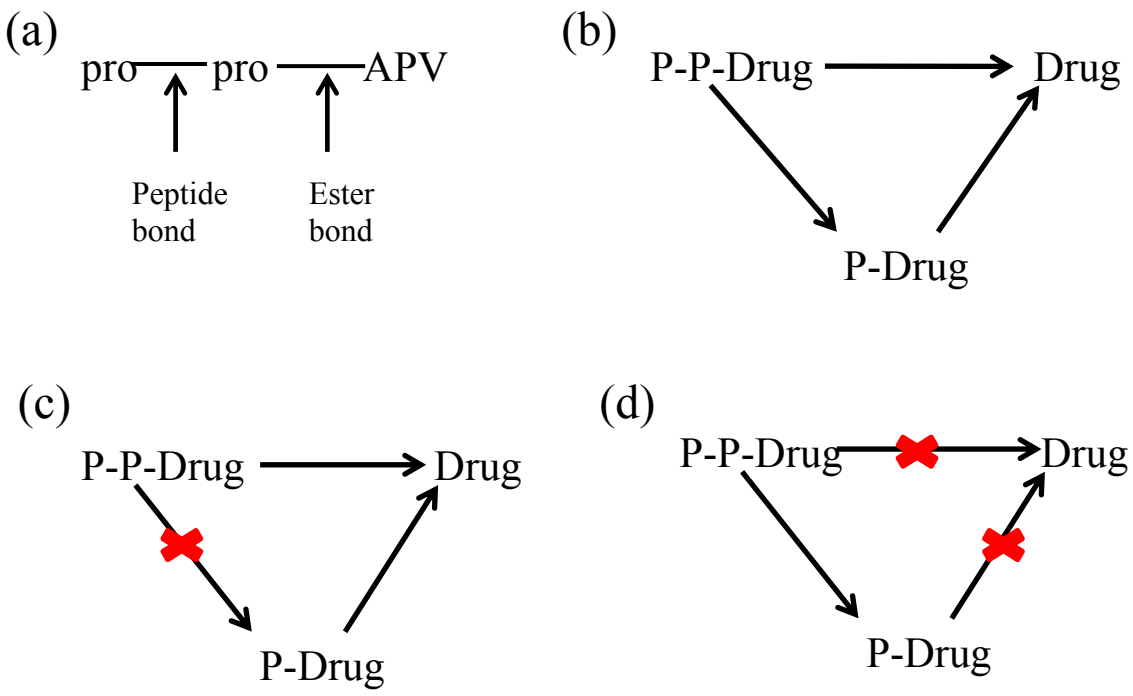

Figure 19. (a) Position of ester and peptide bonds in di-peptide pro-pro-drug (PPD). (b) Possible enzymatic degradation pathways involved in bioreversion of PPD. (c) Pathway inhibited by peptidase enzyme inhibitors. (d) Pathways inhibited by esterase inhibitors.

Table 9. Degradation rate constant and half-life of APV and prodrugs in presence and absence of enzyme inhibitors: Bestatin (aminopeptidase inhibitor), Eserine (cholinesterase inhibitor), PCMB (carboxylesterase inhibitor). Study was performed at 37^{o} for 24 hours. *Values are expressed as mean ±S.D. n=3.*

	G-V-APV		V-V-APV		V-APV	
Control	2.46 ± 0.08	28.1 ± 1.9	1.08 ± 0.09	64 ± 9	1.38 ± 0.08	50 ± 13
Eserine (1mM)	2.0 ± 0.4	37 ± 9	1.3 ± 0.2	57 ± 11	0.1 ± 0.01	722 ± 94

ND: No significant degradation; ---: not determined

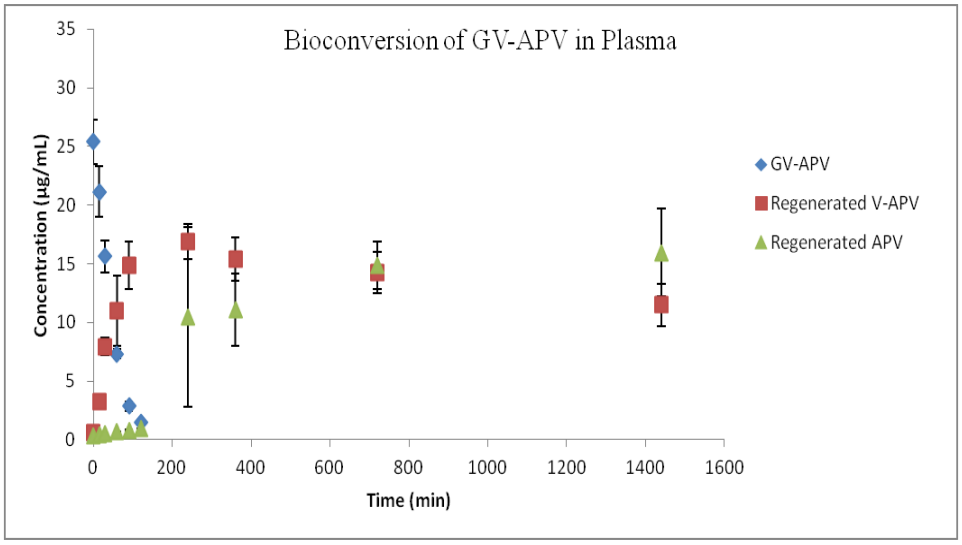
Bioconversion of GV-APV in Plasma
Concentration (µg/mL)
Time (min)
GV-APV
Regenerated V-APV
Regenerated APV

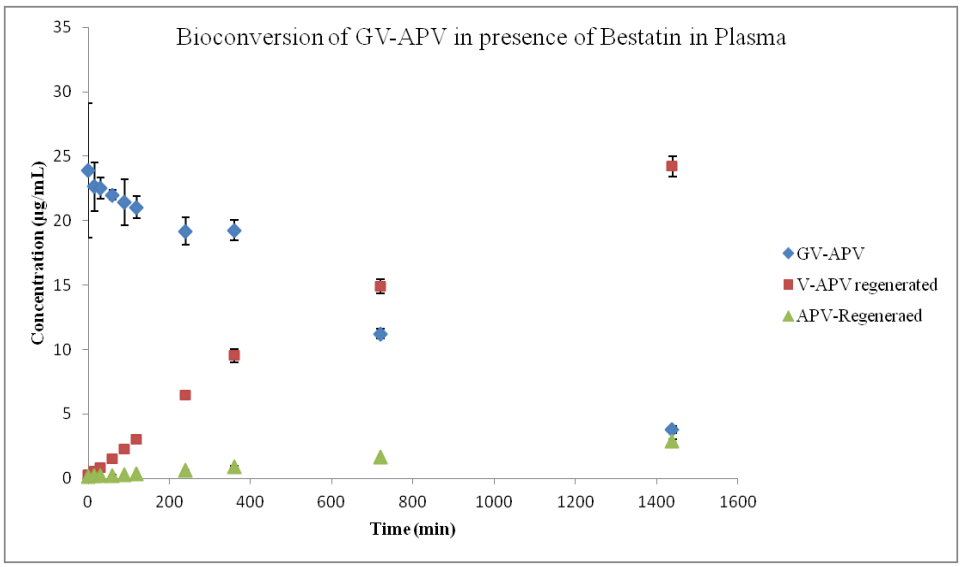
Bioconversion of GV-APV in presence of Bestatin in Plasma
Concentration (µg/mL)
Time (min)
GV-APV
V-APV regenerated
APV-Regeneraed

Figure 20. Concentration vs. time degradation of profile of GV-APV in 85% rat plasma in absence (control) (top) and presence of bestatin (0.5mM) (bottom). *Data points are expressed as mean ± SD, n=3*

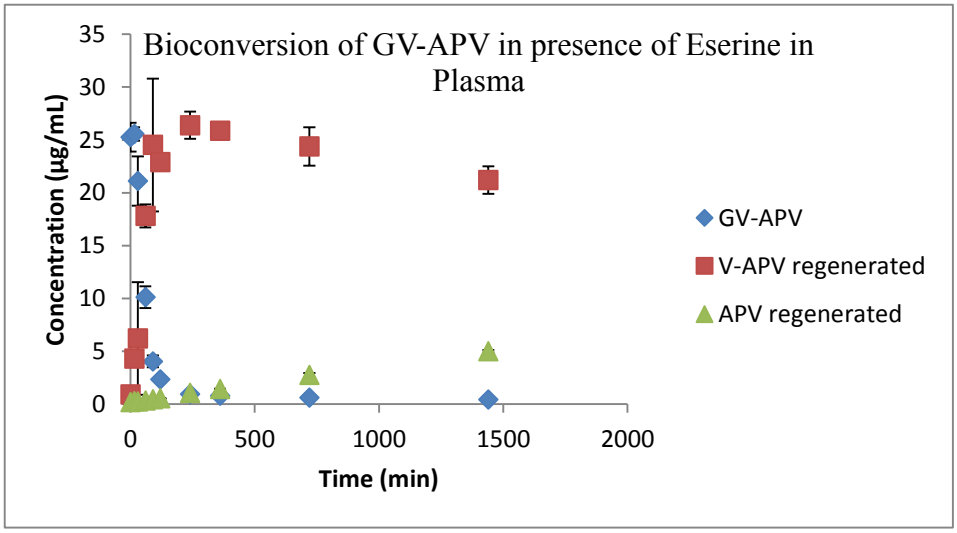

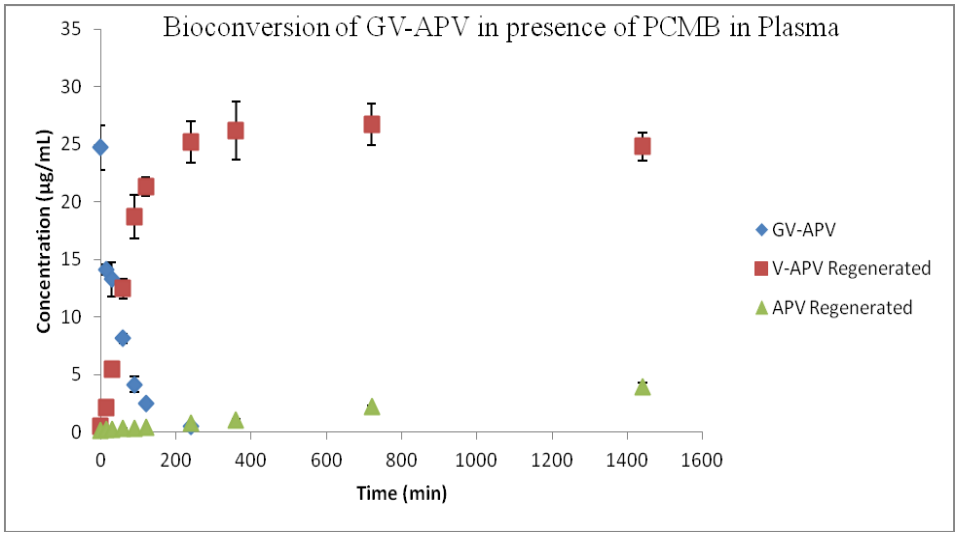

Figure 21. Concentration vs. time degradation of profile of GV-APV in 85% rat plasma in presence of eserine (1mM) (top) and presence of PCMB (1 mM) (bottom). *Data points are expressed as mean ± SD, n=3*

In presence of bestatin rate of degradation of GVA was reduced from $2.46 \times 10^{-2}min^{-1}$ (control) to 0.124×10^{-2} min^{-1}. This clearly suggests that when bestatin inhibited peptidase enzyme activity half-life of GVA increased from 28 minutes to 561 minutes. It is clear that GVA did not undergo enzymatic hydrolysis by esterases to a significant amount. Rate of degradation of GVA in presence of Eserine and PCMB (both esterase inhibitors) was found to be $2.0 \times 10^{-2}min^{-1}$ and $2.6 \times 10^{-2}min^{-1}$ respectively, which is comparable with control without any inhibitors. These results suggest that peptidase inhibitors increased degradation rate tremendously whereas esterase inhibitors have little or no effect on degradation rate. Similar trend was observed with VVA. In presence of bestatin no significant degradation of VVA was observed. However in presence of eserine and PCMB no significant difference in rate of degradation was observed. From these results it is clear that bioreversion of GVA and VVA to VA is the predominant pathway compared to GVA and VVA regenerating drug directly by esterase activity. Enzymatic stability of amino acid prodrug VA was also tested. Surprisingly VA exhibited better enzymatic stability with degradation rate of $1.38 \times 10^{-2}min^{-1}$ which is inhibited approximately ten times by eserine. In presence PCMB no significant degradation of VA was observed.

Even though these results give a clear indication that GVA and VVA undergo sequential hydrolysis, we determined different rate constants for GVA. Degradation profile

of GVA in plasma control and in presence of bestatin was depicted in Figure 20. Similarly degradation profile of GVA in presence of eserine and PCMB was depicted in Figure 21. In control GVA degraded completely in about 150 minutes and regeneration of VA and APV can be clearly seen. However in presence of bestatin rate of degradation of GVA, formation of VA and APV was significantly slowed down. In presence of eserine and PCMB, no significant difference in rate of degradation of GVA was observed. However rate of formation of APV was significantly slowed which is due to inhibition of esterase activity. Different rates k11, k21 were estimated by using Phoenix WinNonlin® software and fitting amount of amino acid prodrug, VA, generated vs. time in one compartmental model with first order elimination. Results are given in Table 10. GV-APV in plasma control exhibited degradation rate k11 as $1.8 \times 10^{-2}min^{-1}$ and k21 $0.4 \times 10^{-2}min^{-1}$. In presence of bestatin rate of formation of VA, k11 was reduced by 20 times to $0.09 \times 10^{-2}min^{-1}$, which in turn increase degradation half-life of VA regenerated from GV-APV. However in presence of PCMB, no significant difference in k11 compared to control was observed but k21 was reduced to $0.05 \times 10^{-2}min^{-1}$ and is comparable with k21 in presence of bestatin. Overall, in presence of peptidase inhibitor, rate of formation of VA was inhibited which in turn affected rate of degradation of VA. However in presence of PCMB, rate of formation of VA is same as rate of degradation of GV-APV control but degradation of VA to APV was significantly inhibited. This negligible k21 in presence of enzyme inhibitors clearly suggest that undergoes sequential hydrolysis of di-peptide pro-pro-drug is more prominent compared to ester hydrolysis of pro-pro-drug to drug.

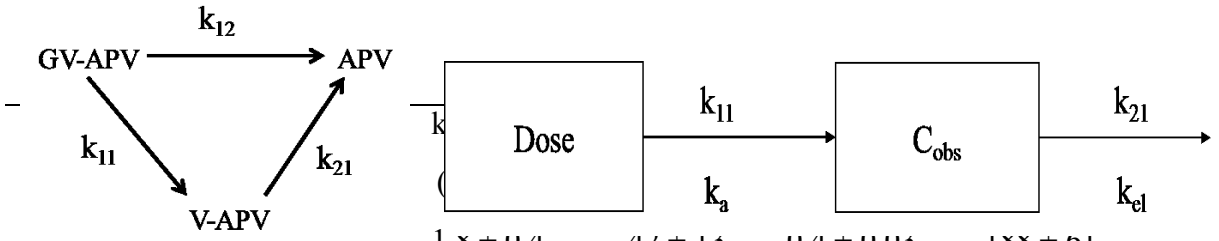

	1.8 ± 0.4	42 ± 13	0.4 ± 0.03	188 ± 61	
GV- APV + Bestatin(0.5mM)	0.09 ± 0.02	720 ± 122	0.04 ± 0.005	1460 ± 298	
GV-APV + PCMB (1 mM)	1.4 ± 0.2	48 ± 8	0.05 ± 0.008	1589 ± 339	

Note: k_{11} is rate of formation of V-APV and k_{21} rate of degradation of V-APV

Table 10. Degradation rate constants of GV-APV in plasma in presence and absence of bestatin (0.5mM) and PCMB (1mM). *Values are expressed as mean ± SD. n=3.*

Conclusions

APV binds to plasma proteins and 90% of the drug binds to AAG. Protein binding of drugs significantly alters both pharmacokinetic and pharmacodynamics properties of drugs. Protein binding studies performed in rat plasma using ultrafiltration technique revealed that 7% of APV is unbound to plasma proteins. Prodrugs VVA and GVA has 13 and 12 % drug was unbound to plasma proteins. Since only unbound fraction of drug can exert pharmacological action, in terms of unbound fraction, approximately 60 % increase is observed. To further determine the affinity of APV and prodrugs with AAG, concentration dependent binding to AAG was performed. The K_d values clearly indicate that prodrugs have less affinity for AAG compared to APV. However the maximum binding B_{max} is comparable for drug and prodrugs. The saturation binding data clearly suggest that prodrugs are binding to single binding site at AAG. With low affinity and comparable maximum binding, prodrugs can be easily displaceable compared to drug which may result in high protein unbound fractions compared to APV are possible with prodrugs. Metabolic stability studies clearly demonstrate that prodrugs exhibited better stability than drug itself. Intrinsic clearance of

drugs *in vitro* was significantly reduced for prodrugs. It is clear from the metabolism studies that prodrugs have better metabolic stability and less affinity for CYP enzymes. Results from enzymatic stability studies clearly suggest that di-peptide prodrugs undergo sequential hydrolysis. Di-peptide PPDs can be cleaved by esterases and peptidases. Degradation rate constants and half-lives of prodrugs in plasma in presence and absence of enzyme inhibitors clearly demonstrates that peptide hydrolysis following ester hydrolysis is predominant pathway compared to direct ester hydrolysis generating drug directly from PPD. This may result in longer residence time of amino acid PD in systemic circulation following oral administration. It is clear that esterase activity in rat plasma is higher than human plasma. Slower ester hydrolysis of prodrugs may result in much longer residence time of amino acid prodrug in humans. Surprisingly V-APV exhibited good stability compared to other amino acid prodrugs synthesized in our laboratory. From the data obtained in this study and previous work from our laboratory suggests that valine- ester prodrugs has better stability due to bulky β-alkyl substitution may be responsible for good enzymatic stability of valine-prodrug. Overall, from these studies VA, VVA, and GVA exhibited less affinity for plasma protein and CYP enzymes. Moreover VVA and GVA undergo sequential hydrolysis (from PPD to PD to D).

CHAPTER 5

ORAL PHARMACOKINETICS OF AMPRENAVIR AND PRODRUGS

Rationale

Protease inhibitors (PIs) constitute an important class in highly active antiretroviral therapy for the treatment of acquired immune deficiency syndrome (AIDS). However oral bioavailability of PIs is limited due to low aqueous solubility, interaction with membrane efflux proteins, extensive systemic metabolism. Hence very high doses of PIs are administered. For example Amprenavir (Agenerase®) dose is 1200 mg (twenty four 50 mg capsules) twice daily in combination with other antiviral agents. Transporter-targeted prodrug modification could be a good approach to improve its oral bioavailability of PIs. Structural modification of drug molecules compromises the interaction between parent drug and transporters/enzymes. Peptide transporters, mainly expressed in intestinal epithelial cell membranes, are attractive targets for prodrug design due to their broad substrate specificity and high capacity. Therefore "peptidomimetic" prodrugs, designed by conjugating parent drug to small peptides, can be recognized easily by the peptide transporter-mediated influx system and ferried across the epithelial membranes at absorption site (Ganapathy et al., 1995). In the previous chapters 3 and 4, it was clearly demonstrated that prodrugs of

amprenavir (APV), V-APV, VV-APV and GV-APV exhibited better intrinsic aqueous solubility and low affinity for efflux proteins such as P-gp compared to APV. We clearly demonstrated that with the di-peptide and amino acid prodrug approach, P-gp mediated efflux can be circumvented as well as prodrugs can be translocated across cell membrane via nutrient influx transporters. Moreover the prodrugs exhibited better hydrolytic and metabolic stability. These prodrugs also possess less affinity for plasma AAG compared to drug. The aim of this study was to investigate whether prodrug modification can result in enhanced oral absorption of poorly absorbed protease inhibitor APV. *In vitro* permeability studies were carried out using Caco2 as a model. To further substantiate our results, *in vivo* oral pharmacokinetics of di-peptide ester prodrugs, V-APV, VV-APV, and GV-APV were investigated. Pharmacokinetic parameters were evaluated for prodrugs relative to the parent drug, APV followed by single dose oral administration in Sprague-Dawley rats.

Materials and Methods

Materials

APV was a generous gift from GlaxoSmithKline USA, (Philadelphia, PA). All the prodrugs used in the study were synthesized according to the methods noted in Chapter 3. Colon carcinoma cell line, Caco-2 (passages 20-30) obtained from ATCC (Manassas, VA, USA). High-performance liquid chromatographic grade DMSO and methanol were obtained from Fisher Scientific Co. (Pittsburgh, PA, USA). These solvents were used neat for preparing stock solutions of all drugs and inhibitors. Trypsin-EDTA solution, Dulbecco's modified Eagle's medium (DMEM), Ham's F-10 medium and Minimum Essential Medium (MEM) were obtained from Invitrogen (Carlsbad, CA, USA). Fetal Bovine Serum (FBS) was obtained from Atlanta biologicals (Lawrenceville, GA, USA). Transwell® and uptake plates

were procured from Corning Costar Corp (Cambridge, MA, USA). All other chemicals were of analytical reagent grade and were obtained from Fisher Scientific or Sigma Chemicals. Jugular vein cannulated rats male Sprague-Dawley rats were obtained from Charles River Laboratories (Wilmington, MA). All the experiments were conducted in accordance to protocols approved by the IACUC at University of Missouri-Kansas City.

Methods

Cell Culture

Caco-2 cells were cultured in T-75 flasks with DMEM (with high glucose and glutamine concentrations) supplemented with 10% FBS, 1% nonessential amino acids, penicillin 100μg/mL and streptomycin 100U/mL. The medium was changed every alternate day; cells were harvested and passaged *via* trypsinization at 80 to 90% confluence (about 4 days of growth). Cells were also grown on collagen coated Transwell® inserts (12-mm) with transparent polyester membranes. Transwell® inserts were coated with type 1 rat tail collagen (100μg/cm^2), equilibrated with medium, and seeded at a 25,000 cells/cm^2 density. Following seeding, medium was changed every alternate day, and transport or uptake studies were performed after incubation of 17-21 days.

Transport Studies

APV transport was evaluated with monolayers of each cell line. All transport studies were performed with Dulbecco's modified phosphate-buffered saline (DPBS) containing glucose (1g/L) and HEPES (20mM) at pH 7.4. Drug solutions were prepared immediately prior to initiating a transport study. APV and prodrugs (VA, VVA and GVA) were dissolved in DMSO (not exceeding 2% v/v as the final concentration) to prepare a stock solution and

then diluted with DPBS to the specified final concentrations. Volumes of test solutions added were 0.5 and 1.5mL, for apical (A) and basolateral (B) chambers respectively. Prior to initiating an experiment, cultured monolayers were rinsed and equilibrated for 30min with DPBS. Drug solution was added either in the donor or receiving chamber for A to B transport study. Samples (100μL) were withdrawn from the receiving chamber at predetermined time points (15, 30, 60, 90, 120, 150 and 180) and were replaced with equal volume of DPBS to maintain sink conditions. Dilutions were taken into account for the calculations. Samples were stored at −80˚C until further analysis. All the experiments were performed at 37˚C in triplicate. Similar transport studies were performed for prodrugs in presence of 10 and 20 mM of glysar.

Oral Absorption Studies

Oral absorption studies of APV and its prodrugs were carried out by administering 49.5 μmol/kg to male Sprague-Dawley rats. Equimolar dose corresponds to 25 mg/kg of APV. Rats weighing 200-300 g, were fasted overnight 8-12 hrs but were allowed water *ad libitum* prior to an experiment. Drug solutions were prepared by dissolving in 40% v/v of PEG400 and 60% v/v water. Drugs/prodrugs were administered by oral gavage (maximum of 0.8 mL) to jugular vein cannulated rats. Blood samples (200 μL) were collected from the jugular vein cannula at predetermined time intervals over 8 hours. The withdrawn blood will be replaced with 200 μL of 100IU/mL of sterile heparin saline solution to constantly maintain the fluid volume and avoid clogs in the cannula. Plasma was separated immediately by centrifugation and samples were stored at –80°C until further analysis.

Sample Preparation and Analysis

Transport and rat plasma samples were analyzed using a highly robust and sensitive LC-MS/MS technique. Samples were prepared using liquid-liquid extraction technique and verapamil (100 nM) as internal standard. Briefly, 100 µL of verapamil and acetonitrile was added to each sample. Then, 600 µL of water saturated ethyl acetate was added and samples were vortexed for 2 min. This process allowed test compounds to partition between organic and aqueous phase. Following vortexing, samples were centrifuged at the speed of 10,000 rpm for 7 min for separation of two layers. Approximately, 500 µL of organic layer was carefully separated and evaporated under reduced pressure for 45 min. The residue was reconstituted in 100 µL solution of 70 % acetonitrile and 30% water containing 0.1% formic acid and analyzed using LC-MS/MS technique. Similarly, standard solution of test compounds (0.3-5 µg/mL) were extracted and analyzed with LC-MS/MS.

LC-MS/MS Analysis

Both *in vitro* transport and *in vivo* plasma samples were analyzed using LC–MS/MS technique. QTrap® LC–MS/MS mass spectrometer (Applied Biosystems/Sciex) equipped with Agilent 1100 series quaternary pump (Agilent G1311A), vacuum degasser (Agilent G1379A), and autosampler (Agilent G1367A) was used. Electrospray ionization (ESI) in positive mode was used for sample analysis. Test compounds were detected in multiple-reaction monitoring (MRM) mode. Briefly, test compounds were separated using a reverse phase XTerra® MS C18column with dimensions of 4.6 x 50 mm and particle size of 5 um. Mobile phase (70% acetonitrile and 30% water containing 0.1% formic acid) was continuously pumped through the column at a constant flow rate of 0.25 mL/min. 20uL of samples were injected in the system and chromatographs were obtained for 5.5 min. Precursor ions of test compounds were determined from spectra which are generated with the

infusion of standard solutions to the electrospray source with the aid of an infusion pump. Each of these precursor ions is subjected to collision-induced dissociation to produce product ions. Precursor and product ion for test compounds were APV + 506.3/155.9; VVA + 704.4/156.1; GVA + 662.4/156.0; VA + 605.4/156.0 and Verapamil (IS) + 455.3/165.1. The turbo ion spray setting and parameters were optimized (IS voltage: 5500 V, temperature: 300° C, nebulizer gas: 40 psi, curtain gas: 40 psi). Nitrogen gas was used as collision gas. Other operational parameters included declustering potential (DP): 95 V; collision energy (CE): 70 V; entrance potential (EP): 8.5 V; and collision cell exit potential (CXP): 4.0 V. These parameters were generated by running analytes of interest in quantitative optimization mode. The analytical data for each test compounds generated with MRM method generated a significant linearity up to nanogram range. With the help of this method, rapid and reproducible results were successfully obtained. Peak areas for test compounds and internal standard were determined using Analyst ^{TM} software.

Data Analysis

Cumulative amounts of prodrugs (VVA or GVA), the intermediate VA and the parent drug APV, generated during transport across the cell monolayers were plotted as a function of time to determine permeability coefficients. Linear regression of the amounts transported as a function of time yielded the rate of transport across the cell monolayer (dM/dt). Rate divided by the cross-sectional area available for transport (A) generated the steady state flux as shown in Eq. 1.

$$\text{Flux}=(dM/dt)/A \qquad \text{Eq. 1}$$

In all the transport studies, slopes obtained from the linear portion of the curve were used to calculate permeability values. Permeability was calculated by normalizing the steady state flux to the donor concentration (C_d) of the drug or prodrug as shown in Eq. 2.

$$\text{Permeability} = \text{Flux}/C_d \qquad \text{Eq. 2}$$

All relevant pharmacokinetic parameters were calculated using non-compartmental analyses of plasma-time curves after oral administration of APV, and the amino acid and di-peptide prodrugs of APV using a pharmacokinetic software package Phoenix® WinNonlin®, version 6.3 (Pharsight, Mountain View, CA). Maximum plasma concentrations (C_{max}) and area under the plasma concentration time curves ($AUC_{0\text{-}inf}$) were obtained from the plasma-concentration time profiles using non-compartmental analysis. The slopes of the terminal phase of plasma profiles were estimated by log-linear regression and the terminal rate constant (λz) was derived from the slope. The terminal plasma half-lives were calculated from the equation: $t_{1/2} = 0.693 / \lambda z$. Mean residence time (MRT) was calculated as area under the first moment curve (AUMC)/AUC, respectively. The total concentration parameters were calculated by adding the concentrations of the administered prodrug (PPD) and the regenerated PD and APV

Statistical Analysis

All experiments were conducted at least in triplicate and results are expressed as mean ± S.E.M/S.D. Statistical comparison of mean values were performed with one way analysis of variance (ANOVA) or Student t test (Graph Pad INSTAT, version 3.1). $*P < 0.05$ was considered to be statistically significant.

Results and Discussion

Permeability of the Prodrugs across Caco-2 Cells

Caco-2 cell line is an established *in vitro* model for intestinal absorption. Hence permeabilities of prodrugs in comparison with APV was determined across apical cell monolayers. Permeability of prodrugs was compared with APV. Equimolar concentration of (25 μM) APV, V-APV, VV-APV and GV-APV have been used for transport study. Permeability values are presented in Table 11. All prodrugs exhibited 2-3 time high apparent permeability compared to drug. Significantly higher permeabilities of V-APV, VV-APV and GV-APV (9.5×10^{-6}, 6.97×10^{-6}, 7.28×10^{-6} cm/s respectively) as compared to 2.3×10^{-6} cm/s for APV. Approximately 3.5 fold improvement in flux of prodrugs was observed. To further determine role of peptide transporter in the flux of prodrugs, permeabilities of prodrugs in presence of glysar (GS, 10 and 20mM) was determined (Figure 22.). Permeabilities of V-APV, VV-APV and GV-APV were found to be 4.8×10^{-6}, 3.2×10^{-6} and 4.2×10^{-6} cm/sec in the presence of 10mM GS and 3.6×10^{-6}, 2.9×10^{-6} and 3.9×10^{-6} cm/sec in the presence of 20mM GS respectively. This result confirmed our previous conclusion from uptake studies that absorptive flux of prodrugs is significantly inhibited in the presence of GS. This study also indicated that prodrugs are good substrates for the peptide transporters expressed on the intestinal barrier and may be translocated efficiently resulting in higher oral bioavailability.

Table 11. A→BTransport of APV and its prodrugs across Caco2 cell monolayers. Permeability values are expressed as mean ±SD, n=4

Drug	**Permeability (10^{-6} cm/s)**
APV	2.32 ± 1.07

V-APV	9.5 ± 2.8
VV-APV	6.97 ± 1.6
GV-APV	7.28 ± 2.1

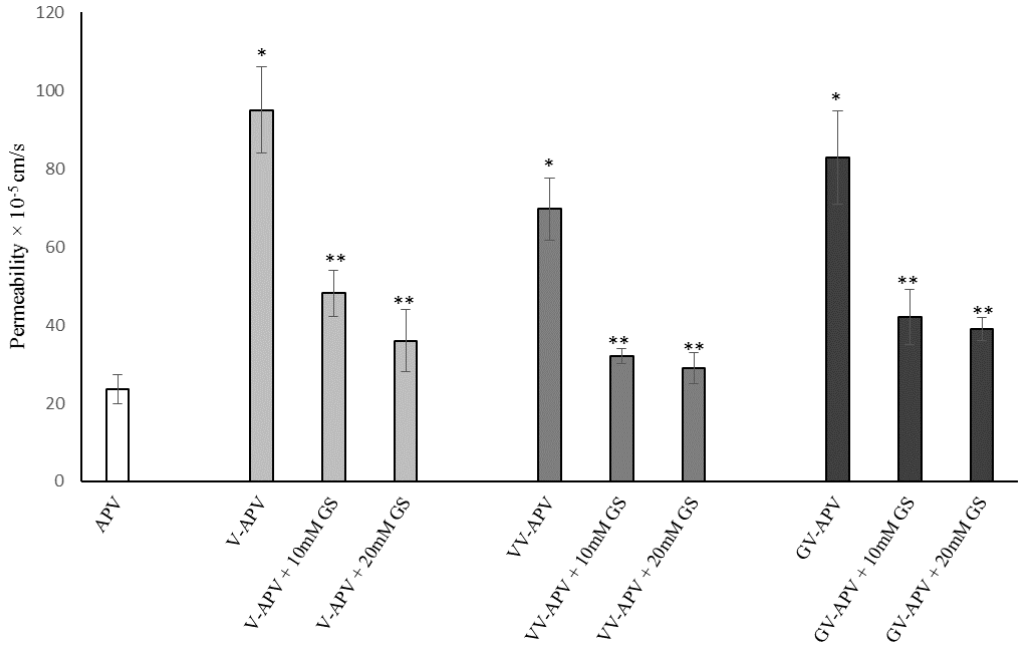

Figure 22. Permeability of APV, V-APV, VV-APV and GV-APV across Caco-2 cell monolayers. Asterisk (*) represents significant difference from control (APV) ($p < 0.05$). Two asterisks (**) represent significant difference from control (when GS is absent) ($p < 0.05$)

Oral Absorption Studies

Plasma concentrations of APV following single dose oral administration were determined and plotted against time. Plasma concentration vs. time profile for APV is provided as Figure 23 and pharmacokinetic parameters are given in table 2. Area under curve for APV was 248 ± 68 min*nmoles/mL. The maximum plasma concentration observed was 1.07 ± 0.2 nmoles/mL at time 55 ± 9 minutes post dosing. Elimination rate constant calculated from elimination phase was 0.017 ± 0.002 with half-life of 43 ± 5 min. Oral absorption of prodrugs with V-APV, VV-APV and GV-APV were also carried out to investigate absorption following oral dosing in Sprague-Dawley rats. All possible breakdown moieties of prodrugs, such as VV-APV, V-APV, and APV for VVA, were monitored. Plasma concentration vs. time profiles were plotted and pharmacokinetic parameters were calculated for all possible breakdown products. Drug plasma concentrations were determined in terms of nmoles/mL and pharmacokinetic parameters of prodrugs and APV were compared. High plasma levels in terms of APV were observed with V-APV, VV-APV and GV-APV. Plasma concentration vs. time profiles APV in comparison with V-APV, VV-APV, and GV-APV are provided in Figures 23, 24, 25 and 26 respectively. Pharmacokinetic parameters for drug and prodrugs are listed in Table 12. Area under plasma concentration time curves expressed as min*nmoles/mL for V-APV (1067 ± 323), VV-APV (1580 ± 261) and GV-APV (1529 ± 455) are significantly higher than APV (248 ± 68). High systemic concentrations of prodrugs might be due to circumvention of P-gp mediated efflux, minimized presystemic metabolism and translocation via peptide transporter expressed on intestinal epithelium. All the prodrugs exhibited higher C_{max} expressed as nmoles/mL compared to APV (1.07 ± 0.2 for APV, 8.08 ± 1.74 for V-APV, 7.06 ± 0.3 for VV-APV, 9.44 ± 1.8 for GV-APV). Elimination half-lives of prodrugs are 2-3 times longer than APV.

Pharmacokinetic parameters for all possible breakdown moieties for VV-APV and GV-APV are summarized in Tables 13 and 14 respectively.

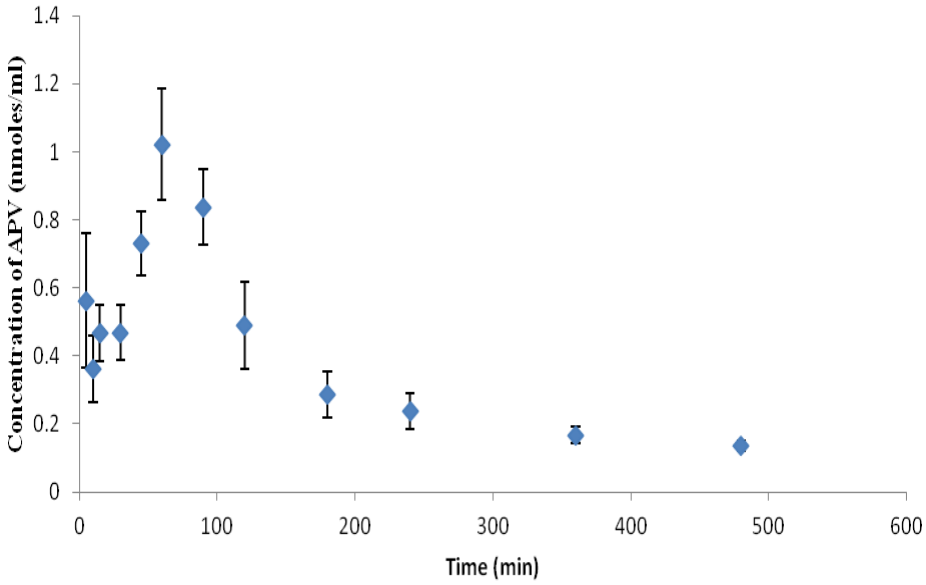

Figure 23. Plasma concentration *vs* time profile of APV in male Sprague Dawley rats following single dose (49.5 µmoles/kg) oral administration. Values are expressed as mean ± SD. n=3

Table 12. Pharmacokinetic Parameters of APV, V-APV, VV-APV and GV-APV after single dose (49.5μmoles/kg) oral administration in rats. Values expressed as mean ± SEM

Parameter	APV	V-APV	VV-APV	GV-APV
AUC_{∞} (min.nmol/mL)	248 ± 68	1067 ± 323	1580 ± 261	1529 ± 455
C_{max} (nmol/mL)	1.07 ± 0.2	8.08 ± 1.74	7.06 ± 0.3	9.44 ± 1.8
T_{max} (min)	55 ± 9	50 ± 8	60 ± 12	45 ± 10
λ_z (min^{-1})	0.017 ± 0.002	0.011 ± 0.002	0.005 ± 0.001	0.007 ± 0.002
$t_{1/2}$ (min)	43 ± 5	94 ± 22	142 ± 30	99 ± 17
MRT_{inf} (min)	67 ± 15	107 ± 18	208 ± 40	162 ± 29

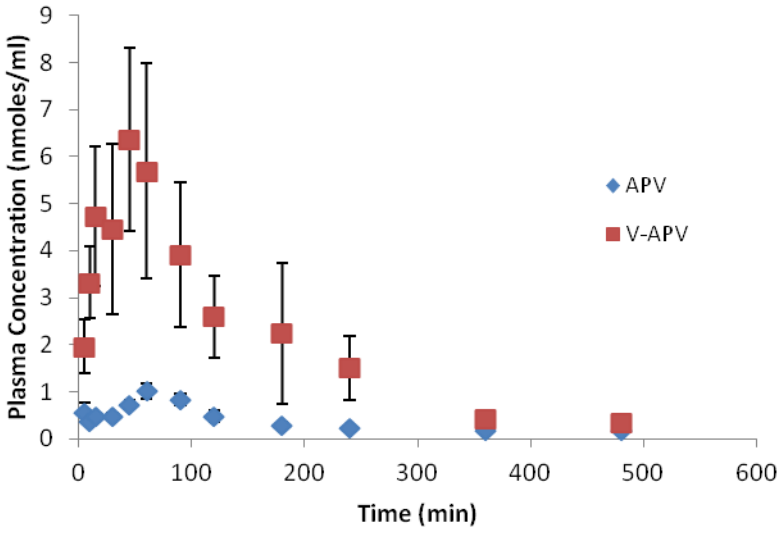

Figure 24. Plasma concentration *vs* time profile of APV and V-APV in male Sprague Dawley rats following single dose (49.5µmoles/kg) oral administration. Values are expressed as mean ± SD. n=3

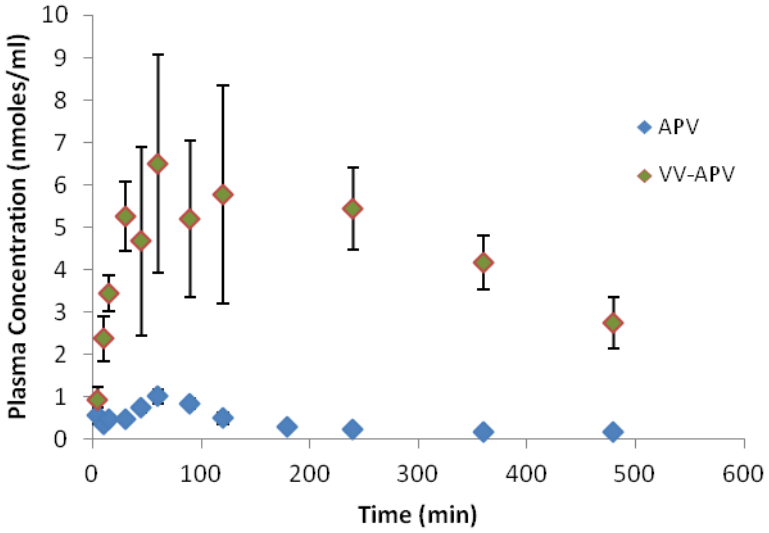

Figure 25. . Plasma concentration *vs* time profile of APV and VV-APV in male Sprague Dawley rats following single dose (49.5µmoles/kg) oral administration. Values are expressed as mean ± SD. n=3

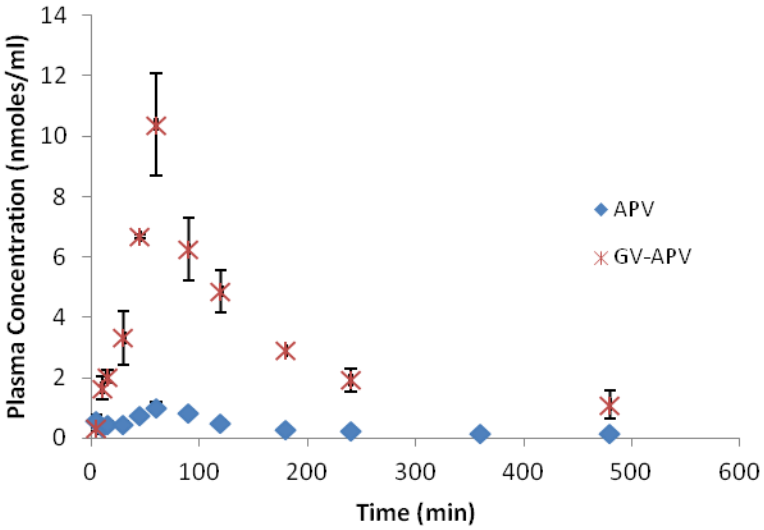

Figure 26. . Plasma concentration *vs* time profile of APV and GV-APV in male Sprague Dawley rats following single dose (49.5 µmoles/kg) oral administration. Values are expressed as mean ± SD. n=3

Plasma concentrations vs. time profile of all breakdown moieties were depicted in Figures 27 and 28. When VV-APV was administered, area under plasma concentration vs. time curve expressed as min*nmoles/mL for VV-APV alone (474 ± 90), V-APV (868 ± 170) and APV (542 ± 125) are significantly higher than APV (248 ± 68). AUC of regenerated APV from VV-APV is two fold higher than APV itself. Among all the fragments observed AUC of V-APV is higher. Moreover elimination of V-APV regenerated is slower than VV-APV alone and regenerated APV. Interestingly mean residence time expressed as min for V-APV moiety (213 ± 12) is longer than VV-APV alone (146 ± 29) and regenerated APV (151± 29). This observation clearly suggests that V-APV is more stable in plasma and elimination is slower. Similarly for GV-APV, AUC expressed as min*nmoles/mL for GV-APV alone (287 ± 43), regenerated V-APV (767 ± 101) and regenerated APV (412 ± 106) was higher than APV (248 ± 68). Like VV-APV, among all possible moieties from GV-APV, regenerated V-APV has higher AUC compared to GV-APV alone and regenerated APV. Mean residence time expressed as min of V-APV (193 ± 32) is much longer than GV-APV alone and regenerated APV. However GV-APV moiety has faster elimination rate with half-life of 29± 6 minutes, unlike VV-APV which exhibited elimination half-life of 106 ± 19 min. Presence of V-APV for longer duration is may be due to lower esterase activity due to stearic hindrance offered by bulk secondary β-alkyl group. These results clearly suggest that V-APV is the major fragment observed in plasma following VV-APV and GV-APV administration. Moreover in both cases the area under plasma concentration time curve (min*nmoles/mL) for regenerated APV from VV-APV (542 $\pm$ 125) and GV-APV (412 $\pm$ 106) is higher than APV (248 ± 68).

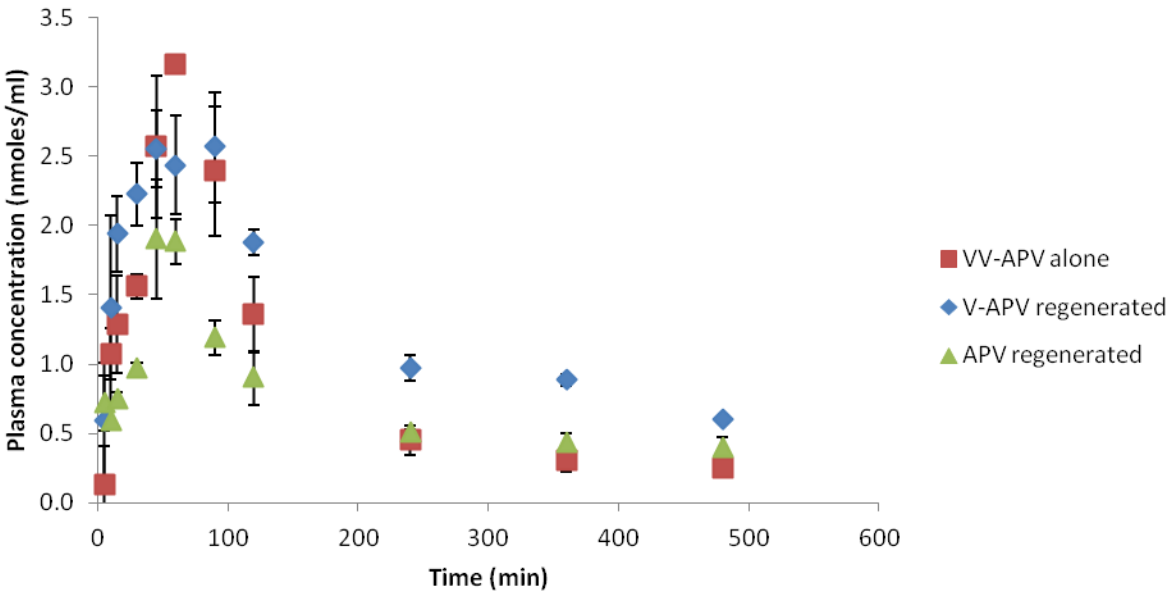

Figure 27. Plasma concentration *vs* time profile of VV-APV alone, APV and V-APV regenerated from VV-APV in male Sprague Dawley rats following single dose (49.5 µmoles/kg) oral administration. Values are expressed as mean ± SD. n=3

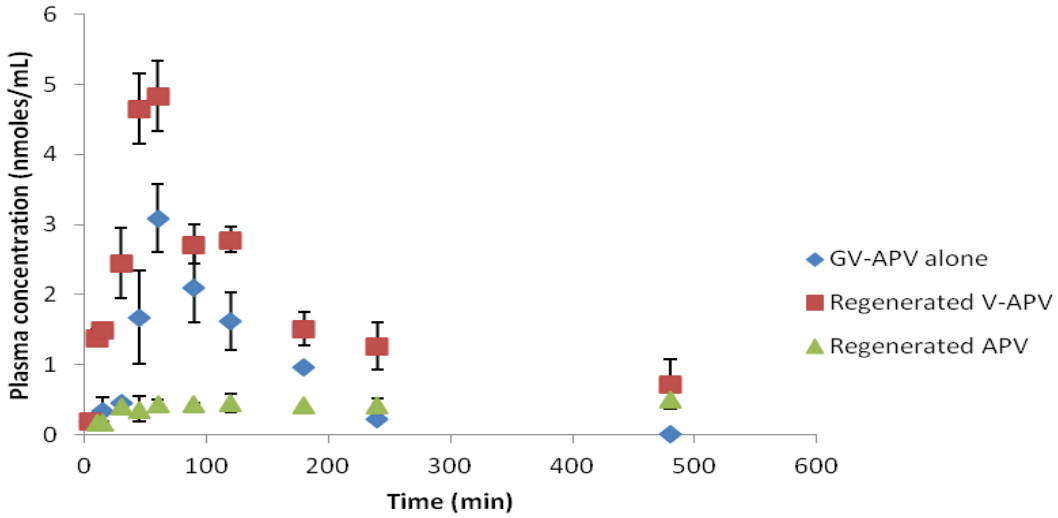

Figure 28. Plasma concentration *vs* time profile of GV-APV alone, APV and V-APV regenerated from GV-APV in male Sprague Dawley rats following single dose (49.5 µmoles/kg) oral administration. Values are expressed as mean ± SD. n=3

Table 13. Pharmacokinetic Parameters for VV-APV alone, V-APV, APV regenerated from VV-APV in comparison with APV after single dose (49.5 μmoles/kg) oral administration in rats. Values expressed as mean ± SEM

Parameters	Val-Val-APV (alone)	Regenerated Val-APV	Regenerated APV	APV
AUC_{∞} (min.nmol/mL)	474 ± 90	868 ± 170	542 ± 125	248 ± 68
C_{max} (nmol/mL)	3.3 ± 0.6	2.9 ± 1.0	1.91 ± 0.75	1.07 ± 0.2
λ_z (min^{-1})	0.008 ± 0.001	0.0045 ± 0.0005	0.006 ± 0.001	0.017 ± 0.002
t1/2 (min)	106 ± 19	159 ± 34	114 ± 27	43 ± 5
MRT_{∞} (min)	146 ± 29	213 ± 12	151 ± 29	67 ± 15

Table 14. Pharmacokinetic Parameters for GV-APV alone, V-APV, APV regenerated from GV-APV in comparison with APV after single dose (49.5 μmoles/kg) oral administration in rats. Values expressed as mean ± SEM

Parameters	Gly-Val-APV (Alone)	Regenerated Val-APV	Regenerated APV	APV
AUC_{∞} (min.nmol/mL)	287 ± 43	767 ± 101	412 ± 106	248 ± 68
C_{max} (nmol/mL)	4.3 ± 1.2	5.8 ± 1.3	0.64 ± 0.2	1.07 ± 0.2
λ_z (min^{-1})	0.02 ± 0.003	0.006 ± 0.001	--	0.017 ± 0.002
$t_{1/2}$ (min)	29 ± 6	132 ± 34	--	43 ± 5
MRT_{∞} (min)	66 ± 19	193 ± 32	--	67 ± 33

(--) Not determined

Conclusions

The permeability studies clearly demonstrated that prodrugs possess better permeability characteristics compared to APV. Reduced permeability of prodrugs in presence of GS clearly suggest that prodrugs are interacting with peptide transporters. Single dose oral absorption studies in Sprague-Dawley rats demonstrate that $AUC_{0-\infty}$ for APV prodrugs V-APV, VV-APV and GV-APV is much higher than parent drug APV indicating that the total amount of APV absorbed in the case of prodrugs is more than APV itself. VV-APV and GV-APV exhibited longer MRT_{∞} and slower elimination compared with APV indicating that prodrugs possess better enzymatic and metabolic stability. Moreover $AUC_{0-\infty}$ for regenerated APV from prodrugs is two to three fold higher than APV itself. As discussed in earlier chapters, prodrugs have low affinity for efflux proteins and are substrates for peptide transporters which lead to high concentrations of drugs. Increased systemic drug levels and longer residence times, bypassing the efflux proteins may lead to better absorption into brain which serve as sanctuary site for HIV.

CHAPTER 6

ABSORPTION OF AMPRENAVIR PRODRUGS ACROSS BLOOD BRAIN INTERFACES

Rationale

Protease inhibitors (PIs) are an important class of anti-HIV drugs. Their continuous use in the highly active anti-retroviral therapy (HAART) led to lowering deaths due to HIV infections. Despite of excellent anti-HIV efficacies of PIs, severely low and variable oral bioavailabilities have been reported when administered in humans. Brain availability of most of the PIs is unknown. Blood brain barrier (BBB) presents a significant challenge to the delivery of therapeutic agents to the brain. Tight junctions prevent free diffusion of small polar molecules across this barrier. However, entry of large lipid soluble molecules is also limited across BBB by the presence of several ABC (ATP binding cassette) efflux transporters i.e., P-glycoprotein (P-gp) and multi-drug resistance associated proteins (MRPs) which efficiently prevent entry of drug molecules into the central nervous system (CNS). Extensive metabolism by CYP3A4, efflux by membrane efflux transporters present on the absorptive membrane of the intestine and the blood-brain barrier (BBB) and extensive plasma protein binding are believed to contribute to such low and variable absorption of PIs. Low brain concentrations of PIs lead to development of safe haven for HIV in the brain tissues.

In the previous chapters amprenavir prodrugs have been evaluated for their interaction with efflux protein P-glycoprotein and influx peptide transporters. All the prodrugs exhibited better absorption than parent drug APV. As per our hypothesis, peptide transporters are targeted at intestinal epithelium and amino acid transporters at blood brain

barrier (BBB). Peptide transporters are not expressed on BBB and the di-peptide prodrugs are good substrates of peptide transporter. In the oral absorption studies it is clear that di-peptide pro-pro-drug (PPD) undergoes enzymatic hydrolysis and bioreverse to amino acid prodrug and some amount to drug. We anticipate that the amino acid prodrug (PD) can evade the efflux by P-gp at BBB and translocates across BBB via amino acid transport system. We name this transporters targeted approach as pro-pro-drug approach as explained in Chapter 2. We hypothesized that systemically generated amino acid prodrug of APV will evade the efflux and permeate into the brain utilizing the amino acid transporters on the BBB. This pro-prodrug strategy will not only result in enhanced oral absorption of poorly absorbed APV but also in higher brain concentrations of APV. In order to test our hypothesis, permeability characteristics of prodrugs of APV were investigated utilizing an *in vitro* BBB model. Further *in vivo* brain concentrations of drugs were determined in Sprague-Dawley rats following intravenous injection. Brain microdialysis technique was employed to study brain pharmacokinetics. To confirm our pro-prodrug hypothesis in possibly enhancing both systemic and brain concentrations of APV, it was imperative to corroborate our *in vitro* permeability results with *in vivo* pharmacokinetics (PK) as seen in rats. Therefore, we conducted brain absorption studies for pro-pro-drug (VV-APV and GV-APV) and amino acid prodrug (V-APV) respectively. Brain PK parameters were evaluated for GV-APV and V-APV following intravenous administration in cannulated rats.

Materials and Methods

Materials

APV was a generous gift from GlaxoSmithKline USA, (Philadelphia, PA). All the prodrugs used in the study were synthesized according to the methods noted in Chapter 3.

High-performance liquid chromatographic grade DMSO and methanol were obtained from Fisher Scientific Co. (Pittsburgh, PA, USA). These solvents were used neat for preparing stock solutions of all drugs and inhibitors. Rat brain endothelial cells (RBE4), an immortal rat brain endothelial cell line, was generously provided by INSERM, France and rat astroctyes were purchased from ATCC (Manassas, VA, USA). Trypsin-EDTA solution, Dulbecco's modified Eagle's medium (DMEM), Ham's F-10 medium and Minimum Essential Medium (MEM) were obtained from Invitrogen (Carlsbad, CA, USA) and fetal bovine serum (FBS) was obtained from Atlanta Biologicals (Lawrenceville, GA, USA). Culture flasks (75 and 25 cm^2), Transwell® and 12-well plates (3.8 cm^2 growth area/well) were obtained from Costar (Bedford, MA, USA). All other chemicals were of analytical reagent grade and were obtained from Fisher Scientific or Sigma Chemicals. Jugular vein-cannulated and carotid artery-cannulated male Sprague-Dawley rats were obtained from Charles River Laboratories (Wilmington, MA). CMA 12 Elite 14/02 PAES probes and guide cannulae were obtained from CMA/Microdialysis AB (Stockholm, Sweden). All the experiments were conducted in accordance to protocols approved by the IACUC at University of Missouri-Kansas City.

RBE4 and Astroytes Cell Culture

The media used to grow these cells and other cell culture conditions were similar to those described for MDCK cells. Cellular accumulation studies were performed on RBE4 cell monolayers using the same protocol followed as described in Chapter 3. Transport of drug and prodrug was studied in RBE4 and astrocytes co-culture (Figure 29). RBE4 cells at a density of 250,000 cells per well grown on collagen coated A side of Transwell® inserts placed in uptake plates plated with astroctytes at a density of 250,000 cells per well (RBE4 &

AST). Transport experiments were performed and apparent permeability was measured for APV and prodrugs.

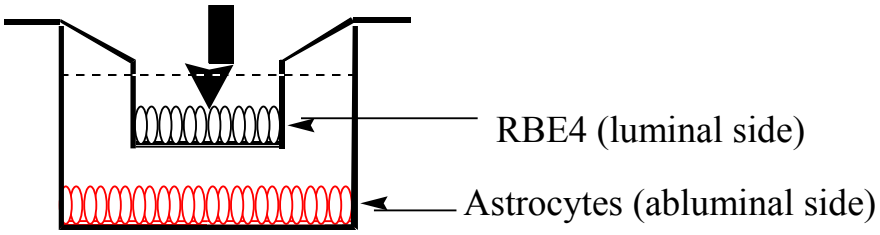

Figure 29. Graphical representation of Rat brain endothelial cells (RBE4) and rat astrocytes co-culture model.

Uptake Studies

Cellular uptake studies in RBE4 were performed according to procedures described in previously published protocol from our laboratory (Patel et al. 2012). Briefly, cells were plated at the density of 3 x 10^6 cells in 12 well culture plates. Medium was aspirated and cell monolayer was washed with Dulbecco's Phosphate Buffered Saline (DPBS) buffer (130 mM NaCl, 0.03 mM KCl, 7.5 mM Na_2HPO_4, 1.5 mM KH_2PO_4, 1 mM $CaCl_2$, 0.5 mM $MgSO_4$, and 5 mM glucose, pH 7.4) for 10 min, three times at 37^0 C. Uptake studies were initiated by incubating cells with radioactive substrates in DPBS at 37^0 C for 15 min. Following incubation, radioactive solution was quickly removed and plates were washed with ice-cold stop solution (210 mM KCl, 2 mM HEPES, pH of 7.4) to terminate the uptake process. One mL of lysis buffer (0.1% Triton-X solution in 0.3% NaOH) was added to each well for cell lysis. Approximately, 500 µL solutions were added from each well to scintillation vials

containing 3 mL of scintillation cocktail. Radioactivity associated with cells was analyzed with a scintillation counter (Beckman Instruments Inc., Model LS-6500; Fullerton, CA). Uptake rate was normalized to protein count using human serum albumin, quantified with BioRad protein estimation kit (BioRad protein; Hercules, CA).

Transport Studies across RBE4 and Astrocyte Co-culture

Transport studies were carried out according to previously published protocols (Luo et al., 2006). Briefly, cells were cultivated in 12-well Transwell® plates as mentioned in the previous section. Before initiation of transport study, cell monolayers were washed with DBPS (pH7.4) for 15 min at 37° C (three washes). For determining A-B permeability, 0.5 mL test solution (25 µM) was added in the apical chamber of 12-well Transwell® plates. Similarly, 1.5 mL test solution (25 µM) was added in the basolateral chamber to determine B-A permeability. Transport study was performed for 3 h at 37° C. At predetermined time points (5, 15, 30, 45, 60, 120 and 180 min), 100 µL sample was withdrawn from the receiving chamber and replaced with fresh DPBS to maintain sink conditions. Samples were stored at − 80° C until further analysis with LC/MS/MS technique. To study the effect of P-gp inhibitors on transepithelial permeability of test compounds, cells were treated with inhibitors such as GF 120918 prior to the initiation of the experiment. Transport study of test compounds in presence of inhibitors was also determined for 3 h at 37° C.

***In vitro* Probe Calibration**

Microdialysis probe recovery was determined in artificial CSF and a known concentration of APV and prodrugs (1-5µM). The probe was perfused at a constant flow rate of 2µL/min and samples were collected every 40 min for a period of 2h. The recovery factor (RF) for APV and prodrugs was calculated as a percentage according to the equation, RF =

$C_{out}/C_{in,}$ where, C_{out} is the concentration of the drug in the dialysate flowing out of the probe and C_{in} is the known concentration of the dialysate in which the probe is dipped. Actual brain concentrations were then derived by dividing the dialysate concentrations by the recovery factor. Probe recovery efficiency for APV is 20% whereas for V-APV and GV-APV was 12-15%.

Brain Microdialysis Studies

For *in vivo* brain microdialysis studies, V-APV was administered via intravenous route through jugular vein cannula. Equimolar doses of APV and prodrugs (19.8 μmoles/kg) which is equivalent to 10mg/kg of APV. Doses were prepared by dissolving drug/prodrug in PEG400 40%v/v and water 50%v/v. The rats were anesthetized before implanting microdialysis probe in the brain by an intra-peritoneal (IP) injection of ketamine hydrochloride (90mg/kg) and xylazine (10mg/kg). Thereafter ketamine (30mg/kg) was administered intramuscularly (IM) every 45min for maintenance of anesthesia. Animals were then placed on the Kopf® stereotaxic instrument. The head was fixed on this instrument at three places: two bony ear canals and the upper jaw. The skin over the head was shaved and cleaned with alcohol swabs. Using a clean, sharp sterile scalpel blade, a midline scalp incision was made to expose the skull. After the skin was incised, the periosteum was cleaned to expose the skull by a pair of tweezers. Surface of the skull was cleaned with cotton swabs. Bregma and lamda sites were exposed and marked. A guide cannula was fixed in the stereotaxic instrument and placed just above the bregma. Coordinates of the X, Y and Z axis on the instrument were noted and set as zero points for reference. Using the stereotaxic instruments guide cannula was moved 2.6mm medio-lateral and 0.9mm anterior relative to bregma (Roiko et al.; Zhang et al.). A hole was drilled in this area with a 2mm

trephine drill. The guide cannula (CMA12) was then lowered 3.9 mm ventral to the bregma and sealed in the place with the help of dental cement. Paxinos brain atlas was used to determine the *brain* coordinates. CMA12 microdialysis probe (2mm membrane) was inserted into the brain through the guide cannulae. The probe was perfused with an artificial cerebrospinal fluid (CSF) (140 mM NaCl, 3 mM KCl, 2.5 mM $CaCl_2$, 1 mM $MgCl_2$, 1.2 mM Na_2HPO_4, 0.3 mM NaH_2PO_4, 3 mM glucose, 2% w/v bovine serum albumin pH 7.2) (Roiko et al.; Zhang et al.). The perfusion fluid was pumped at a flow rate of 2µL/min for 1h to attain equilibration. At this time, APV, V-APV and GV-APV were administered via jugular vein. Dialysate was collected every 40min to study the brain concentrations of APV and prodrugs. Samples were stored at -80°C until further analysis. Animals were kept under anesthesia for the entire duration of the experiment and euthanized under deep anesthesia by an over dose of sodium pentobarbital injection USP at the end of an experiment.

LC-MS/MS Sample Preparation

Transport, *in vivo* plasma and brain samples were analyzed using sensitive LC-MS/MS technique. Samples were prepared using liquid-liquid extraction technique and verapamil (100 nM) as internal standard. Briefly, 100 µL of verapamil and acetonitrile was added to each sample. Then, 600 µL of water saturated ethyl acetate was added and samples were vortexed for 2 min. This process allowed test compounds to partition between organic and aqueous phase. Following vortexing, samples were centrifuged at the speed of 10,000 rpm for 7 min for separation of two layers. Approximately, 500 µL of organic layer was carefully separated and evaporated under reduced pressure for 45 min. The residue was reconstituted in 100 µL solution of 70 % acetonitrile and 30% water containing 0.1% formic acid and analyzed using LC-MS/MS technique. Similarly, standard solution of test

compounds (0.3-5 μg) were extracted and analyzed with LC-MS/MS. Samples were analyzed as described in Chapter 5.

Data Analysis

Cumulative amounts of prodrugs (VVA or GVA), the intermediate VA and the parent drug APV, generated during transport across the RBE4 and Astrocyte co-culture model were plotted as a function of time to determine permeability coefficients. Flux and permeability values were determined as described in Chapter 3 and Chapter 5.

All relevant pharmacokinetic parameters were calculated using non-compartmental analyses of plasma-time and brain concentration vs. time curves after IV administration of APV, and the amino acid and di-peptide prodrugs of APV using a pharmacokinetic software package Phoenix® WinNonlin®, version 6.3 (Pharsight, Mountain View, CA). Maximum plasma concentrations (C_{max}) and area under the plasma concentration time curves ($AUC_{0\text{-}inf}$) were obtained from the plasma-concentration time profiles using non-compartmental analysis. The slopes of the terminal phase of plasma profiles were estimated by log-linear regression and the terminal rate constant (λz) was derived from the slope. The terminal plasma half-lives were calculated from the equation: $t_{1/2}= 0.693 / \lambda z$. Mean residence time (MRT) was calculated as area under the first moment curve (AUMC)/AUC. The total concentration parameters were calculated by adding the concentrations of the administered prodrug (PPD) and the regenerated PD and APV

Statistical Analysis

All experiments were conducted at least in triplicate and results are expressed as mean ± S.E.M/S.D. Statistical comparison of mean values were performed with one way

analysis of variance (ANOVA) or Student t test (Graph Pad INSTAT, version 3.1). *P <0.05 was considered to be statistically significant.

Results and Discussion

Transport Studies across RBE4

Various publications about BBB and valid *in vitro* models led us to various possible co-cultures with different components of the BBB, such as brain endothelial cells, astrocytes, perictyes, and glial cells. Good permeabilities were found with co-cultures of brain endothelial cells and astrocytes (Ayres, 1977; Gumbleton and Audus, 2001; Deli et al., 2005; Nicolazzo et al., 2006). Hence in our laboratory co-culture of RBE4 and astrocytes was developed. Agarwal et al., studied all possible models which can be developed with RBE4 and astrocytes and compared the permeabilities of drugs with MDCK cells. Among all the models developed with RBE4 and astrocytes treated with 25µg/mL of rifampicin exhibited better barrier properties. Rifampicin is a well know inducer of efflux protein expression. Transport of lopnavir was studied in our laboratory across a co-culture, containing RBE4-Rif cells (RBE4 cells treated with rifampicin) and astrocytes generated an efflux ratio of 2.3 indicating significant efflux transporter activities in RBE4 cells after treatment with rifampicin. Hence we adapted this model study *in vitro* permeability characteristics of APV prodrugs. The concentration of APV and all the prodrugs utilized for the transport studies was 25µM. Figure 30, shows the A-B permeabilities obtained for all the prodrugs across RBE4-Rif cells. A-B (absorptive) permeability of APV, APV in presence of GF, V-APV, VV-APV and GV-APV were determined. Approximately three fold increase in apprent permeability of APV in presence of P-gp inhibitor was observed. Similarly V-APV exhibited three fold increase in the permeability whereas VV-APV and GV-APV exhibited two fold

increase in permeability. Among all the prodrugs tested, V-APV exhibited better flux across the cell monolayer. It is evident from the P-gp interaction studies that all prodrugs exhibited low affinity for P-gp. Hence all the prodrugs tested can evade the P-gp mediated efflux. Moreover all prodrugs are good substrates of peptide transporters in cluding V-APV. It is clear from the literature that valine is the only amino acid with good affinity for peptide transporters (Terada and Inui, 2004; Bhardwaj et al., 2005). However, unfortunately peptide transporter is not expressed on BBB. The enhanced permeability of V-APV triggers a question whether any other transport system in responsible in translocation of V-APV. We wanted to further investigate the amino acid transport system involved in translocation of V-APV.

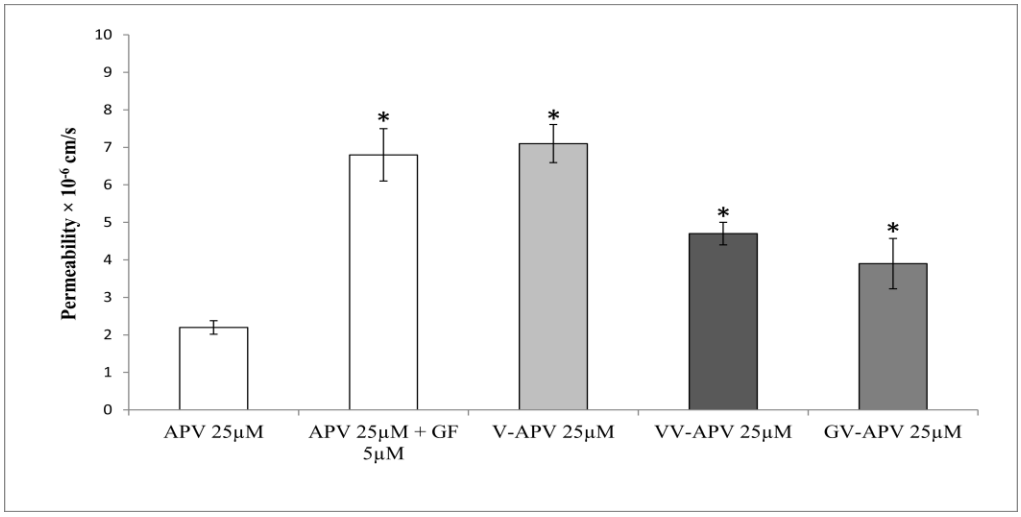

Figure 30. Permeability across RBE4-rif Astrocytes co-culture for APV and prodrugs of APV. Equimolar concentration of all the drugs was used (25 µM). Study was performed at pH 7.4. Values are expressed as mean ± S.D. n=4). (*) is considered as statistically significant from control.

Characterization of Valine Transport across RBE4

After observing the permeability across BBB model, we investigated for transporters involved in translocation of valine. Cellular accumulation studies were performed using valine and substrates of amino acid transport systems. In the process of characterization of valine transport, uptake of [3H]-tyrosine in presence of phenylalanine (100µM) and valine (100µM) was studied. Tyrosine and phenylalanine are good substrates of system L amino acid transporter (Pardridge, 1998). Results obrained are shown as Figure 31. Approximately 80% of [3H]-tyrosine uptake was inhibited in presence of phenylalanine. Both tyrosine and phenylalanine are well known substrates for large amino acid transport system 1(LAT1). Similar inhibition in uptake of [3H]-tyrosine was observed in presence of valine. This result clearly demonstrates that valine is interacting with LAT1 on RBE4 cells. We further characterized the active transport process using [3H]-valine, unlabled valne, tyrosine and phenyl alanine.

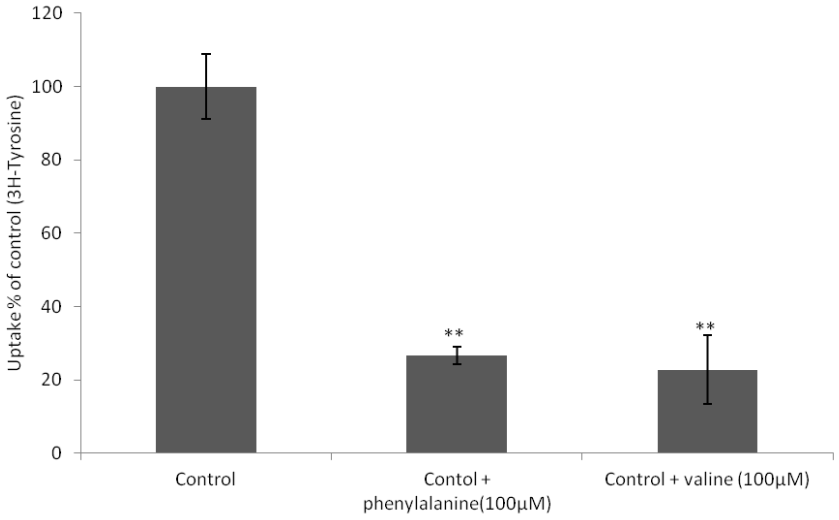

Figure 31. Uptake of [3H] tyrosine in presence of Phenylalanine and valine in RBE4 cell monolayers. Values reported are mean±S.D. (n = 4). (**) is considered as statistically significant from control at $p<0.01$.

Time and pH dependant uptake of [3H]-valine was determined. For time dependent uptake studies, [3H]-tyrosine uptake is carried out over various time points (5, 15, 30 and 45 min). The effect of pH on [3H]-tyrosine uptake is studied by adjusting buffer pH to 4, 5, 6, 7.4 and 8. The uptake study is carried out as described earlier at different pHs. [3H]-valine uptake is found to be linear up to 45 min (Figure 32). Incubation time of 15 min is selected for further uptake studies unless or otherwise specified. The involvement of inward proton gradient for [3H]-valine uptake is examined by adjusting buffer pH to 4, 5, 6 and 7.4. The uptake remains unaltered within a pH range of 4–7.4 indicating that the process is pH independent (Figure 33).

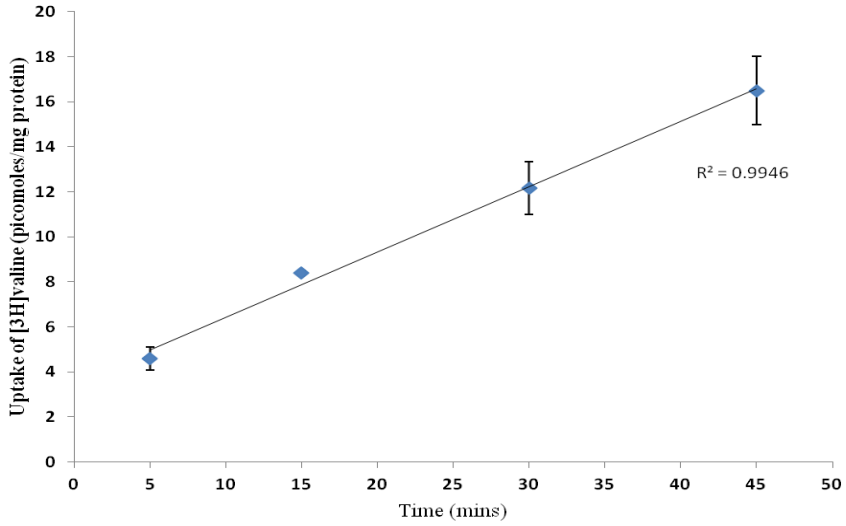

Figure 32. Time dependent uptake of [3H]-valine in RBE4. Values are expressed as mean ± SD., n=4

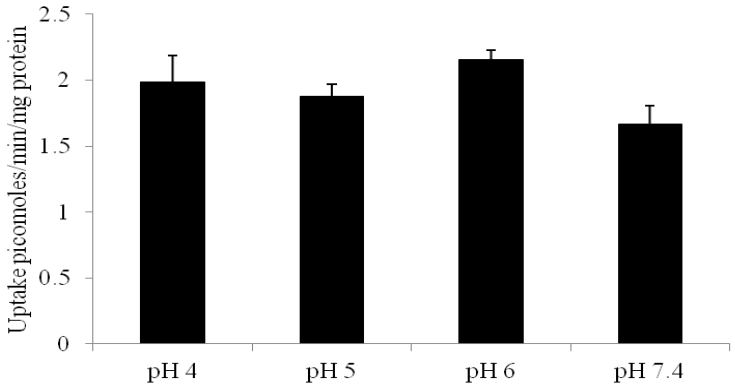

Figure 33. pH dependent uptake of [3H]-valine in RBE4. Values are expressed as mean ± SD., n=4

The role of sodium ions on [3H]-valine uptake is delineated by substituting sodium chloride (NaCl) and sodium phosphate dibasic (Na_2HPO4) in DPBS with equimolar quantities of choline chloride and potassium phosphate dibasic (KH_2PO4), respectively. The absence of sodium ions in incubation buffer does not significantly influence [3H]-tyrosine uptake (Figure 34). This result clearly suggests that the uptake process is sodium independent.

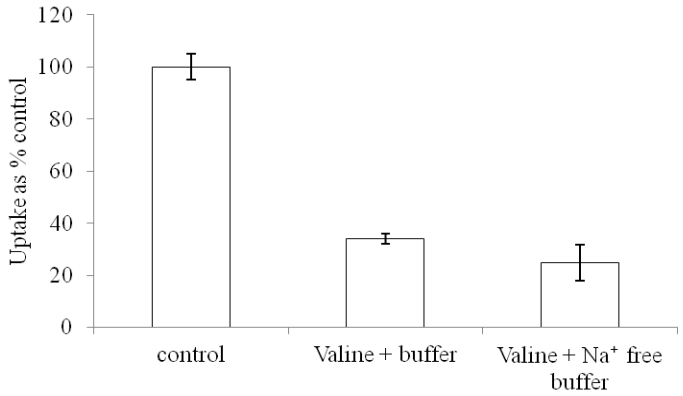

Figure 34. Uptake of [3H]-valine in RBE4 in absence (control) and presence of valine and buffer and sodium free buffer. Values are expressed as mean ± SD., n=4

For studying saturation kinetics, [3H]-valine uptake was performed as a function of substrate (valine, tyrosine and phenylalanine) concentration over the range 0.01–100 μM. Figure 35 clearly shows the involvement of a saturable carrier mediated process. The data obtained is fitted to classical Michaelis-Menten inetic model and kinetic parameters, K_m and V_{max} were determined. The results are summmarised in Table 15.

Table 15. K_m and V_{max} values obtained by fitting data obtained from Uptake of [3H] valine in presence of various concentrations of valine, tyrosine and phenylalanine into classic Michaelis-Menten equation. Values expressed as mean±SD. n=4.

	Km(μM)	**Vmax** (nmoles/mg/min)
Valine	41.3 ± 7.8	148 ± 12
Tyrosine	36.3 ± 4.6	176 ± 18
Phenylalanine	41.9 ± 13.16	159 ± 13

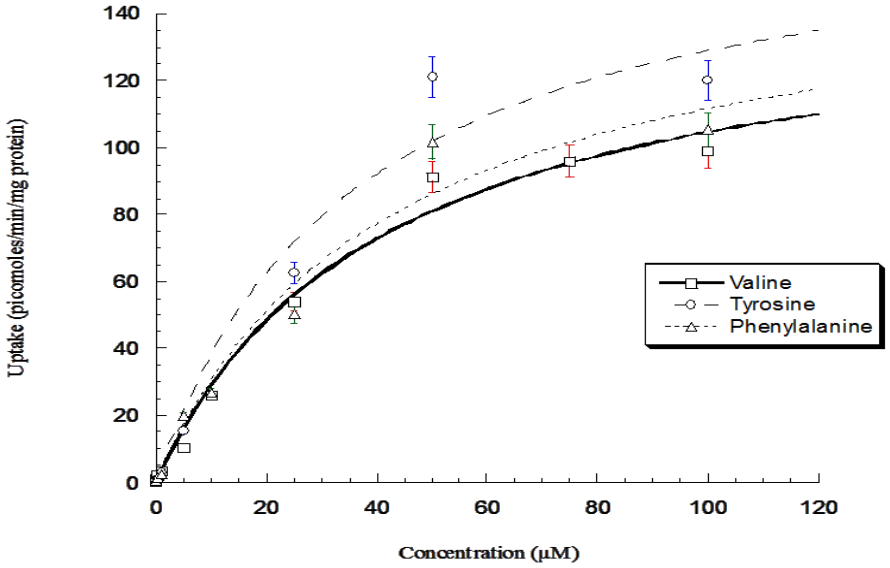

Figure 35. Uptake of [3H] valine in presence of various concentrations of valine, tyrosine and phenylalanine (1-100µM). K_m and V_{max} are calculated by fitting data into classic Michaelis-Menten equation. Each data point is expressed as mean±SD. n=4.

The K_m values for valine, tyrosine and phenylalanine are comparable which indicates affinity of valine for LAT1 is comparable with that of tyrosine and phenylalanine. Extent of binding is also similar to that of tyrosine and phenylalanine. These results clearly demonstrate that valine is translocated by LAT1 across RBE4. In order to investigate the interaction of V-APV with LAT1, we performed cellular accumulation studies of [3H]-valine in presence of various concentrations of V-APV and unlabeled valine (100µM) was used as positive control. The results obtained from this study are depicted as Figure 36. At all the concentrations tested (25, 50 and 100 µM) uptake of [3H]-valine is significantly inhibited by 30-50%. The results clearly indicate V-APV is a substrate for LAT1 and translocated across BBB via system L transporter. Affinity of V-APV for LAT1 could be the reason for high permeability of V-APV compared with VV-APV and GV-APV.

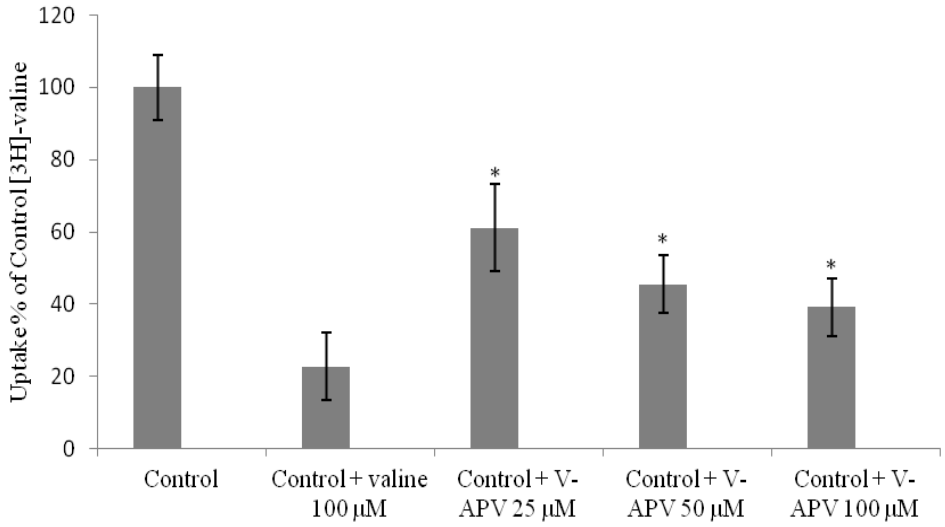

Figure 36. Uptake of [3H]-valine in presence unlabled valine (100 µM) and V-APV (25, 50 and 100 µM) in RBE4 cells. Data points are expressed as mean ± SD. n=4. (*) indicated statistical significant difference from control at $p<0.05$

Brain Absorption Studies *in vivo*

Brain microdialysis studies were carried out with APV, V-APV and GV-APV in male Sprague-Dawley rats. *In vitro* transport studies clearly demonstrated that prodrugs have better permeability characteristics compared to APV in BBB co-culture model. Further *in vivo* evaluation of these prodrugs was conducted by intravenous administration of equimolar doses of drug/prodrug (19.8 μmoles/kg). Both plasma and brain samples were collected and analyzed for drug/prodrug concentrations. CMA12 Elite PAES microdialysis probes were implanted in rat brain and artificial CSF buffer was perfused continuously throughout the experiment and samples were collected. Brain microdialysis probe and experimental setup was shown in Figure 37.

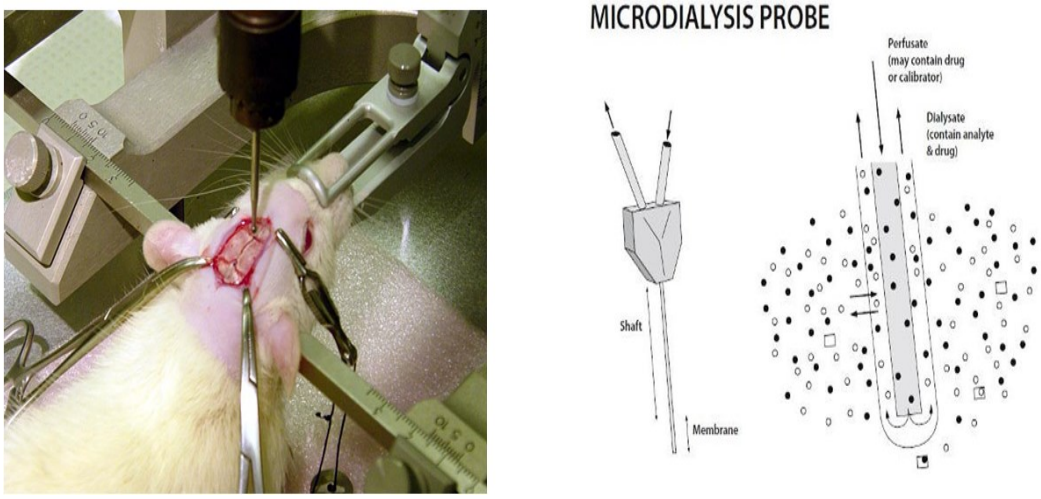

Figure 37. Brain microdialysis experimental set up. (Left) Sprague-Dawley rat mounted on stereotaxic instrument and skull was exposed with clear visibility of bregma and lambda. (Right) CMA 12 elite PAES probe with 2mm semipermeable membrane.

From plasma and brain concentrations, pharmacokinetic parameters were estimated. Figure 38, shows the concentration (nmoles/mL) vs. time profile in plasma and brain for APV. All the pharmacokinetic parameters are summarized in Table 16. $AUC_{0\text{-last}}$ in plasma expressed as min*nmoles/mL in plasma and brain was found to be 678 ± 148 and 66 ± 13 respectively for APV. $AUC_{0\text{-last}}$ observed from brain concentrations was almost ten times less than that of plasma concentrations. Elimination of APV from brain is slower with half life of 69 ± 22 min compared to elimination from blood with half life of 38 ± 15 min. The mean residence time calculated from ratio of area under moments curve and area under curve was found to be 42 ± 9 and 81 ± 17 min in plasma and brain respectively.

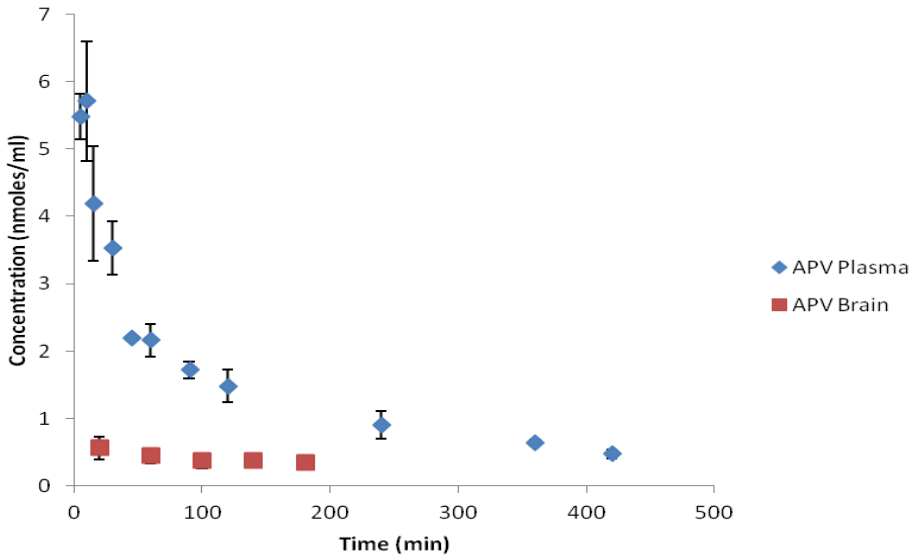

Figure 38. Comparative plasma and brain concentration vs time profile for APV following intravenous administration (19.8 µmoles/kg) in Sprague Dawley rats. Values are expressed as mean ± SE. n=3.

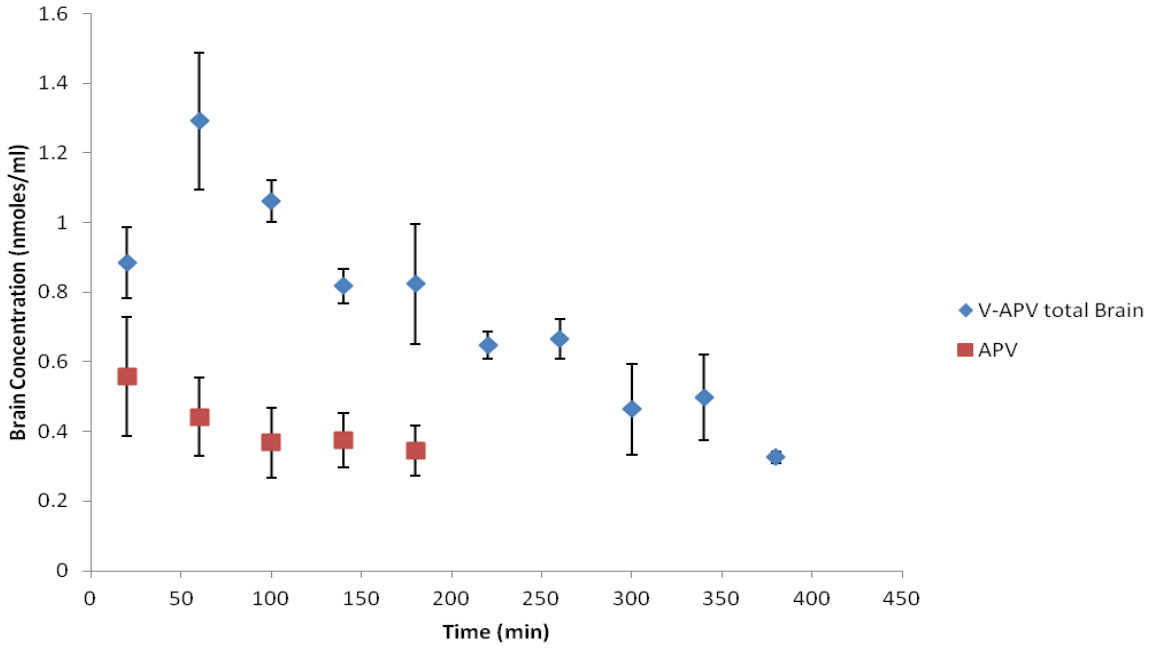

Figure 39. Comparative brain concentration vs time profile for APV and V-APV (cumulative) following intravenous administration (19.8 µmoles/kg) in Sprague Dawley rats. Values are expressed as mean ± SE. n=3.

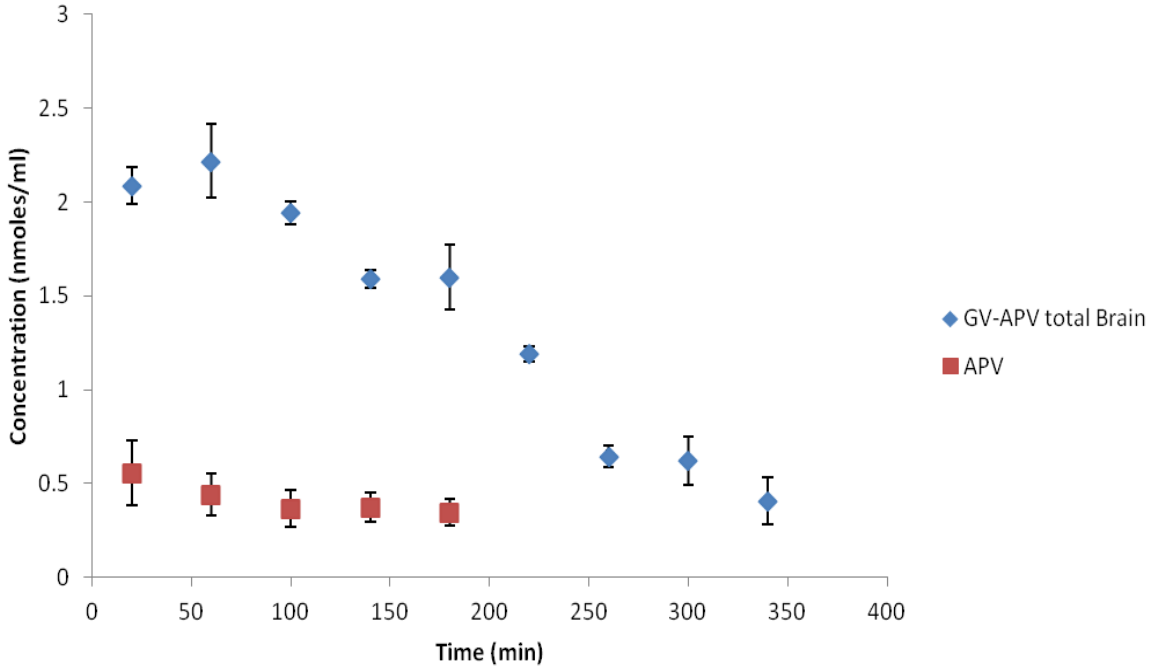

Figure 40. Comparative brain concentration vs time profile for APV and GV-APV (cumulative) following intravenous administration (19.8 µmoles/kg) in Sprague Dawley rats. Values are expressed as mean ± SE. n=3.

Table 16. Comparative pharmacokinetic parameters of APV, V-APV and GV-APV estimated from plasma and brain concentrations following intravenous administration (19.8 μmoles/kg) in Sprague Dawley rats. Values are expressed as mean±SD, n=3.

	APV		**V-APV**		**GV-APV**	
	Plasma	**Brain**	**Plasma**	**Brain**	**Plasma**	**Brain**
$AUC_{0\text{-last}}$ (min*nmoles/ml)	678 ± 138	66 ± 13	1131 ± 400	312 ± 26	1335 ± 316	363 ± 112
C_{max} (nmoles/ml)	6.8 ± 0.8	0.55 ± 0.17	7.4 ± 0.53	1.29 ± 0.32	11.5 ± 2.1	2.18
λ_z ($x10^2 min^{-1}$)	2.1± 0.4	1.2 ± 0.2	0.77 ± 0.1	0.6 ± 0.2	0.79 ± 0.2	0.6 ± 0.2
$t_{1/2}$ (min)	38 ± 15	69 ± 22	80 ± 21	115 ± 28	93 ± 19	121 ± 33
MRT_{last} (min)	42 ± 9	81 ± 17	132 ± 32	175 ± 43	256 ± 52	184 ± 19

Prodrugs V-APV and GV-APV exhibited better brain absorption compared to APV. However when GV-APV was administered, we were able to determine only concentrations of amino acid intermediate V-APV and parent APV. The cumulative $AUC_{0\text{-last}}$ obtained from brain concentrations vs. time profile expressed as min*nmoles/mL for V-APV was found to be 312 ± 26 and 363 ± 112 for GV-APV. These AUCs were 4-5 folds higher than that of parent drug, APV. The brain concentration vs. time profiles for $V\text{-}APV_{total}$ (V-APV and regenerated APV) and $GV\text{-}APV_{total}$ (regenerated V-APV and regenerated APV) in comparison with APV are depicted in Figures 39 and 40. Both prodrugs exhibited comparable $AUC_{0\text{-last}}$ values. Even though Cmax values for $V\text{-}APV_{total}$ in brain (1.29 ± 0.32 nmoles/mL) and $GV\text{-}APV_{total}$ (2.18 ± 0.4 nmoles/mL), are 2-3 fold higher than APV (0.55 ±0.17nmoles/mL), a 4-5 fivefold difference in $AUC_{0\text{-last}}$ was observed. This difference is due to slower elimination of both regenerated V-APV and APV, and regeneration of APV slowly from V-APV. Moreover mean residence times of prodrugs (175 ± 43 for V-APV and 184± 19 for GV-APV) are longer than for APV (81 ± 17minutes). Brains vs. plasma ratios were calculated. Extent of brain absorption, calculated from 100× (AUC_{brain}/AUC_{plasma}) was found to be 9.7 for APV, 27.5 for $V\text{-}APV_{total}$, and 26.1 for GV-APV. Typically extent of brain absorption is calculated from ratios of steady state AUCs in brain and plasma. However for the comparison purposes we calculated the extent of brain absorption following single IV administration. Approximately three fold difference in extent of brain absorption was observed between APV and prodrugs.

In order to further conclude that prodrugs have better pharmacokinetic properties and result in improved therapeutic efficacy, we determined regenerated APV

concentrations from V-APV and GV-APV in brain and pharmacokinetic parameters were determined.

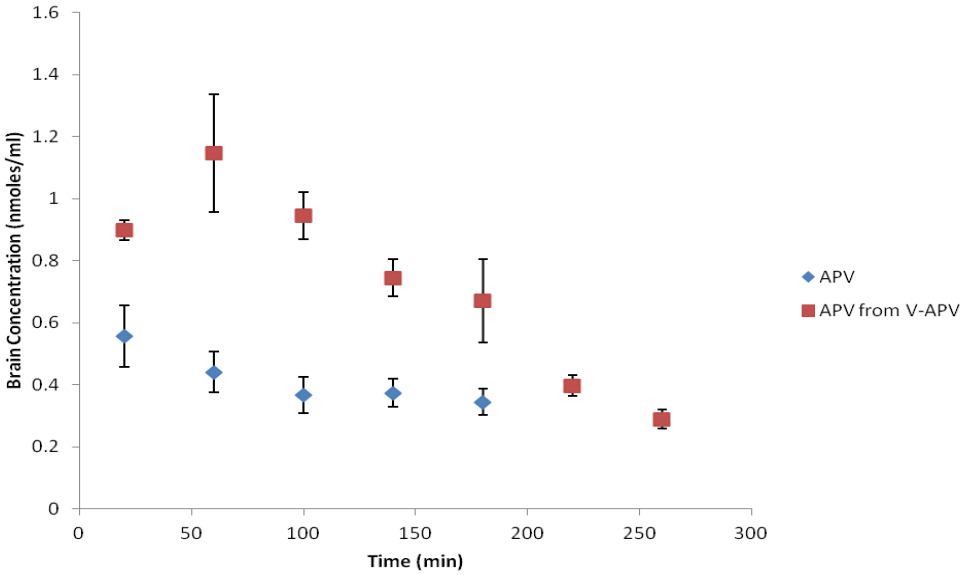

Figure 41. Comparative brain concentration vs. time profile for APV and APV regenerated from V-APV following intravenous administration (19.8 µmoles/kg) in Sprague Dawley rats. Values are expressed as mean ± SE. n=3

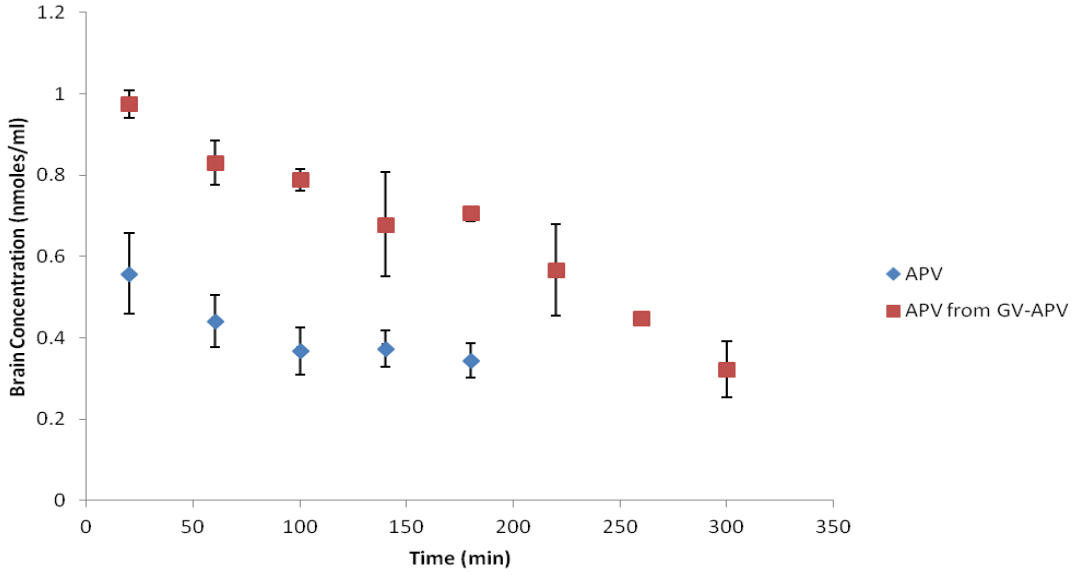

Figure 42. Comparative brain concentration vs. time profile for APV and APV regenerated from GV-APV following intravenous administration (19.8 µmoles/kg) in Sprague Dawley rats. Values are expressed as mean ± SE. n=3.

Table 17. Comparative pharmacokinetic parameters of APV, APV regenerated from V-APV and GV-APV estimated from brain concentrations following intravenous administration (19.8 μmoles/kg) in Sprague Dawley rats. Values are expressed as mean±SD, n=3.

	APV	**APV regenerated from V-APV**	**APV regenerated from GV-APV**
$AUC_{0\text{-last}}$ (min*nmoles/mL)	66 ± 13	182 ± 56	261.5 ± 64
C_{max} (nmoles/mL)	0.55 ± 0.17	0.67 ± 0.06	0.73 ± 0.04
λ_z ($x10^2 min^{-1}$)	1.2 ± 0.2	0.7 ± 0.2	0.6 ± 0.1
$t_{1/2}$ (min)	69 ± 22	106 ± 19	127 ± 29
MRT_{last} (min)	81 ± 17	152 ± 41	141 ± 22

Comparative brain concentration (nmoles/mL) vs. time profile for APV and regenerated APV from V-APV is shown in Figure 6.13. Similarly comparative brain concentration vs. time profile for APV and regenerated APV from GV-APV is shown in Figure 6.14. $AUC_{0\text{-last}}$ expressed as min*nmoles/mL for regenerated APV from V-APV (182 ± 56) and GV-APV (261.5 ±64) are two and three fold higher than that of APV (66 ± 13). High and steady concentrations of APV from V-APV and GV-APV were observed in brain. Elimination rate of regenerated APV was approximately 1.5 times slower than that of APV. Mean residence times of regenerated APV (152 ± 41min for V-APV and 141 ±22 min for GV-APV) are longer than that of APV (69 ±22). Moreover another important observation was 50-60% of V-APV and GV-APV cumulative amounts observed constitute regenerated APV. These results clearly suggest that pro-pro-drug (PPD) approach can result in enhanced oral and brain absorption provided with lowered affinity for efflux transporters, good affinity for influx transporters and good enzymatic stability.

Conclusions

From the *in vitro* permeability evaluation it is clear that V-APV, VV-APV, and GV-APV exhibited better permeability compared to APV. However V-APV exhibited better permeability than di-peptide prodrugs. Observed enhancement in permeability of VV-APV and GV-APV could be due to reduced affinity for efflux protein P-gp. V-APV exhibited better flux which is attributed to evasion of efflux and active transport. Transport of valine was characterized and found to be translocated via system L-amino acid transporter LAT1 with comparable affinity with tyrosine and phenylalanine. Considering *in vitro* stability, bioreversion and oral absorption results, GV-APV was evaluated from brain absorption along with V-APV. *In vivo* brain absorption studies clearly indicate the

concentration of regenerated APV from prodrugs is 1.5 to 2 times higher than APV. Moreover bidirectional functionality of LAT1 is well studied. Hence V-APV needs to be converted to APV in brain tissue. Our tissue homogenate stability study clearly demonstrated regeneration of APV from prodrugs. This couls be the reason for high concentrations of APV in brain parenchyma. All these results clearly prove that PPD approach is a viable strategy to improve brain absorption of antiviral agents resulting in better therapeutic efficacy.

CHAPTER 7

SUMMARY AND RECOMMENDATIONS

Summary

Presence of efflux proteins on epithelial and endothelial membranes plays a major role in pharmacokinetic and pharmacodynamic properties of drugs. In the recent years importance of efflux proteins in drug therapeutic efficacy and drug-drug interactions is gaining importance. Hence the USFDA guidelines suggest that every new and existing drug should be studied for their affinity for efflux proteins such as P-glycoprotein (P-gp) and CYP metabolizing enzymes. Considerable amount of research has been performed to circumvent these efflux proteins by various approaches. In this dissertation project nutrient transporter targeted prodrug approach has been employed to circumvent P-gp mediated cellular efflux. Besides efflux transporters, such as P-gp being expressed in the inner leaflet of the apical membrane, a number of nutrient transporters are also expressed on the outer leaflet of cellular membranes. These nutrient transporters are responsible for the influx of various nutrients and drugs into various epithelial cells (enterocytes) and endothelial cells (e.g. blood brain barrier). In the transporter targeted prodrug approach chemical modifications to drug molecule were made such that evasion of efflux and recognition by influx transporters occur simultaneously.

In this dissertation project, Amprenavir (APV) was selected as model compound to test our hypothesis. We attempted to improve both oral and brain absorption of APV simultaneously by prodrug derivatization. Di-peptide and amino acid prodrugs (Val-APV, Val-Val-APV, and Gly-Val-APV) were synthesized and evaluated for interaction with P-gp. These prodrugs exhibited less affinity for P-gp mediated efflux and are good substrates of

peptide transporter expressed on intestinal epithelium. Moreover these prodrugs exhibited low protein binding and better metabolic stability compared to parent drug. These prodrugs are readily converted to parent drug by enzymatic hydrolysis. These prodrugs underwent sequential hydrolysis, peptide hydrolysis followed by slow ester hydrolysis. Oral absorption studies demonstrated that prodrugs have very good oral absorption compared to APV. VV-APV and GV-APV exhibited significant increase in AUC values relative to APV. One important observation in oral absorption studies was, longer mean residence times of V-APV than other breakdown moieties of di-peptide prodrugs. High concentrations of amino acid prodrug in systemic circulation were observed. Permeability characteristics of prodrugs were studied using *in vitro* BBB model. All the prodrugs exhibited 2-3 fold better permeability than APV. Since V-APV is observed in systemic circulation in high amounts, we characterized transport of valine across BBB to investigate interaction of valine prodrug with system L amino acid transport system. Finally brain absorption of APV and prodrugs was studied following intravenous administration in Sprague-Dawley rats. Only amino acid and parent drug were in brain following GV-APV administration. The AUC of regenerated APV from prodrug is at least twice higher than that of APV. From all the observations in this dissertation project, we can clearly conclude that this pro-drug/pro-pro-drug approach can be successfully employed to deliver PIs and other substrates of efflux proteins effectively.

Recommendations

Transporter targeted pro-pro-drug strategy evaluated in this project, is a viable strategy to circumvent efflux pumps expressed on both epithelial (intestinal) and endothelial (BBB) membranes. Utilization of nutrient transporters to translocate drugs can enhance oral and brain absorption of poorly permeable compounds. However knowledge about various

tissue specific transporters may aide in better tissue targeted delivery. Novel transporters such as histidine peptide transporter (PHT1) can be explored and utilized for drug delivery. Since ester hydrolysis of pro-drug to drug is rate limiting step in the current approach, various amino acid promoieties can be studied in terms of hydrolytic and metabolic stability. Better understanding of transporters expressed on both absorptive and secretory membranes, their functionality and directionality can result in various promoities which can be conjugated to drugs. This knowledge may help designing better prodrugs with improved apical influx and basolateral secretion at epithelial and endothelial barrier mebranes.

APPENDIX

AMERICAN SOCIETY FOR NUTRITION LICENSE TERMS AND CONDITIONS

Aug 14, 2013

This is a License Agreement between Nanda K Mandava ("You") and American Society for Nutrition ("American Society for Nutrition") provided by Copyright Clearance Center ("CCC"). The license consists of your order details, the terms and conditions provided by American Society for Nutrition, and the payment terms and conditions.

All payments must be made in full to CCC. For payment instructions, please see information listed at the bottom of this form.

License Number	3207640655172
License date	Aug 14, 2013
Volume number	130
Issue number	4
Licensed content publisher	American Society for Nutrition
Licensed content publication	The Journal of Nutrition
Licensed content title	Transport of Glutamate and Other Amino Acids at the Blood-Brain Barrier
Licensed content author	Quentin R. Smith
Licensed content date	Apr 1, 2000
Type of Use	Thesis/Dissertation
Requestor type	Student
Portion	Figures/table/illustration
Number of Figures/table/illustration	1
List of figures/table/ illustration	FIGURE 1
Order reference number	
Title of your dissertation / thesis	Evasion of Efflux and improved permeability of APV by prodrug derivatization
Expected completion date	Sep 2013

NATURE PUBLISHING GROUP LICENSE
TERMS AND CONDITIONS

Aug 12, 2013

This is a License Agreement between Nanda K Mandava ("You") and Nature Publishing Group ("Nature Publishing Group") provided by Copyright Clearance Center ("CCC"). The license consists of your order details, the terms and conditions provided by Nature Publishing Group, and the payment terms and conditions.

All payments must be made in full to CCC. For payment instructions, please see information listed at the bottom of this form.

License Number	3206680057941
License date	Aug 12, 2013
Licensed content publisher	Nature Publishing Group
Licensed content publication	Nature Reviews Neuroscience
Licensed content title	Drug resistance in brain diseases and the role of drug efflux transporters
Licensed content author	Wolfgang Loscher and Heidrun Potschka
Licensed content date	Aug 1, 2005
Volume number	6
Issue number	8
Type of Use	reuse in a thesis/dissertation
Requestor type	academic/educational
Format	print and electronic
Portion	figures/tables/illustrations
Number of figures/tables/illustrations	1
High-res required	no
Figures	Figure 1
Author of this NPG article	no
Your reference number	
Title of your thesis / dissertation	Evasion of Efflux and improved permeability of APV by prodrug derivatization
Expected completion date	Sep 2013

Original Message-----
From: dominique.duchene [mailto:dominique.duchene@editionsdesante.fr]
Sent: Monday, August 26, 2013 5:24 AM
To: Mandava, Nanda (UMKC-Student)
Subject: Re: TR: [JDDST] Customer message from contact form [no_sync]

Dear Nanda Mandava,

Yes, you can use this article for your dissertation, with complete reference of its origine.
Yours sincerely,

Prof. Dominique Duchene

>
>
> Message from a JDDST customer
>
>
>
>
>
> Customer e-mail address: <mailto:nkmxb3@mail.umkc.edu>
> nkmxb3@mail.umkc.edu
>
> Customer message: Hello, I am a graduate student in Division of
> Pharmaceutical Sciences, at University of Missouri Kansas City. I am
> the author of publication â€œTransporter targeted drug delivery, JDDST, J.
> DRUG DEL. SCI. TECH., 20 (2) 89-99 2010. I would like to request your
> permission to use the write up in my dissertation.
>
> Regards
> Nanda Mandava
>
>
>
>
>
> <http://www.jddst.com/index.php> JDDST powered by
> <http://www.prestashop.com/> PrestaShopâ„¢
>
>
>
>

REFERENCES

Aarnoutse RE, Schapiro JM, Boucher CA, Hekster YA and Burger DM (2003) Therapeutic drug monitoring: an aid to optimising response to antiretroviral drugs? *Drugs* 63:741-753.

Abbott NJ (2002) Astrocyte-endothelial interactions and blood-brain barrier permeability. *J Anat* 200:629-638.

Abbott NJ (2005) Dynamics of CNS barriers: evolution, differentiation, and modulation. *Cell Mol Neurobiol* 25:5-23.

Abbott NJ, Patabendige AA, Dolman DE, Yusof SR and Begley DJ Structure and function of the blood-brain barrier. *Neurobiol Dis* 37:13-25.

Acharya P, Tran TT, Polli JW, Ayrton A, Ellens H and Bentz J (2006) P-Glycoprotein (P-gp) expressed in a confluent monolayer of hMDR1-MDCKII cells has more than one efflux pathway with cooperative binding sites. *Biochemistry* 45:15505-15519.

Adkins JC and Faulds D (1998) Amprenavir. *Drugs* 55:837-842; discussion 843-834.

Agarwal S, Boddu SH, Jain R, Samanta S, Pal D and Mitra AK (2008) Peptide prodrugs: improved oral absorption of lopinavir, a HIV protease inhibitor. *Int J Pharm* 359:7-14.

Allt G and Lawrenson JG (2001) Pericytes: cell biology and pathology. *Cells Tissues Organs* 169:1-11.

Ambudkar SV, Kimchi-Sarfaty C, Sauna ZE and Gottesman MM (2003) P-glycoprotein: from genomics to mechanism. *Oncogene* 22:7468-7485.

Anand BS, Dey S and Mitra AK (2002) Current prodrug strategies via membrane transporters/receptors. *Expert Opin Biol Ther* 2:607-620.

Anand BS, Patel J and Mitra AK (2003) Interactions of the di-peptide ester prodrugs of acyclovir with the intestinal oligopeptide transporter: competitive inhibition of glycylsarcosine transport in human intestinal cell line-Caco-2. *J Pharmacol Exp Ther* 304:781-791.

Anderson PL, Brundage RC, Bushman L, Kakuda TN, Remmel RP and Fletcher CV (2000) Indinavir plasma protein binding in HIV-1-infected adults. *AIDS* 14:2293-2297.

Ayres S, 3rd (1977) Prevention and correction of unaesthetic results of hair transplantation for male pattern baldness. *Cutis* 19:117-121.

Bakos E, Hegedus T, Hollo Z, Welker E, Tusnady GE, Zaman GJ, Flens MJ, Varadi A and Sarkadi B (1996) Membrane topology and glycosylation of the human multidrug resistance-associated protein. *J Biol Chem* 271:12322-12326.

Barrail A, Le Tiec C, Paci-Bonaventure S, Furlan V, Vincent I and Taburet AM (2006) Determination of amprenavir total and unbound concentrations in plasma by high-performance liquid chromatography and ultrafiltration. *Ther Drug Monit* 28:89-94.

Barry M, Mulcahy F, Merry C, Gibbons S and Back D (1999) Pharmacokinetics and potential interactions amongst antiretroviral agents used to treat patients with HIV infection. *Clin Pharmacokinet* 36:289-304.

Belpaire FM and Bogaert MG (1989) Pharmacokinetic and pharmacodynamic consequences of altered binding of drugs to alpha 1-acid glycoprotein. *Prog Clin Biol Res* 300:337-350.

Benet LZ and Cummins CL (2001) The drug efflux-metabolism alliance: biochemical aspects. *Adv Drug Deliv Rev* 50 Suppl 1:S3-11.

Bertucci C and Domenici E (2002) Reversible and covalent binding of drugs to human serum albumin: methodological approaches and physiological relevance. *Curr Med Chem* 9:1463-1481.

Bhardwaj RK, Herrera-Ruiz D, Sinko PJ, Gudmundsson OS and Knipp G (2005) Delineation of human peptide transporter 1 (hPepT1)-mediated uptake and transport of substrates with varying transporter affinities utilizing stably transfected hPepT1/Madin-Darby canine kidney clones and Caco-2 cells. *J Pharmacol Exp Ther* 314:1093-1100.

Boffito M, Back DJ, Blaschke TF, Rowland M, Bertz RJ, Gerber JG and Miller V (2003) Protein binding in antiretroviral therapies. *AIDS Res Hum Retroviruses* 19:825-835.

Bradford MM (1976) A rapid and sensitive method for the quantitation of microgram quantities of protein utilizing the principle of protein-dye binding. *Anal Biochem* 72:248-254.

Cameron DW, Heath-Chiozzi M, Danner S, Cohen C, Kravcik S, Maurath C, Sun E, Henry D, Rode R, Potthoff A and Leonard J (1998) Randomised placebo-controlled trial of ritonavir in advanced HIV-1 disease. The Advanced HIV Disease Ritonavir Study Group. *Lancet* 351:543-549.

Chang SC, Bundgaard H, Buur A and Lee VH (1987) Improved corneal penetration of timolol by prodrugs as a means to reduce systemic drug load. *Invest Ophthalmol Vis Sci* 28:487-491.

Conway B, Routy JP and Sekaly RP (1998) Combination therapy for HIV: towards long term control of disease progression. *Expert Opin Investig Drugs* 7:941-961.

Cordon-Cardo C, O'Brien JP, Casals D, Rittman-Grauer L, Biedler JL, Melamed MR and Bertino JR (1989) Multidrug-resistance gene (P-glycoprotein) is expressed by endothelial cells at blood-brain barrier sites. *Proc Natl Acad Sci U S A* 86:695-698.

Crone C and Christensen O (1981) Electrical resistance of a capillary endothelium. *J Gen Physiol* 77:349-371.

Crowe SM and Sonza S (2000) HIV-1 can be recovered from a variety of cells including peripheral blood monocytes of patients receiving highly active antiretroviral therapy: a further obstacle to eradication. *J Leukoc Biol* 68:345-350.

Dalgleish AG, Beverley PC, Clapham PR, Crawford DH, Greaves MF and Weiss RA (1984) The CD4 (T4) antigen is an essential component of the receptor for the AIDS retrovirus. *Nature* 312:763-767.

Das M and Radhakrishnan AN (1976) Role of peptidases and peptide transport in the intestinal absorption of proteins. *World Rev Nutr Diet* 24:58-87.

Dayton PG, Israili ZH and Perel JM (1973) Influence of binding on drug metabolism and distribution. *Ann N Y Acad Sci* 226:172-194.

de Maat MM, Ekhart GC, Huitema AD, Koks CH, Mulder JW and Beijnen JH (2003) Drug interactions between antiretroviral drugs and comedicated agents. *Clin Pharmacokinet* 42:223-282.

Deli MA, Abraham CS, Kataoka Y and Niwa M (2005) Permeability studies on in vitro blood-brain barrier models: physiology, pathology, and pharmacology. *Cell Mol Neurobiol* 25:59-127.

Dorkoosh FA, Broekhuizen CA, Borchard G, Rafiee-Tehrani M, Verhoef JC and Junginger HE (2004) Transport of octreotide and evaluation of mechanism of opening the paracellular tight junctions using superporous hydrogel polymers in Caco-2 cell monolayers. *J Pharm Sci* 93:743-752.

Doyon L, Croteau G, Thibeault D, Poulin F, Pilote L and Lamarre D (1996) Second locus involved in human immunodeficiency virus type 1 resistance to protease inhibitors. *J Virol* 70:3763-3769.

Eagling VA, Profit L and Back DJ (1999) Inhibition of the CYP3A4-mediated metabolism and P-glycoprotein-mediated transport of the HIV-1 protease inhibitor saquinavir by grapefruit juice components. *Br J Clin Pharmacol* 48:543-552.

Edwards JE, Brouwer KR and McNamara PJ (2002) GF120918, a P-glycoprotein modulator, increases the concentration of unbound amprenavir in the central nervous system in rats. *Antimicrob Agents Chemother* 46:2284-2286.

Engelhardt B and Sorokin L (2009) The blood-brain and the blood-cerebrospinal fluid barriers: function and dysfunction. *Semin Immunopathol* 31:497-511.

Falcoz C, Jenkins JM, Bye C, Hardman TC, Kenney KB, Studenberg S, Fuder H and Prince WT (2002) Pharmacokinetics of GW433908, a prodrug of amprenavir, in healthy male volunteers. *J Clin Pharmacol* 42:887-898.

Flexner C (2007) HIV drug development: the next 25 years. *Nat Rev Drug Discov* 6:959-966.

Frankel AD and Young JA (1998) HIV-1: fifteen proteins and an RNA. *Annu Rev Biochem* 67:1-25.

Ganapathy ME, Brandsch M, Prasad PD, Ganapathy V and Leibach FH (1995) Differential recognition of beta -lactam antibiotics by intestinal and renal peptide transporters, PEPT 1 and PEPT 2. *J Biol Chem* 270:25672-25677.

Golden PL and Pollack GM (2003) Blood-brain barrier efflux transport. *J Pharm Sci* 92:1739-1753.

Goldenberg GJ, Lam HY and Begleiter A (1979) Active carrier-mediated transport of melphalan by two separate amino acid transport systems in LPC-1 plasmacytoma cells in vitro. *J Biol Chem* 254:1057-1064.

Graffner-Nordberg M, Sjodin K, Tunek A and Hallberg A (1998) Synthesis and enzymatic hydrolysis of esters, constituting simple models of soft drugs. *Chem Pharm Bull (Tokyo)* 46:591-601.

Greene WC, Debyser Z, Ikeda Y, Freed EO, Stephens E, Yonemoto W, Buckheit RW, Este JA and Cihlar T (2008) Novel targets for HIV therapy. *Antiviral Res* 80:251-265.

Guengerich FP, Martin MV, Beaune PH, Kremers P, Wolff T and Waxman DJ (1986) Characterization of rat and human liver microsomal cytochrome P-450 forms involved in nifedipine oxidation, a prototype for genetic polymorphism in oxidative drug metabolism. *J Biol Chem* 261:5051-5060.

Gulick RM, Mellors JW, Havlir D, Eron JJ, Gonzalez C, McMahon D, Richman DD, Valentine FT, Jonas L, Meibohm A, Emini EA and Chodakewitz JA (1997) Treatment with indinavir, zidovudine, and lamivudine in adults with human immunodeficiency virus infection and prior antiretroviral therapy. *N Engl J Med* 337:734-739.

Gumbleton M and Audus KL (2001) Progress and limitations in the use of in vitro cell cultures to serve as a permeability screen for the blood-brain barrier. *J Pharm Sci* 90:1681-1698.

Han HK and Amidon GL (2000) Targeted prodrug design to optimize drug delivery. *AAPS PharmSci* 2:E6.

Hipfner DR, Almquist KC, Leslie EM, Gerlach JH, Grant CE, Deeley RG and Cole SP (1997) Membrane topology of the multidrug resistance protein (MRP). A study of glycosylation-site mutants reveals an extracytosolic NH2 terminus. *J Biol Chem* 272:23623-23630.

Ho GT, Moodie FM and Satsangi J (2003) Multidrug resistance 1 gene (P-glycoprotein 170): an important determinant in gastrointestinal disease? *Gut* 52:759-766.

Hodges GM, Carr EA, Hazzard RA and Carr KE (1995) Uptake and translocation of microparticles in small intestine. Morphology and quantification of particle distribution. *Dig Dis Sci* 40:967-975.

Hsu A, Granneman GR and Bertz RJ (1998) Ritonavir. Clinical pharmacokinetics and interactions with other anti-HIV agents. *Clin Pharmacokinet* 35:275-291.

Huang Z and Ung T Effect of alpha-1-acid glycoprotein binding on pharmacokinetics and pharmacodynamics. *Curr Drug Metab* 14:226-238.

Hundal HS and Taylor PM (2009) Amino acid transceptors: gate keepers of nutrient exchange and regulators of nutrient signaling. *Am J Physiol Endocrinol Metab* 296:E603-613.

Hunter J, Jepson MA, Tsuruo T, Simmons NL and Hirst BH (1993) Functional expression of P-glycoprotein in apical membranes of human intestinal Caco-2 cells. Kinetics of vinblastine secretion and interaction with modulators. *J Biol Chem* 268:14991-14997.

Israili ZH and Dayton PG (2001) Human alpha-1-glycoprotein and its interactions with drugs. *Drug Metab Rev* 33:161-235.

Jain R, Agarwal S, Majumdar S, Zhu X, Pal D and Mitra AK (2005) Evasion of P-gp mediated cellular efflux and permeability enhancement of HIV-protease inhibitor saquinavir by prodrug modification. *Int J Pharm* 303:8-19.

Jain R, Agarwal S, Mandava NK, Sheng Y and Mitra AK (2008) Interaction of di-peptide prodrugs of saquinavir with multidrug resistance protein-2 (MRP-2): evasion of MRP-2 mediated efflux. *Int J Pharm* 362:44-51.

Jain R, Duvvuri S, Kansara V, Mandava NK and Mitra AK (2007) Intestinal absorption of novel-di-peptide prodrugs of saquinavir in rats. *Int J Pharm* 336:233-240.

Jayakanthan M, Chandrasekar S, Muthukumaran J and Mathur PP Analysis of CYP3A4-HIV-1 protease drugs interactions by computational methods for Highly Active Antiretroviral Therapy in HIV/AIDS. *J Mol Graph Model* 28:455-463.

Johanson CE, Duncan JA, Stopa EG and Baird A (2005) Enhanced prospects for drug delivery and brain targeting by the choroid plexus-CSF route. *Pharm Res* 22:1011-1037.

Juliano RL and Ling V (1976) A surface glycoprotein modulating drug permeability in Chinese hamster ovary cell mutants. *Biochim Biophys Acta* 455:152-162.

Kamerman PR, Wadley AL and Cherry CL HIV-associated sensory neuropathy: risk factors and genetics. *Curr Pain Headache Rep* 16:226-236.

Katragadda S, Budda B, Anand BS and Mitra AK (2005) Role of efflux pumps and metabolising enzymes in drug delivery. *Expert Opin Drug Deliv* 2:683-705.

Kempf DJ, Marsh KC, Kumar G, Rodrigues AD, Denissen JF, McDonald E, Kukulka MJ, Hsu A, Granneman GR, Baroldi PA, Sun E, Pizzuti D, Plattner JJ, Norbeck DW and Leonard JM (1997) Pharmacokinetic enhancement of inhibitors of the human immunodeficiency virus protease by coadministration with ritonavir. *Antimicrob Agents Chemother* 41:654-660.

Kim RB, Fromm MF, Wandel C, Leake B, Wood AJ, Roden DM and Wilkinson GR (1998) The drug transporter P-glycoprotein limits oral absorption and brain entry of HIV-1 protease inhibitors. *J Clin Invest* 101:289-294.

Klatzmann D, Champagne E, Chamaret S, Gruest J, Guetard D, Hercend T, Gluckman JC and Montagnier L (1984) T-lymphocyte T4 molecule behaves as the receptor for human retrovirus LAV. *Nature* 312:767-768.

Kolars JC, Schmiedlin-Ren P, Schuetz JD, Fang C and Watkins PB (1992) Identification of rifampin-inducible P450IIIA4 (CYP3A4) in human small bowel enterocytes. *J Clin Invest* 90:1871-1878.

Kopecky V, Jr., Ettrich R, Hofbauerova K and Baumruk V (2003) Structure of human alpha1-acid glycoprotein and its high-affinity binding site. *Biochem Biophys Res Commun* 300:41-46.

Kotze AF, Luessen HL, de Leeuw BJ, de Boer AG, Verhoef JC and Junginger HE (1998) Comparison of the effect of different chitosan salts and N-trimethyl chitosan chloride on the permeability of intestinal epithelial cells (Caco-2). *J Control Release* 51:35-46.

Kremer JM, Wilting J and Janssen LH (1988) Drug binding to human alpha-1-acid glycoprotein in health and disease. *Pharmacol Rev* 40:1-47.

Kwara A, Delong A, Rezk N, Hogan J, Burtwell H, Chapman S, Moreira CC, Kurpewski J, Ingersoll J, Caliendo AM, Kashuba A and Cu-Uvin S (2008) Antiretroviral drug concentrations and HIV RNA in the genital tract of HIV-infected women receiving long-term highly active antiretroviral therapy. *Clin Infect Dis* 46:719-725.

Legare D, Richard D, Mukhopadhyay R, Stierhof YD, Rosen BP, Haimeur A, Papadopoulou B and Ouellette M (2001) The Leishmania ATP-binding cassette protein PGPA is an intracellular metal-thiol transporter ATPase. *J Biol Chem* 276:26301-26307.

Leslie EM, Deeley RG and Cole SP (2001) Toxicological relevance of the multidrug resistance protein 1, MRP1 (ABCC1) and related transporters. *Toxicology* 167:3-23.

Louis JM, Ishima R, Torchia DA and Weber IT (2007) HIV-1 protease: structure, dynamics, and inhibition. *Adv Pharmacol* 55:261-298.

Luo S, Kansara VS, Zhu X, Mandava NK, Pal D and Mitra AK (2006) Functional characterization of sodium-dependent multivitamin transporter in MDCK-MDR1 cells and its utilization as a target for drug delivery. *Mol Pharm* 3:329-339.

Mammano F, Petit C and Clavel F (1998) Resistance-associated loss of viral fitness in human immunodeficiency virus type 1: phenotypic analysis of protease and gag coevolution in protease inhibitor-treated patients. *J Virol* 72:7632-7637.

Meijer DK and Van der Sluijs P (1987) The influence of binding to albumin and alpha 1-acid glycoprotein on the clearance of drugs by the liver. *Pharm Weekbl Sci* 9:65-74.

Miller DS, Nobmann SN, Gutmann H, Toeroek M, Drewe J and Fricker G (2000) Xenobiotic transport across isolated brain microvessels studied by confocal microscopy. *Mol Pharmacol* 58:1357-1367.

Moyle G and Gazzard B (1996) Current knowledge and future prospects for the use of HIV protease inhibitors. *Drugs* 51:701-712.

Nath A and Sacktor N (2006) Influence of highly active antiretroviral therapy on persistence of HIV in the central nervous system. *Curr Opin Neurol* 19:358-361.

Nicolazzo JA, Charman SA and Charman WN (2006) Methods to assess drug permeability across the blood-brain barrier. *J Pharm Pharmacol* 58:281-293.

Nolan D, Reiss P and Mallal S (2005) Adverse effects of antiretroviral therapy for HIV infection: a review of selected topics. *Expert Opin Drug Saf* 4:201-218.

Oroszlan S and Luftig RB (1990) Retroviral proteinases. *Curr Top Microbiol Immunol* 157:153-185.

Pardridge WM (1998) Blood-brain barrier carrier-mediated transport and brain metabolism of amino acids. *Neurochem Res* 23:635-644.

Park S and Sinko PJ (2005) P-glycoprotein and mutlidrug resistance-associated proteins limit the brain uptake of saquinavir in mice. *J Pharmacol Exp Ther* 312:1249-1256.

Patel J and Mitra AK (2001) Strategies to overcome simultaneous P-glycoprotein mediated efflux and CYP3A4 mediated metabolism of drugs. *Pharmacogenomics* 2:401-415.

Patel M, Vadlapatla RK, Pal D and Mitra AK Molecular and functional characterization of riboflavin specific transport system in rat brain capillary endothelial cells. *Brain Res* 1468:1-10.

Pearl LH and Taylor WR (1987) A structural model for the retroviral proteases. *Nature* 329:351-354.

Piafsky KM (1980) Disease-induced changes in the plasma binding of basic drugs. *Clin Pharmacokinet* 5:246-262.

Piliero PJ (2002) The utility of inhibitory quotients in determining the relative potency of protease inhibitors. *AIDS* 16:799-800.

Pokorna J, Machala L, Rezacova P and Konvalinka J (2009) Current and Novel Inhibitors of HIV Protease. *Viruses* 1:1209-1239.

Potschka H and Loscher W (2001) In vivo evidence for P-glycoprotein-mediated transport of phenytoin at the blood-brain barrier of rats. *Epilepsia* 42:1231-1240.

Price RW, Brew B, Sidtis J, Rosenblum M, Scheck AC and Cleary P (1988) The brain in AIDS: central nervous system HIV-1 infection and AIDS dementia complex. *Science* 239:586-592.

Ranki A, Nyberg M, Ovod V, Haltia M, Elovaara I, Raininko R, Haapasalo H and Krohn K (1995) Abundant expression of HIV Nef and Rev proteins in brain astrocytes in vivo is associated with dementia. *AIDS* 9:1001-1008.

Redzic Z Molecular biology of the blood-brain and the blood-cerebrospinal fluid barriers: similarities and differences. *Fluids Barriers CNS* 8:3.

Roiko SA, FelmLee MA and Morris ME Brain uptake of the drug of abuse gamma-hydroxybutyric acid in rats. *Drug Metab Dispos* 40:212-218.

Rowland M (1984) Protein binding and drug clearance. *Clin Pharmacokinet* 9 Suppl 1:10-17.

Roy SD and Manoukian E (1994) Permeability of ketorolac acid and its ester analogs (prodrug) through human cadaver skin. *J Pharm Sci* 83:1548-1553.

Rubio-Aliaga I and Daniel H (2002) Mammalian peptide transporters as targets for drug delivery. *Trends Pharmacol Sci* 23:434-440.

Rubio-Aliaga I and Daniel H (2008) Peptide transporters and their roles in physiological processes and drug disposition. *Xenobiotica* 38:1022-1042.

Sadler BM, Gillotin C, Lou Y and Stein DS (2001) In vivo effect of alpha(1)-acid glycoprotein on pharmacokinetics of amprenavir, a human immunodeficiency virus protease inhibitor. *Antimicrob Agents Chemother* 45:852-856.

Sadler BM, Hanson CD, Chittick GE, Symonds WT and Roskell NS (1999) Safety and pharmacokinetics of amprenavir (141W94), a human immunodeficiency virus (HIV) type 1 protease inhibitor, following oral administration of single doses to HIV-infected adults. *Antimicrob Agents Chemother* 43:1686-1692.

Sadler BM and Stein DS (2002) Clinical pharmacology and pharmacokinetics of amprenavir. *Ann Pharmacother* 36:102-118.

Salama NN, Kelly EJ, Bui T and Ho RJ (2005) The impact of pharmacologic and genetic knockout of P-glycoprotein on nelfinavir levels in the brain and other tissues in mice. *J Pharm Sci* 94:1216-1225.

Sarafian TA, Montes C, Imura T, Qi J, Coppola G, Geschwind DH and Sofroniew MV Disruption of astrocyte STAT3 signaling decreases mitochondrial function and increases oxidative stress in vitro. *PLoS One* 5:e9532.

Scherrmann JM (2002) Drug delivery to brain via the blood-brain barrier. *Vascul Pharmacol* 38:349-354.

Schinkel AH and Jonker JW (2003) Mammalian drug efflux transporters of the ATP binding cassette (ABC) family: an overview. *Adv Drug Deliv Rev* 55:3-29.

Schmidt S, Barbour A, Sahre M, Rand KH and Derendorf H (2008) PK/PD: new insights for antibacterial and antiviral applications. *Curr Opin Pharmacol* 8:549-556.

Shao Z, Li Y, Chermak T and Mitra AK (1994) Cyclodextrins as mucosal absorption promoters of insulin. II. Effects of beta-cyclodextrin derivatives on alpha-chymotryptic degradation and enteral absorption of insulin in rats. *Pharm Res* 11:1174-1179.

Shen DD, Kunze KL and Thummel KE (1997) Enzyme-catalyzed processes of first-pass hepatic and intestinal drug extraction. *Adv Drug Deliv Rev* 27:99-127.

Shibuyama S, Gevorkyan A, Yoo U, Tim S, Dzhangiryan K and Scott JD (2006) Understanding and avoiding antiretroviral adverse events. *Curr Pharm Des* 12:1075-1090.

Smith QR (2000) Transport of glutamate and other amino acids at the blood-brain barrier. *J Nutr* 130:1016S-1022S.

Sparreboom A, van Asperen J, Mayer U, Schinkel AH, Smit JW, Meijer DK, Borst P, Nooijen WJ, Beijnen JH and van Tellingen O (1997) Limited oral bioavailability and active epithelial excretion of paclitaxel (Taxol) caused by P-glycoprotein in the intestine. *Proc Natl Acad Sci U S A* 94:2031-2035.

St Clair MH, Millard J, Rooney J, Tisdale M, Parry N, Sadler BM, Blum MR and Painter G (1996) In vitro antiviral activity of 141W94 (VX-478) in combination with other antiretroviral agents. *Antiviral Res* 29:53-56.

Stoll J, Wadhwani KC and Smith QR (1993) Identification of the cationic amino acid transporter (System y+) of the rat blood-brain barrier. *J Neurochem* 60:1956-1959.

Su TZ, Lunney E, Campbell G and Oxender DL (1995) Transport of gabapentin, a gamma-amino acid drug, by system l alpha-amino acid transporters: a comparative study in astrocytes, synaptosomes, and CHO cells. *J Neurochem* 64:2125-2131.

Talluri RS, Samanta SK, Gaudana R and Mitra AK (2008) Synthesis, metabolism and cellular permeability of enzymatically stable di-peptide prodrugs of acyclovir. *Int J Pharm* 361:118-124.

Tamai I and Tsuji A (2000) Transporter-mediated permeation of drugs across the blood-brain barrier. *J Pharm Sci* 89:1371-1388.

Tanaka E (1998) Clinically important pharmacokinetic drug-drug interactions: role of cytochrome P450 enzymes. *J Clin Pharm Ther* 23:403-416.

Terada T and Inui K (2004) Peptide transporters: structure, function, regulation and application for drug delivery. *Curr Drug Metab* 5:85-94.

Terao T, Hisanaga E, Sai Y, Tamai I and Tsuji A (1996) Active secretion of drugs from the small intestinal epithelium in rats by P-glycoprotein functioning as an absorption barrier. *J Pharm Pharmacol* 48:1083-1089.

Thiebaut F, Tsuruo T, Hamada H, Gottesman MM, Pastan I and Willingham MC (1987) Cellular localization of the multidrug-resistance gene product P-glycoprotein in normal human tissues. *Proc Natl Acad Sci U S A* 84:7735-7738.

Thomas NW, Jenkins PG, Howard KA, Smith MW, Lavelle EC, Holland J and Davis SS (1996) Particle uptake and translocation across epithelial membranes. *J Anat* 189 (Pt 3):487-490.

Thomas SA (2004) Anti-HIV drug distribution to the central nervous system. *Curr Pharm Des* 10:1313-1324.

Tolcher AW, Cowan KH, Solomon D, Ognibene F, Goldspiel B, Chang R, Noone MH, Denicoff AM, Barnes CS, Gossard MR, Fetsch PA, Berg SL, Balis FM, Venzon DJ and O'Shaughnessy JA (1996) Phase I crossover study of paclitaxel with r-verapamil in patients with metastatic breast cancer. *J Clin Oncol* 14:1173-1184.

Tornatore C, Chandra R, Berger JR and Major EO (1994) HIV-1 infection of subcortical astrocytes in the pediatric central nervous system. *Neurology* 44:481-487.

Tran TT, Mittal A, Aldinger T, Polli JW, Ayrton A, Ellens H and Bentz J (2005) The elementary mass action rate constants of P-gp transport for a confluent monolayer of MDCKII-hMDR1 cells. *Biophys J* 88:715-738.

Treluyer JM, Bowers G, Cazali N, Sonnier M, Rey E, Pons G and Cresteil T (2003) Oxidative metabolism of amprenavir in the human liver. Effect of the CYP3A maturation. *Drug Metab Dispos* 31:275-281.

Tsuji A and Tamai II (1999) Carrier-mediated or specialized transport of drugs across the blood-brain barrier. *Adv Drug Deliv Rev* 36:277-290.

Urbatsch IL, Sankaran B, Bhagat S and Senior AE (1995) Both P-glycoprotein nucleotide-binding sites are catalytically active. *J Biol Chem* 270:26956-26961.

van der Sandt IC, Vos CM, Nabulsi L, Blom-Roosemalen MC, Voorwinden HH, de Boer AG and Breimer DD (2001) Assessment of active transport of HIV protease inhibitors in various cell lines and the in vitro blood--brain barrier. *AIDS* 15:483-491.

Veronese L, Rautaureau J, Sadler BM, Gillotin C, Petite JP, Pillegand B, Delvaux M, Masliah C, Fosse S, Lou Y and Stein DS (2000) Single-dose pharmacokinetics of amprenavir, a human immunodeficiency virus type 1 protease inhibitor, in subjects with normal or impaired hepatic function. *Antimicrob Agents Chemother* 44:821-826.

Vogelgesang S, Warzok RW, Cascorbi I, Kunert-Keil C, Schroeder E, Kroemer HK, Siegmund W, Walker LC and Pahnke J (2004) The role of P-glycoprotein in cerebral amyloid angiopathy; implications for the early pathogenesis of Alzheimer's disease. *Curr Alzheimer Res* 1:121-125.

Wacher VJ, Silverman JA, Zhang Y and Benet LZ (1998) Role of P-glycoprotein and cytochrome P450 3A in limiting oral absorption of peptides and peptidomimetics. *J Pharm Sci* 87:1322-1330.

Washington CB, Wiltshire HR, Man M, Moy T, Harris SR, Worth E, Weigl P, Liang Z, Hall D, Marriott L and Blaschke TF (2000) The disposition of saquinavir in normal and P-glycoprotein deficient mice, rats, and in cultured cells. *Drug Metab Dispos* 28:1058-1062.

Watanabe KA, Matsuda A, Halat MJ, Hollenberg DH, Nisselbaum JS and Fox JJ (1981) Nucleosides. 114. 5'-O-Glucuronides of 5-fluorouridine and 5-fluorocytidine. Masked precursors of anticancer nucleosides. *J Med Chem* 24:893-897.

Watkins PB (1997) The barrier function of CYP3A4 and P-glycoprotein in the small bowel. *Adv Drug Deliv Rev* 27:161-170.

Wilkinson GR (1983) Plasma and tissue binding considerations in drug disposition. *Drug Metab Rev* 14:427-465.

Wlodawer A and Erickson JW (1993) Structure-based inhibitors of HIV-1 protease. *Annu Rev Biochem* 62:543-585.

Wohl DA, McComsey G, Tebas P, Brown TT, Glesby MJ, Reeds D, Shikuma C, Mulligan K, Dube M, Wininger D, Huang J, Revuelta M, Currier J, Swindells S, Fichtenbaum C, Basar M, Tungsiripat M, Meyer W, Weihe J and Wanke C (2006) Current concepts in the diagnosis and management of metabolic complications of HIV infection and its therapy. *Clin Infect Dis* 43:645-653.

Yang C, Tirucherai GS and Mitra AK (2001) Prodrug based optimal drug delivery via membrane transporter/receptor. *Expert Opin Biol Ther* 1:159-175.

Yang CY, Dantzig AH and Pidgeon C (1999) Intestinal peptide transport systems and oral drug availability. *Pharm Res* 16:1331-1343.

Yeni PG, Hammer SM, Hirsch MS, Saag MS, Schechter M, Carpenter CC, Fischl MA, Gatell JM, Gazzard BG, Jacobsen DM, Katzenstein DA, Montaner JS, Richman DD, Schooley RT, Thompson MA, Vella S and Volberding PA (2004) Treatment for adult HIV infection: 2004 recommendations of the International AIDS Society-USA Panel. *JAMA* 292:251-265.

Zhang X, Liu L, Ma K, Rao Y, Zhao Q and Li F Analytical methods for brain targeted delivery system in vivo: perspectives on imaging modalities and microdialysis. *J Pharm Biomed Anal* 59:1-12.

VITA

Nanda Mandava was born on August 20th, 1980 in Andhra Pradesh, India. He obtained his Bachelor of Pharmacy degree from The Tamil Nadu Dr. M.G.R. Medical University (Chennai, India) in June 2001. He joined Madras Analytical and Research Labs as research assistant in 2002. Later Nanda Mandava joined Dr. Ashim K. Mitra's laboratory in spring semester of 2005 in pursuit of interdisciplinary doctorate degree in Pharmaceutical Sciences and Chemistry.

Nanda Mandava was member of organizations such as American Association of Pharmaceutical Scientists (AAPS), Association for Research in Vision and Ophthalmology (ARVO). He received outstanding leadership award for serving as Pharmaceutical Sciences Graduate Students Association. He authored/co-authored several peer reviewed publications including review articles and book chapters and made presentations at national conferences.